INFORMATION TO USERS

This manuscript has been reproduced from the microfilm master. UMI films the text directly from the original or copy submitted. Thus, some thesis and dissertation copies are in typewriter face, while others may be from any type of computer printer.

The quality of this reproduction is dependent upon the quality of the copy submitted. Broken or indistinct print, colored or poor quality illustrations and photographs, print bleedthrough, substandard margins, and improper alignment can adversely affect reproduction.

In the unlikely event that the author did not send UMI a complete manuscript and there are missing pages, these will be noted. Also, if unauthorized copyright material had to be removed, a note will indicate the deletion.

Oversize materials (e.g., maps, drawings, charts) are reproduced by sectioning the original, beginning at the upper left-hand corner and continuing from left to right in equal sections with small overlaps.

ProQuest Information and Learning
300 North Zeeb Road, Ann Arbor, MI 48106-1346 USA
800-521-0600

UMI®

LYAPUNOV- BASED CONTROL OF UNBALANCED PULSE-WIDTH MODULATION BOOST TYPE RECTIFIERS

DANIEL TUMA

Bachelor of Science in Electronics
Eastern Kentucky University
May, 1990

Masters of Science in Electronics
Indiana State University
May, 1994

Masters of Science in Industrial Engineering
Cleveland State University
May, 1997

Masters of Science in Electrical Engineering
Cleveland State University
May, 1999

submitted in partial fulfillment of the requirements for degree of
DOCTOR OF ENGINEERING

at the
CLEVELAND STATE UNIVERSITY

November, 2002

© Copyright by Daniel Tuma 2002

This dissertation has been approved

for the Department of Electrical and Computer Engineering,

and the College of Graduate Studies by

Dan Simon / 11-6-02

Dissertation Committee Chairperson, Dr. Dan Simon, Date
Department of Electrical and Computer Engineering

Zhiqiang Gao / 11-6-02

Dr. Zhiqiang Gao, Date
Department of Electrical and Computer Engineering

F. Eugenio Villaseca / 11-6-02

Dr. F. Eugenio Villaseca, Date
Department of Electrical and Computer Engineering

Joseph Svestka / 11/6/02

Dr. Joseph Svestka, Date
Department of Industrial Manufacturing Engineering

Luiz F. Martins / 11/06/2002

Dr. Luiz Martins, Date
Mathematics Department

This work is dedicate to

my beloved mother Julia B. Tuma,

my lovely wife Rose T. Tuma, my beautiful daughter Bih E. Tuma,

my sons Lionel F. Tuma and Ndeke N. Tuma, my mentor Paul A. Tuma

and all of my family for all their love and support.

ACKNOWLEDGEMENTS

Thanks be to God, the Almighty, the Creator, the Giver and the Taker for His guidance, wisdom, and many blessings given to me to be able overcome obstacles.

I would like to thank the Department of Electrical and Computer Engineering and the faculty for giving me the opportunity and preparing me for all that was involved in this undertaking. The completion of this dissertation would not have occurred without the support of Dr. Dan Simon, my committee chair, Dr. Villaseca and Dr. Gao of the Department Electrical Engineering, Dr. Svestka of the Department of Industrial Engineering and Dr. Martins of the Department of Mathematics.

I would like to express my sincere and heartfelt gratitude to Dr. Simon for believing in me, his patience, stimulating suggestions, encouragement and moral support throughout this dissertation. Special thanks to Dr. Villaseca and Dr. Svestka for their encouragement and advise throughout my studies at Cleveland State University, and Dr. Gao and Dr. Martins for taking time and agreeing to serve as part of my dissertation committee.

Special thanks to Adrienne and Jan of the Department of Electrical and Computer Engineering for always willing and able to offer assistance beyond the call.

Finally, many thanks to my beloved parents, my lovely wife Rose, beautiful Daughter Bih, my sons Lionel and Ndeke, my brothers and sisters, and my friends for all their prayers and support throughout my studies in the United State as whole and at Cleveland State University in particular.

LYAPUNOV- BASED CONTROL OF UNBALANCED PULSE-WIDTH MODULATION BOOST TYPE RECTIFIERS

DANIEL TUMA

ABSTRACT

The three-phase pulse-width modulation (PWM) Boost Type Rectifier under balanced operating conditions exhibits instability as the resistance of the input line decreases. Under unbalanced operating conditions the PWM Boost Type Rectifier is subject to instability and severe disturbance such as distortion in the input line current, significant increase in output capacitor voltage and current ripple, generation of sub-harmonic components in the rectifier's output voltage and input current.

The objective of this research was to develop a Lyapunov based controller that could be used to improve the performance of the PWM Boost Type Rectifier under unbalanced operating conditions. By selecting the switching function as the control variable, and by utilizing Lyapunov's stability theory (direct method), a control strategy that not only eliminates sub-harmonics, but also guarantees stability was developed. The objective of this new control strategy is to cancel harmonics at the input and output of the converter and bring the system to stability while provide unity power factor with near sinusoidal input line current.

The study involves numerous computer simulations to ascertain the feasibility of the Lyapunov based controller. The models used for the verification process include: unbalanced input voltage and balanced input line impedance; balanced input voltage and unbalanced input line impedance. The results of the simulations show that the Lyapunov based controller indeed provides system stability and cancellation of harmonics at the

output and at the input of the converter at the same time. The dynamic response of the system is excellent and the input line currents are nearly sinusoidal.

TABLE OF CONTENTS

VI. Computer Simulation

Appendix

LIST OF FIGURES

LIST OF TABLES

CHAPTER I

INTRODUCTION AND STATEMENT OF THE PROBLEM

1.1. Overview of the Controllable Converter

Most power electronic circuit applications involve using power semiconductor device as a switch. The semiconductor device is either off (switch open) or on (switch closed). In the off position, the device must block or hold off in some cases a large AC or DC voltage with minimal leakage current. In the on position, the semiconductor switch will behave as a closed switch and conduct current. It will perform as an imperfect switch in that there will be junction power losses associated with the current flow. In a properly designed switching circuit the junction power losses can be reliably accommodated with good thermal design and the selection of the proper heat dissipation hardware. When operated as an efficient and fast acting switch in different circuit topologies, power semiconductors can satisfy a multitude of power conversion and control application as needed.

For instance, when operating from a fixed DC voltage source, it might be required to modulate the output voltage and power over a wide range. One method to

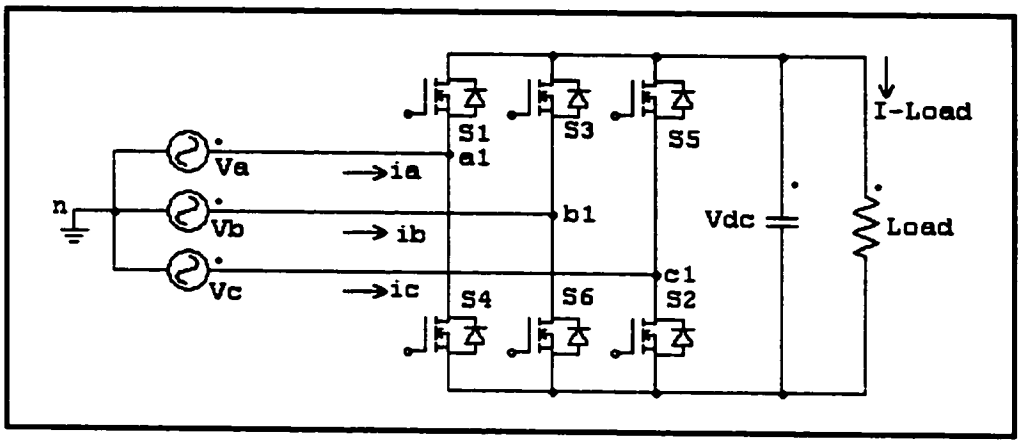

Figure 1-1.1 Three-Phase Six-Pulse Converter

Application of Kirchhoff's voltage law (VL) to any branch shows that only one diode in the upper half (S_1, S_3, S_5) of Figure 1-1.1 may conduct at any time. The conducting diode will have its anode properly biased by the phase voltage that is at its highest potential at that instant. By the same token, only one diode in the bottom half (S_4, S_6, S_2) may conduct an any one time. The conducting diode will have its cathode properly biased by the phase voltage that is at its lowest potential level at that instant. This implies that S_1 and S_4 will never conduct at the same time. Similarly, S_3 and S_6 will never conduct at the same time, and so for S_5 and S_2. The output voltage is determined by the line-to-line voltage of the source; i.e., if S_1 and S_2 are conducting, the output voltage is taken at the points a1 and c1. In total, there are six combinations of line-to-line voltages. For a three-phase voltage source, one period is 360^0, implying that line-to-line voltage transition must occur at every $360^0/6$ or 60^0 intervals. It is from this action that the six-pulse rectifier has a fundamental frequency of 6ω where ω is the source voltage frequency.

From Figure 1-1.1, the switches (thyristors) are arranged such that two of the thyristors are triggered (closed) at 60-degree intervals. That is, suppose the converter has

been on for some time and that S_1 and S_6 are conducting load current i_d. Then at theta equals zero degrees, commutation would occur and S_5 would close and start conducting, taking over from S_1. Sixty degrees later S_4 is closed and the resulting commutation transfers the load current from S_6 to S_4. This process continues indefinitely and the resulting output is a dc voltage with ripple.

As with the line-to-line voltage combinations, there are also eight switching combinations; S_1-S_2, S_1-S_6, S_2-S_3, S_3-S_4, S_4-S_5, S_5-S_6 and two zero states. It is assume that when any of the upper switches is on the corresponding lower switch is zero. Duration for each set of closed switches must be precise for the dc voltage to appear. Because conduction can be initiated at any time, it is possible to control the dc output voltage when the converter operates in a rectifier mode. As stated earlier, the three-phase six-pulse converter can be operated as a converter and as an inverter. As a converter, the switching angle lies between 0^0 and 90^0 while as an inverter, the switch angle lies 90^0 and 180^0. Normally, an optimal ac-dc converter should generate a pure dc voltage or current at unity power factor from a pure ac source. However, this is not the case in practice [2]. Traditionally the three-phase controlled rectifier has inherent problems such as a decrease in power factor and high harmonics in line current as the firing angle of the thyristors increased . Research has shown that using a PWM to operate the three-phase six-pulse converter provides a means to improve its performance.

1.2. Pulse-Width Modulation

Pulse-width modulation (PWM) provides a means to reduce the total harmonic distortion (THD) of load current in a system. In a PWM system, the amplitude of the output voltage can be controlled with the modulating waveforms. Reduced filter requirements needed to decrease harmonics and control of the output voltage amplitude are the two main advantages of the PWM. Disadvantages of the PWM include,

a). Complex control circuits

b). Increase in losses due to more frequent switching.

There are three types of control commonly used to vary the output of a converter: sinusoidal pulse-with modulation (SPWM) Figure 1-2.1, hysteresis pulse-width modulation (HPWM), Figure 1-3.1 and space-vector pulse-width modulation (SV-PWM) Figure 1-4.1. In SPWM, the control of the switches requires (a) a reference signal, sometimes called the modulating or control signal, which is a sinusoidal wave form in this case; and (b) a carrier signal, which is a triangular wave that controls the switching frequency. In general, the number of pulses per half-cycle usually ranges from 1 to 15. In SPWM control the conduction angles of the power semiconductor devices are generated by comparing a reference voltage V_r with a carrier signal V_c as shown below.

The pulse's width which is also the angle of conduction can be varied by varying the carrier voltage V_c. This control technique can be implemented using an op-amp (comparator). The input voltages to the comparator are V_r and V_c, and its output is the conduction angle δ for which the switch remains on. The modulation index M is defined as

$$M = \frac{A_c}{A_r}$$

where A_r is the peak value of the reference voltage V_r and A_c is the peak value of the carrier voltage V_c. The SPWM modulator can be used as a sub-circuit to generate control signals for the triangular reference voltage of one or more pulses per half-cycle and a dc carrier signal. The Fourier series of the PWM output waveform has a fundamental frequency that is the same as that of the reference signal. Harmonic frequencies exist at and around multiples of the switching frequency. These harmonics in some cases have relatively high amplitudes that are higher that the fundamental frequency.

Because these harmonics are located at high frequencies, a simple low ordered filter can be used to eliminate them. The amplitude modulation ratio *ma* is defined as the ratio between the reference and the carrier signals.

$$ma = \frac{V_{m,reference}}{V_{m,carrier}} = \frac{V_{m,\sin e}}{V_{m,tri}}$$

If $ma \leq 1$ the amplitude of the fundamental frequency of the output voltage, V_{out} would be linearly proportional to *ma*. That is,

$$V_{out} = maV_{dc}$$

Therefore, the amplitude of the fundamental frequency of the PWM output is, controlled by *ma*.

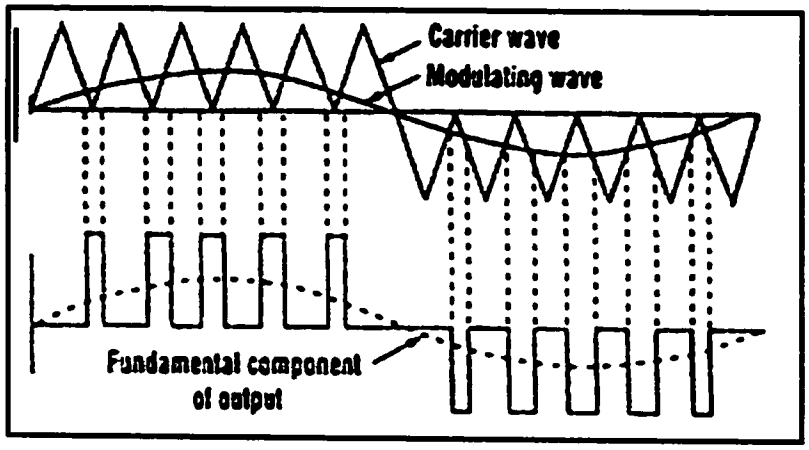

Figure 1-2.1 Sinusoidal Pulse-Width Modulation (PWM) Technique

1.3. Hysteresis PWM

Under this technique the output of the PWM is allowed to oscillate within a predetermined error band. As with sinusoidal technique, the switching instances are generated by the vertices of the high frequency triangular wave. This technique does not require any information about the characteristic of the converter. So long as the reference signal and the converter do not saturate, the output of the converter always follows the reference signal. This technique can be implemented in both digital and analog circuits.

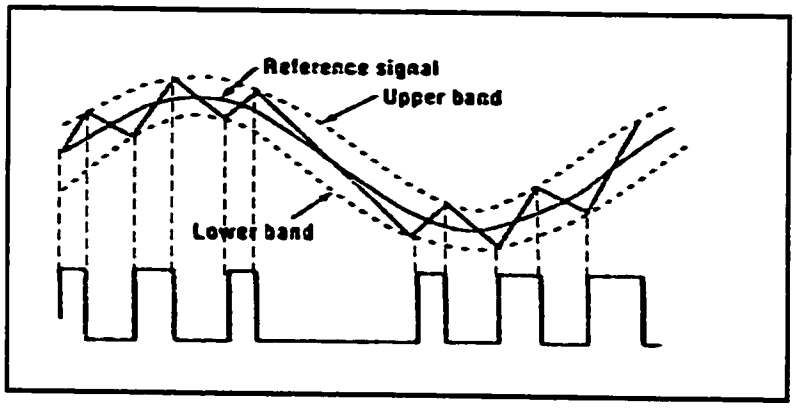

Figure 1-3.1 Hysteresis Pulse-Width Modulation (HPWM) Technique

1.4. Space-Vector PWM

This technique refers to a specific switching sequence of a three-phase voltage source converter, using space-vector to generate the converter output voltage. This technique generally has been known to generate less harmonic distortion in the converter output voltage and current. Under this control technique, the output voltage vector is approximated by using the combinations of eight switching pattern.

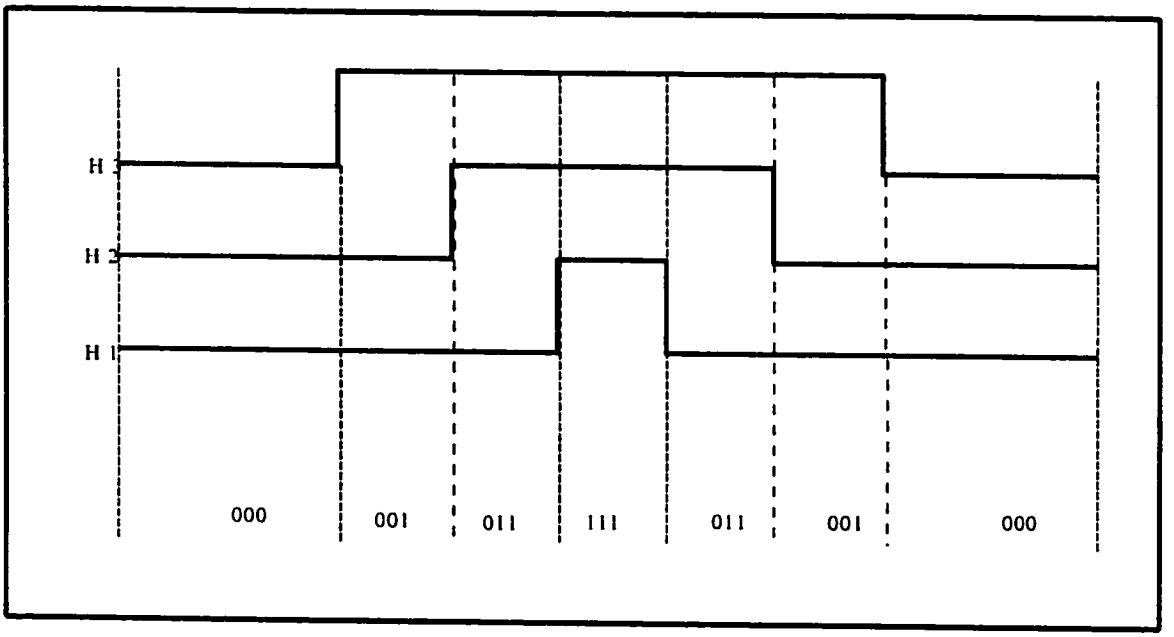

Figure 1-4.1. Symmetrical Space-Vector Pulse-Width Modulation (SV-PWM) Technique

1.5. Pulse-Width Modulation (PWM) Rectifier

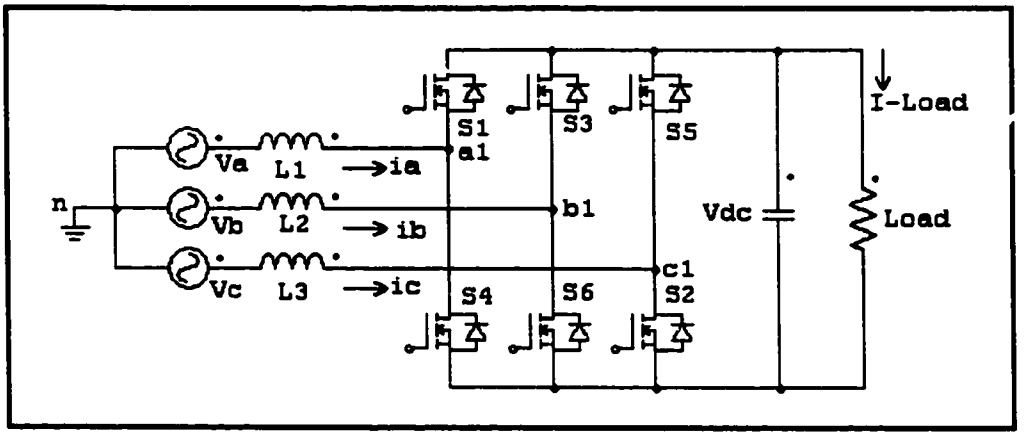

Figure 1-5.1. PWM Boost Type Rectifier.

The review of literature will indeed show that traditionally, the PWM rectifier has several advantages over the traditional phase controlled rectifier.

If Figure 1-5.1 is modified such that the load becomes a dc voltage source and the ac source becomes an induction motor, we obtain the circuit of Figure 1-5.2. which is an inverter with traditional feedback diodes. By gating the thyristors at an angle greater that 90^0 a sinusoidal voltage will be produced at the ac terminal. However, the induction motor in this case will be the three-phase ac voltage source. By properly gating the thyristors on and synchronizing them to go off in relation to the ac input, the Boost-Type PWM Regenerative Rectifier will be able to accept and deliver dc current on both a sub-cycle transient basis and on an average value basis [3]. Traditionally, regenerative PWM circuits consist of two separate rectification circuits connected in anti-parallel. With this configuration energy to the dc load is achieved by phasing off the "motoring" rectifier group of thyristors and phasing on the "generating" group which then operates as a line

commuted inverter. During ac to dc conversion traditional rectification action occurs and the feedback diodes conduct while the thyristors (though gated), carry no current. During dc to ac conversion, traditional forced commutation inverter action occurs and ac power is returned to the ac side. If there is no load but an induction motor requiring a PWM inverter, then factors such as voltage control in converters and frequency coordination become critical issues that must all be addressed

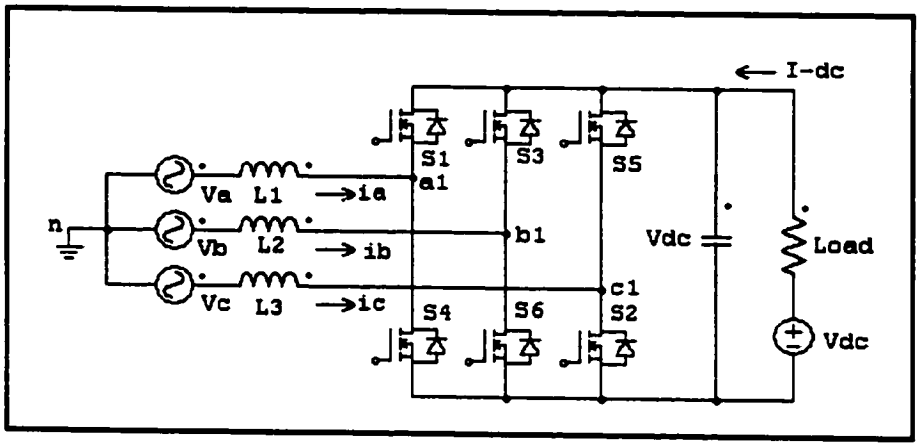

Figure 1-5.2. A Boost Type Regenerative Rectifier

The Boost-Type Regenerative Rectifier could be used to provide power to a PWM Inverter that could then be used to supply power to an induction motor. During this process, as the literature search would show, potentially disastrous harmonics (harmful to electrical equipment requiring absolute accuracy) will be generated. These harmonics, and unbalanced line voltages and impedances are the focus of this research.

1.6. Statement of the Problem

The application of a rectifier/inverter circuit to run an induction motor requires that certain parameters be known and controlled. These parameters include sudden changes in input voltage, changes in dc voltage during regeneration and with respect to the input voltage, changes in frequency, changes in line impedance, or in general, changes in system dynamics.

Unfortunately, the advantages and features of the PWM Boost-Type Rectifier are fully realized only when the three-phase input voltages are balanced and the dynamics of the converter are at steady-state. Under unbalanced conditions there exists distortion in the form of harmonics at the input and the output of the rectifier. It has been shown that in this rectifier the unbalanced input voltage causes an abnormal second order harmonic current at the dc bus, which is then reflected back to the input causing a third harmonic current to flow. This third harmonic current in turn, causes a fourth-order harmonic voltage at the output. This process continues, leading to the presence of odd harmonics in the input current and even harmonics at the dc bus voltage [4].

This research proposes a new control strategy based on Lyapunov stability theory that guarantees a sufficient stability region in state space system in the presence of large signal disturbances and sudden changes in system dynamics. To accomplish this objective, Lyapunov's direct method for nonlinear system control is utilized. Based on Lyapunov's direct method a scalar energy function (Lyapunov function) will be constructed and the variations of the function will be examined.

1.7. Proposed Objectives

The objectives of this research is to develop a control scheme based on Lyapunov's direct method that could be used to eliminate low order harmonics at both the input and output of the Boost Type PWM Rectifier under unbalanced operating conditions and at the same time, guarantee a stability region robust to system's parameter variations and independent of system dynamics. The system will then be examined in closed-loop form with the new control scheme to determined its transient response, level of harmonic distortion in the input line currents, regulation in the dc output voltage, and, if the system is globally asymptotically stable.

1.8. Outline of the Dissertation

Chapter II presents a brief review of current research important to the present research that has been done in relation to harmonics cancellation and stability control of the PWM Boost Type Rectifier. Computer simulations are presented to show that under balanced operating conditions the PWM Boost Type Rectifier contain no harmonics at it input or output. Also, computer simulations are presented to show that under unbalanced operating conditions the PWM Boost Type Rectifier there exist 3^{rd} harmonics at it input and 2^{nd} harmonics at the output of the converter.

Chapter III presents state analysis of Boost Type Rectifier under unbalanced input voltages. Steady state equations developed in section are used to determine the Lyapunov equation. Further more, equations are transformed to their *dq* quantities. Chapter III also presents a theoretical approach to harmonic cancellation in the PWM Boost Type Rectifier under unbalanced input voltages. This is accomplished by determining both the

magnitudes and phase angles of the input current and adjusting so as to eliminate low harmonics and maintain a constant dc output level. System stability is then analyzed using Lyapunov stability theorem. Equations developed in this Chapter are used to simulate the PWM Boost Type Rectifier under unbalanced conditions.

Chapter IV presents derivation of the space vector equations for the magnitudes and phases angles for the switching function. The switching technique is also presented in this section.

Chapter V presents the proposed solution and control techniques for harmonic cancellation and stability control of the PWM Boost Type Rectifier under unbalanced operating condition. Constraints for the space vector are also developed in this section.

Chapter VI presents an overview of different types of simulation packages and PSIM used to conduct simulation for this dissertation. This chapter also presents a series simulations to verify system stability and harmonics elimination under different levels of imbalance. The results of the simulations for the proposed Lyapunov based control for the unbalanced PWM Boost Type Rectifier are presented and discussed.

Finally, Chapter VII presents the concluding remarks and recommendations for future studies in this area.

CHAPTER II

LITERATURE SURVEY

Over the years, the Boost-Type Rectifier has been the main focus of researchers and engineers given its many advantages over the traditional phase-controlled thyristors rectifiers used in AC-DC and DC-AC converters. This is due primarily to the fact that conduction may be initiated at any time enabling the dc output to be varied. This Chapter examines some of the previous research conducted as related to the current research. Simulations are included to verify the theory that unwanted harmonics are generated at the output and input of the PWM boost type rectifier when operating under unbalanced conditions.

2.1. Three-Phase Pulse-Width Modulator (PMW)

The three-phase pulse-width modulator (PWM) rectifier shown in Figure 1-5.1 has the capability of dc-bus voltage control, controllable power factor with reduced current harmonics and bi-directional real power flow. In this rectifier, complete control of the voltage level at the dc bus is achievable only when the voltage at the bus is used under a balanced ac power system. The capacitor connected across the output of the converter limits the ripple current generated by the converter, thereby providing some

control to the dc bus voltage. Acting as first-order filters, the input line inductors minimize the amplitude of the line current harmonics [5], [6]. Therefore, the main objective in the control of the PWM AC/DC converters is to achieve a high power factor and minimum harmonic distortion of the line input currents. Over the years many control strategies have been proposed for this type of PWM converter. Reference [7] and [8] showed that a dc/ac converter using the PWM with phase and amplitude control (PAC) provided a good switching pattern. This control technique like many others has its disadvantage in that the reflected dc current to the ac side of the converter deteriorates the load current and voltage waveform during transient. These control methods require a dc capacitor large enough to improve or increase stability margin leading to slower transients response.

Reference [9] proposed a current controller with both a satisfactory steady-state characteristics and fast transient response. By incorporating a reference modification part with a generally used synchronous-frame proportional plus integral (PI) controller, they showed that fast transient response was achievable with a three-phase ac/dc boost type converter. These control strategies provides excellent switching pattern to reduce output voltage ripple and steady-state current harmonics but the system is assumed to be in steady-state (balanced).

Reference [10] and [11] proposed a hysteresis current control (HCC) that provided fast dynamic response, better accuracy, little or no dc offset, and robustness. Problems with the control technique include sensitivity in changes to system parameters, and uneven and random switching patterns as a result of variations in switching frequencies with respect to the dc load current. Therefore, when employing this control

strategy, the switching frequency must be fixed and the system must be in steady state. Similarly, this control method also requires a dc capacitor large enough to improve or increase stability margin leading to a slower transient response.

Reference [12] proposed a load current control method in which the output voltage of the rectifier is obtained by shifting a unique PWM patterns with respect to the input voltage of rectifier, thereby, changing the power angle and hence changing the amount of power transferred from the ac side to the dc side of the rectifier. With these circumstances they established a relation between the dc current and the input power angle that lead to zero dc voltage regulation for all load current conditions. This implies each time there is a change in load current, the power angle must be modified to maintain a constant dc voltage. Measuring the input current and the output is not required as it is with the "direct current control" method, PWM switching patterns are constant, and power angle is directly controlled by the dc load current.

Reference [13] determined that, though various control strategies proposed over the years yield various advantages and disadvantages depending on control circuit complexity, switching frequencies, and transient responses. However, these control methods had a common disadvantage in that, they did not guarantee system stability against large-signal disturbances. Based on this determination, they proposed a new control strategy based on Lyapunov stability theory that strictly guarantees a sufficient stability region in the state space for systems against large-signal disturbances. However, they assume that the input to the system is balanced.

Earlier, reference [14] and [15] had proposed Lyapunov control strategies that were for dc/dc switching converters. Reference [16] also proposed a new control strategy

for the three-phase voltage type PWM converter in which they used the state variables of an LC filter connected to the ac side of the converter as a feedback to the PWM generator. By optimizing the feedback gain, the proposed control strategy that effectively compensated the offset current, which is a major problem in the PAC control method and reduced the oscillation of the dc current and voltage waveform during transient. The research presented in this proposal differ from previous Lyapunov methods in that input voltage and line impedance are unbalanced and input line resistance is zero. I.e. $V_a(t) \neq V_b(t) \neq V_c(t)$ and $Z = 0 + jX$. This is a more difficult case given the fact that a balanced system become oscillatory as the line resistance decreases (approaching zero).

Reference [17] proposed a feed-forward control technique for eliminating harmonics in an unbalanced PWM ac-dc converter. To illustrate their technique, they computed the sequence component as they counteract the unwanted harmonics generated by the PWM gating signals. Assuming **T** as the converter transfer function given by **T** = $[SW_1, SW_2, SW_3]$ representing converter switches and v as the input voltage given by v = $[\mathbf{V_{ab}}\ \mathbf{V_{bc}}\ \mathbf{V_{ca}}]^{\mathbf{T}}$, the converter output voltage $V_0 = Tv$. Furthermore they showed that by equating the positive switch function angle α to positive sequence voltage angle θ, and, the negative sequence switching function angle λ to the negative sequence voltage β, the magnitude of the negative switching function is given by

$$A_{1n} = -A_{1p}\frac{V_{1n}}{V_{1p}} \tag{2.1.1}$$

where A_{1p} is the magnitude of the positive switching function and V_{1n} and V_{1p} are the magnitude of the negative and positive of input voltage

Reference [18] attempted to eliminate harmonics in the PWM rectifier with a technique in which they developed equations for the positive and the negative sequence separately. From these equations they obtained positive and negative sequence current commands for a constant dc bus voltage and the average zero-reactive power. That is, the dc component of the reactive is zero whereas the second order harmonic ac component may not be zero. As pointed out in later research [19], this is achievable if the positive and the negative sequence component are controlled simultaneously using two controllers. By converting the negative sequence to a positive sequence they eliminated the use of the negative sequence controller by combining the positive sequences and controlling it in the positive synchronous reference frame (SRF).

Stankovic [2] showed that the second harmonic could be eliminated from the input and the output of an unbalanced rectifier by generating unbalanced switching commands to counteract the harmonics in the system. Using symmetrical components she showed that harmonics could be eliminated from the input-output of a three-phase rectifier under unbalanced operating condition under the following conditions.

$$| S^+ || I^- | = | S^- || I^+ | \tag{2.1.2}$$

$$\Theta_s^- + \Theta_i^+ = \pi + \Theta_s^+ + \Theta_i^- \tag{2.1.3}$$

Where $| S^+ |, | S^- |, \Theta_s^+$ and Θ_s^- are the magnitudes and phase angles of the positive and negative switching functions. $| I^+ |, | I^- |, \Theta_i^+$ and Θ_i^- are the magnitudes and phase angles of the positive sequence of the input current. Using the per-phase positive and negative equivalent circuits of the rectifier.

$$ZI^+ = U^+ - V_S^+ \tag{2.1.4}$$

$$ZI^{-} = U^{-} - V_S^{-} \tag{2.1.5}$$

where V_S^{+} and V_S^{-} are the positive and negative voltages at the input of the rectifier and U^{+} and U^{-} are the positive and negative sequence of the input voltages.

$$V_S^{+} = \frac{1}{2\sqrt{2}} V_{dc} S^{+} \tag{2.1.6}$$

$$V_{S_1}^{-} = \frac{1}{2\sqrt{2}} V_{dc} S^{-} \tag{2.1.7}$$

where V_{dc} is the out dc voltage of the converter.

$$P_{dc} = \mathrm{Re}(3U^{+}I^{+} + 3U^{-}I^{-}) \tag{2.1.8}$$

Where P_{dc} is the average output dc power of the converter.

Adding equations (2.1.2, 2.1.3, 2.1.4, 2.1.5, and 2.1.8) gives

$$\frac{|S^{+}|}{|S^{-}|} = \frac{|U^{+}|}{|U^{-}|} \tag{2.1.9}$$

$$\Theta_U^{-} - \Theta_S^{-} = \Theta_U^{+} - \Theta_S^{+} \tag{2.1.10}$$

$$|S^{+}| = \frac{2\sqrt{2}\,|U^{+}|}{V_{dc}} \cos(\Theta_U^{+} - \Theta_S^{+}) \tag{2.1.11}$$

$$\sin 2(\Theta_U^{+} - \Theta_S^{+}) = \frac{2P_{dc}Z}{3(U^{+2} - U^{-2})} \tag{2.1.12}$$

which represents the steady-state solution for input-output harmonics elimination of the PWM Boost Type Rectifier under unbalanced conditions.

2.2. Symmetrical Components

From Sarma and Glover [24], zero-sequence components consisting of three-phasors with equal magnitude and with zero phase displacement are shown in Figure 2-2.1 below.

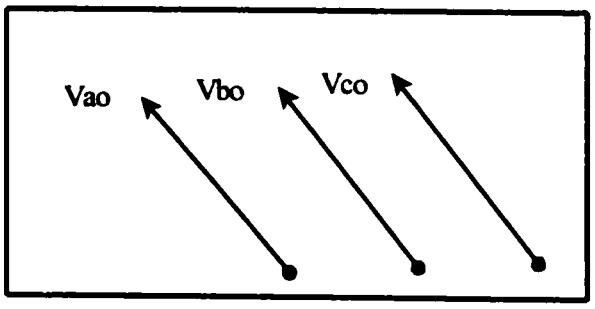

Figure 2-2.1 Zero-Sequence Components

Positive-sequence components consisting of three-phasors with equal magnitude and a $\pm 120^0$ phase displacements are shown in Figure 2-2.2 below.

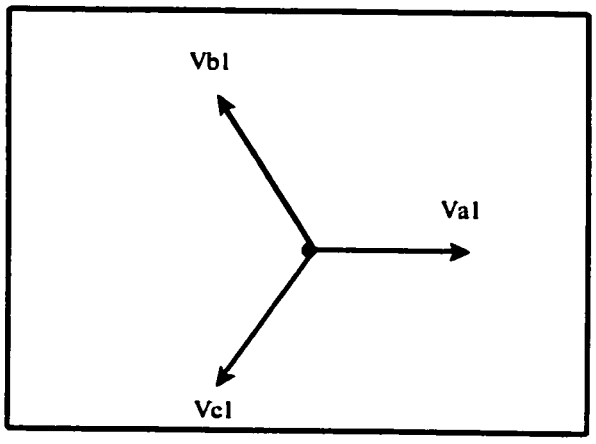

Figure 2-2.2. Positive-Sequence Components

Negative-sequence components consisting of three-phasors with equal magnitude and a $\pm 120^0$ phase displacements are shown in Figure 2-2.3 below.

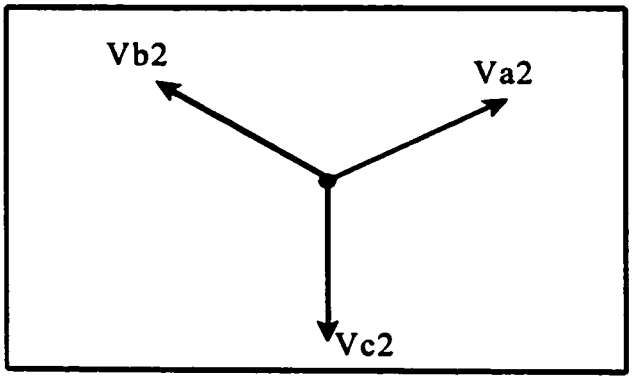

Figure 2-2.3. Negative-Sequence Components

It is common practice however, to deal with only the sequence components of phase a. i.e., V_{a0}, V_{a1}, V_{a2}. These components are then defined by the transformation

$$\begin{bmatrix} V_a \\ V_b \\ V_c \end{bmatrix} = \begin{bmatrix} 1 & 1 & 1 \\ 1 & a^2 & a \\ 1 & a & a^2 \end{bmatrix} \times \begin{bmatrix} V_{a0} \\ V_{a1} \\ V_{a2} \end{bmatrix} \tag{2.2.1}$$

where

$$a = 1\angle 120^0 = \frac{-1}{2} + j\frac{\sqrt{3}}{2} \tag{2.2.2}$$

let

$$A = \begin{bmatrix} 1 & 1 & 1 \\ 1 & a^2 & a \\ 1 & a & a^2 \end{bmatrix} \quad \text{and} \quad A^{-1} = \frac{1}{3}\begin{bmatrix} 1 & 1 & 1 \\ 1 & a & a^2 \\ 1 & a^2 & a \end{bmatrix}$$

Therefore

$$\begin{bmatrix} V_{a0} \\ V_{a1} \\ V_{a2} \end{bmatrix} = \frac{1}{3}\begin{bmatrix} 1 & 1 & 1 \\ 1 & a & a^2 \\ 1 & a^2 & a \end{bmatrix} \times \begin{bmatrix} V_a \\ V_b \\ V_c \end{bmatrix} \tag{2.2.3}$$

Equation (2.2.1) can be written as three separate equations as follows

From equation (2.2.10) and (2.2.13) it follows that

$$I_n = 3I_{a0} \tag{2.2.14}$$

In the absence of the return path through the neutral of the system, I_n is zero and the line currents contain no zero-sequence components.

Generally, a is a complex number with a unit magnitude and a 120^0 phase angle. When a phasor is multiplied by a, that phasor rotates by 120^0 counterclockwise. By the same token, when a phasor is multiplied by a^2 i.e. $((1\angle 120)\times(1\angle 120) = 1\angle 240)$, the phasor rotates by 240^0.

2.3. Boost Type PWM Rectifier under Balanced Operating Conditions

Figure 2-3.1 shows the schematic of the Boost Type Rectifier that offers the following advantages over other types of types Rectifiers that have been investigated over the years

a. instantaneous reversal of power flow

b. provides excellent input power factor characteristics

c. provides a nearly sinusoidal input current at an intermediate dc voltage with fixed polarity

Power flow between the ac input and the dc bus is controlled by adjusting the phase angle δ. When V_a is leading V_{al} real power flows from the ac input to the dc bus. Conversely when V_{al} leads V_a real power flows from the dc bus into the ac lines.

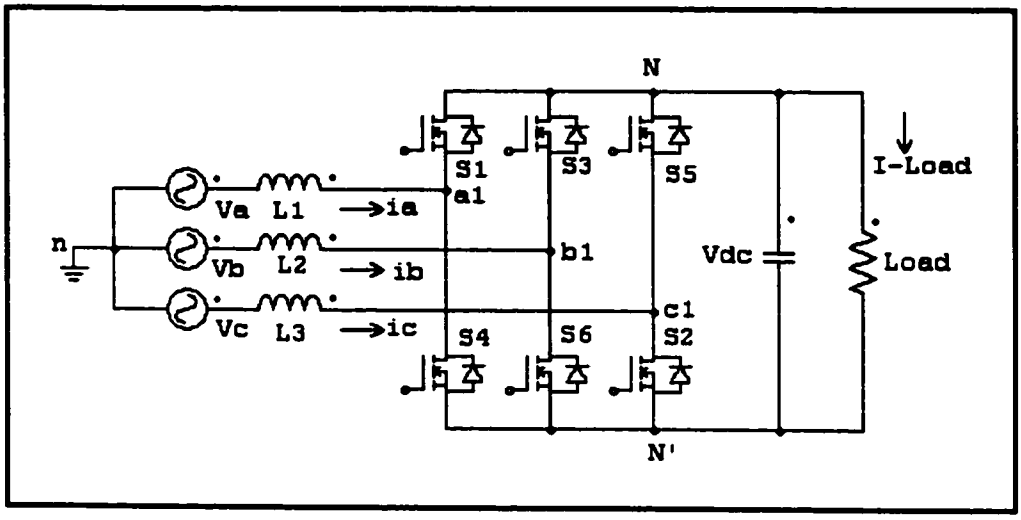

Figure 2-3.1. Boost Type PWM Rectifier

2.3.1. Analysis of the PWM under Balanced Operating Conditions

From Figure 2-3.1.1, real power transfer is determined as follow;

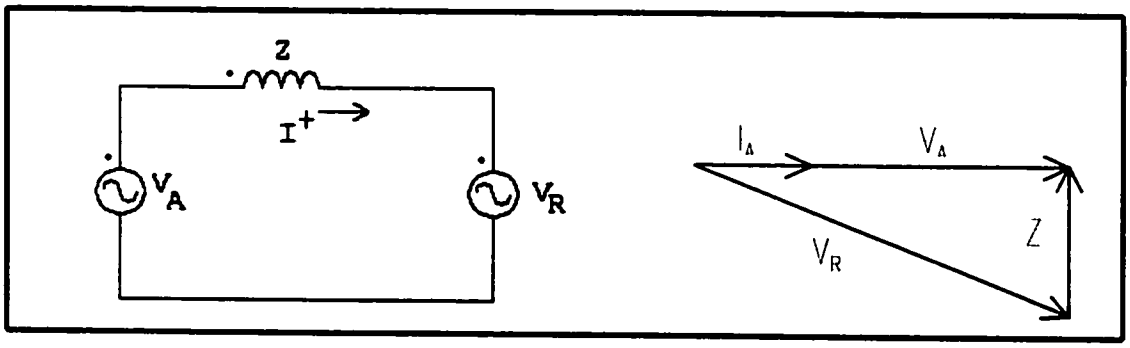

Figure 2-3.1.1 Per-Phase Equivalent circuit and Phasor Diagram for a Balanced Input Voltage

From KVL

$V_A - IZ - V_R = 0$, let $V_A = |V_A|\angle\delta$, $V_R = |V_R|\angle 0$ and $Z = |Z|\angle\theta$

Solving $I\angle\Phi$ we obtain

$$I\angle\Phi = \frac{|V_A|\angle\delta - |V_R|}{|Z|\angle\theta}$$

$$= \frac{V_A}{Z}\angle(\delta-\theta) - \frac{V_R}{Z}\angle -\theta \qquad (2.3.1.1)$$

Apparent power received is $S_R = |V_R|I^*$ and apparent power sent is $S_A = |V_A|I^*$.

Here we use the complex conjugate of I^* to allow the power flow sign convention to be consistent with the selected sign convention for the impedance. Thus

$$I^* = \frac{|V_A|}{|Z|}\angle(\theta-\delta) - \frac{|V_R|}{|Z|}\angle\theta \qquad (2.3.1.2)$$

Substituting I^* into the apparent power equation

$$S_A = |V_A|I^* = \frac{|V_A^2|}{|Z|}\angle\theta - \frac{|V_A||V_R|}{|Z|}\angle(\theta+\delta) \qquad (2.3.1.3)$$

From which

$$P_A = \frac{|V_A^2|}{|Z|}\cos\theta - \frac{+|V_A||V_R|}{|Z|}\cos(\theta+\delta) \qquad (2.3.1.4)$$

From the trigonometric identity $\cos(\beta \pm \alpha) = \cos\beta\cos\alpha \mp \sin\beta\sin\alpha$ (2.3.1.4) becomes

$$P_A = \frac{|V_A^2|}{|Z|}\cos\theta - \frac{|V_A||V_R|}{|Z|}\cos\theta\cos\delta + \frac{|V_A||V_R|}{|Z|}\sin\theta\sin\delta \qquad (2.3.1.5)$$

Let $Z = R + jX$, if R = 0 so that $\theta = 90^\circ$

$$P_A = \frac{|V_A||V_R|}{|X|}\sin\delta \qquad 2.3.1.6)$$

and

$$Q_A = \frac{|V_A||V_R|}{|X|}\cos\delta \qquad (2.3.1.7)$$

Similarly, the real power received is

$$S_R = |V_R| I^* = \frac{|V_A||V_R|}{|Z|}\angle(\theta - \delta) - \frac{|V_R^2|}{|Z|}\angle\theta \qquad (2.3.1.8)$$

From which

$$P_R = -\frac{|V_A^2|}{|Z|}\cos\theta + \frac{|V_A||V_R|}{|Z|}\cos(\theta - \delta)$$

$$P_R = \frac{|V_A||V_R|}{|Z|}\cos\theta\cos\delta + \frac{|V_A||V_R|}{|Z|}\sin\theta\sin\delta - \frac{|V_R^2|}{|Z|}\cos\theta$$

and if R << X so that $\theta \approx 90^\circ$ then P_R and Q_R can be approximated as

$$P_R = \frac{|V_R||V_A|}{|X|}\sin\delta$$

$$Q_R = \frac{|V_R||V_A|}{|X|}\cos\delta$$

Power flow in the PWM inverter is determined by the size of the load. Real power flow from the dc bus to the ac output occurs when the amplitude of the input current I_A is positive. In the regenerative mode I_A becomes negative and real power flows from the ac side to the dc bus.

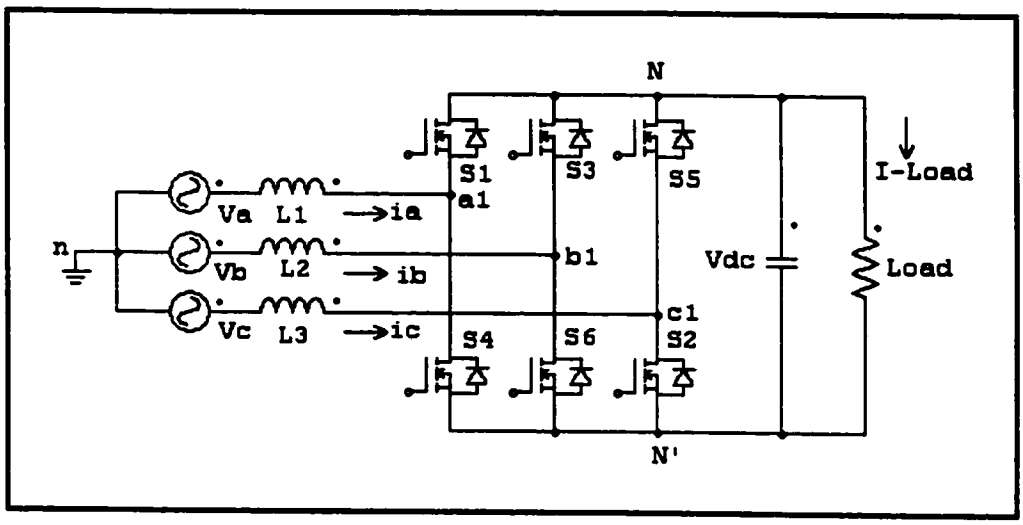

Figure 2-3.2.1. Boost Type PWM Rectifier under Balanced Condition

2.3.2. Simulation Results

To show that balanced operating conditions do not result in harmonics, the Boost Type PWM rectifier Figure 2-3.2.1 was simulated using Pspice.

The parameters are as follows:

Input voltages (peak), $V_a = 120V$, $V_b = 120V$ *and* $V_c = 120V$

Line impedance (per phase), $L1 = L2 = L3 = 1mH$

Fundamental frequency, $f = 50hz$

Output capacitor, $C = 100\mu F$

Switching frequency, f_s = 5Khz

Output load (resistive), $R = 100$ *ohms*

Figures 2-3.2.2 and 2-3.2.3 shows the balanced input voltage and the output voltage and current. A harmonic analysis shows that there is only the fundamental component of the input frequency present at the input current and no harmonics at the output of the converter.

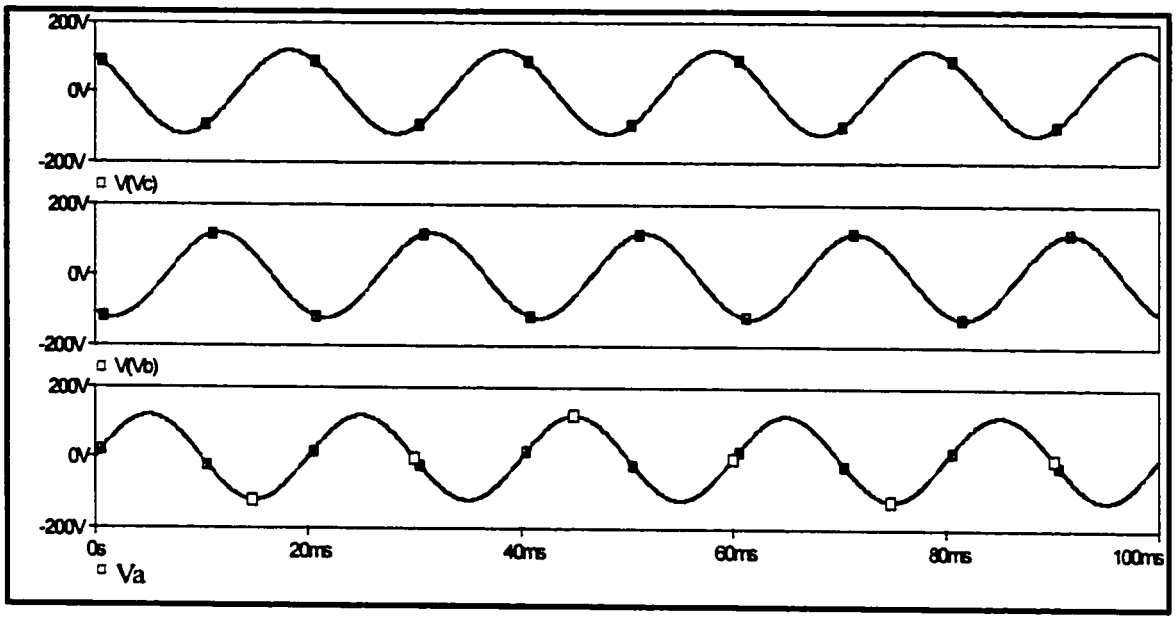

Figure 2-3.2.2. Input Voltages $V_a(t)$, $V_b(t)$ and $V_c(t)$ Balanced Condition

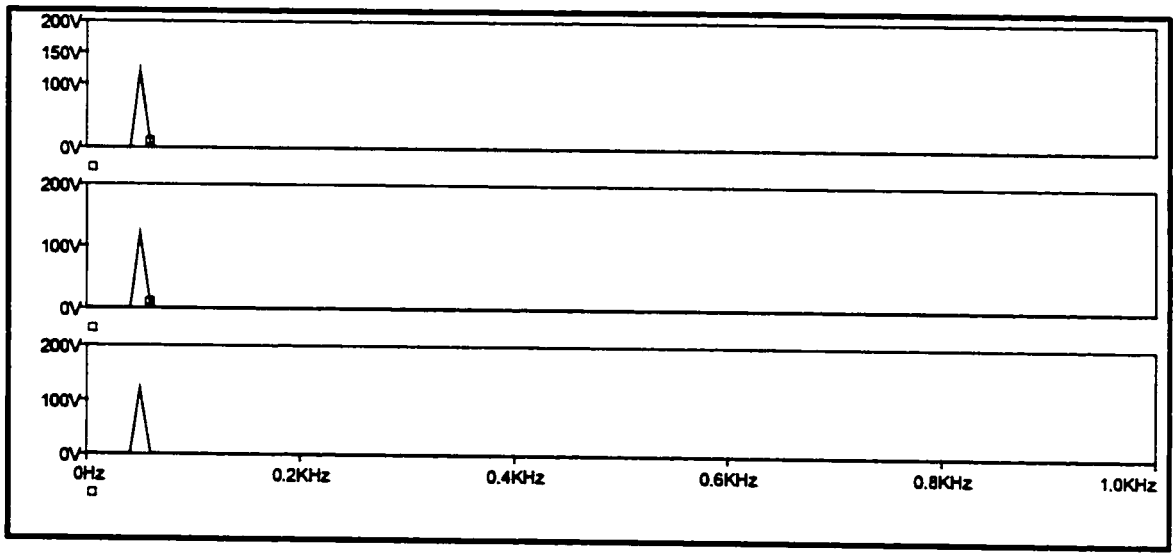

Figure 2-3.2.3. Frequency Spectrum of $V_a(t)$, $V_b(t)$ and $V_c(t)$ under Balanced Condition

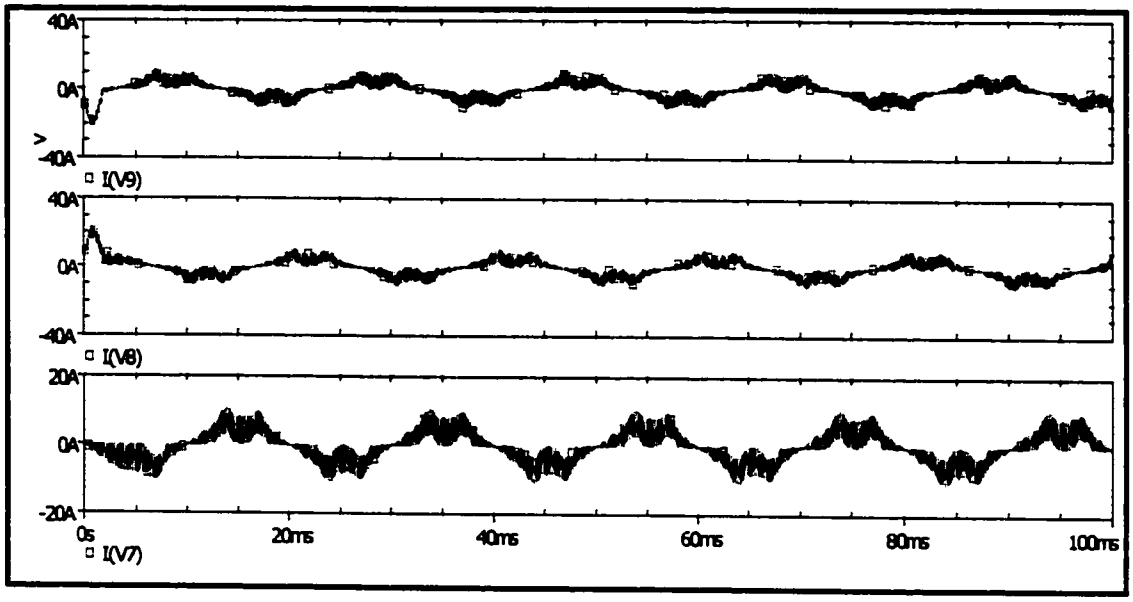

Figure 2-3.2.4. Input Line Current $I_a(t)$, $I_b(t)$ and $I_c(t)$ under Balanced Condition

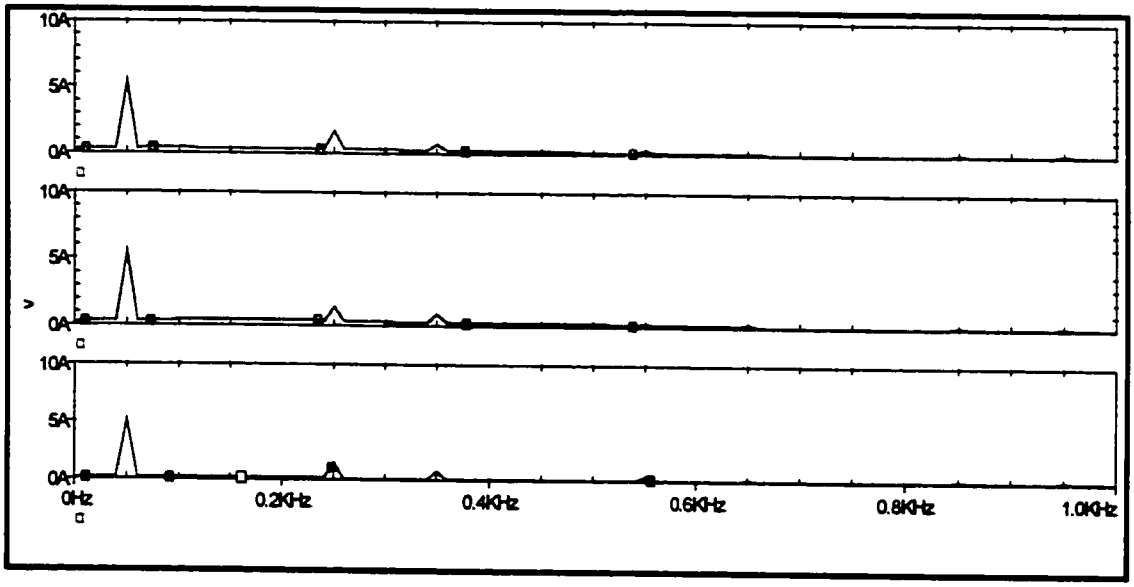

Figure 2-3.2.5. Frequency Spectrum of $I_a(t)$, $I_b(t)$ and $I_c(t)$ under Balanced Condition

Figures 2-3.2.4 and 2-3.2.5 shows the input line currents and their frequency spectrums with only the fundament component of the input voltage frequency present.

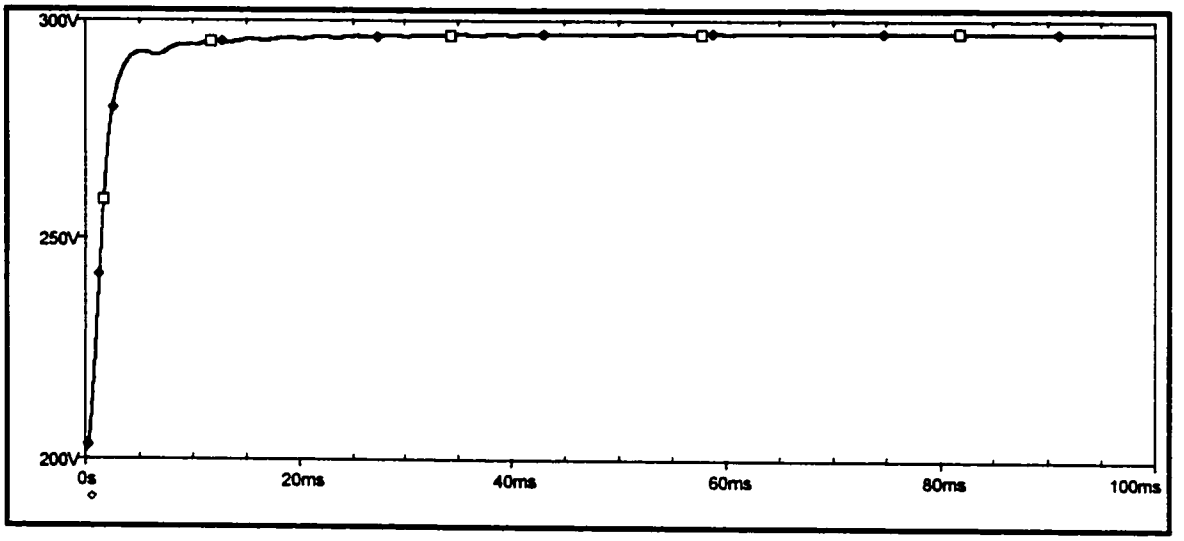

Figure 2-3.2.6. Output dc Voltage under Balanced Condition

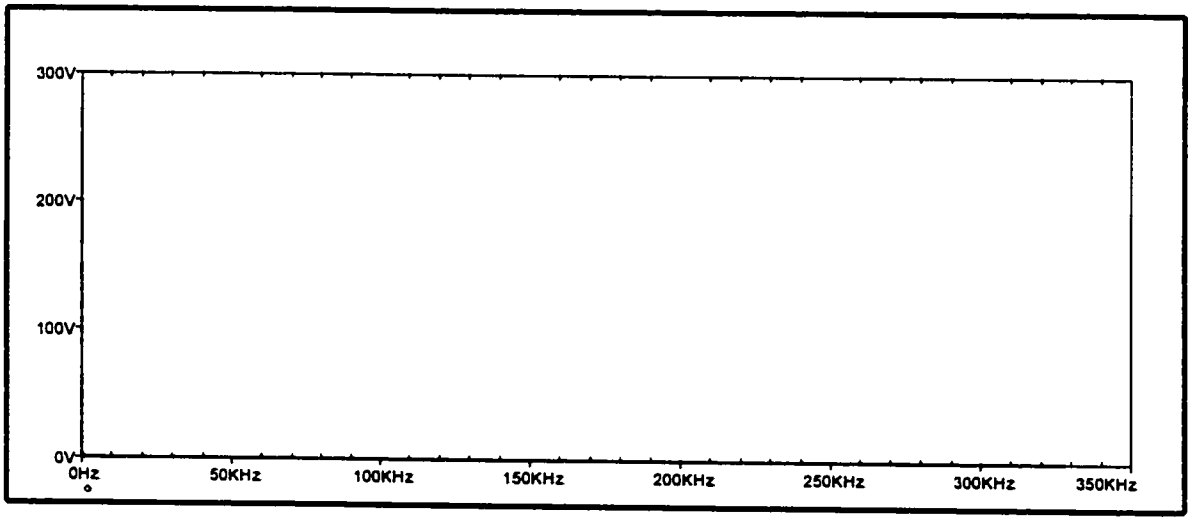

Figure 2-3.7. Frequency Spectrum of the dc Output Voltage under Balanced Condition

Figures 2-3.2.6 and 2-3.2.7 shows the output dc voltage and its frequency spectrum. As can be seen, there are no harmonics present.

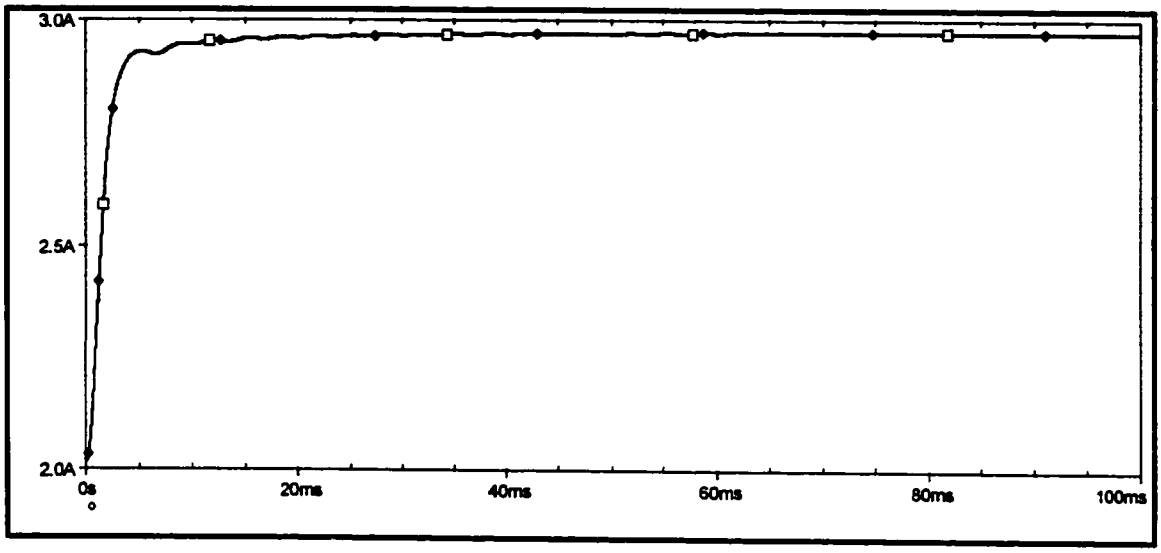

Figure 2-3.2.8. Output dc Current under Balanced Condition

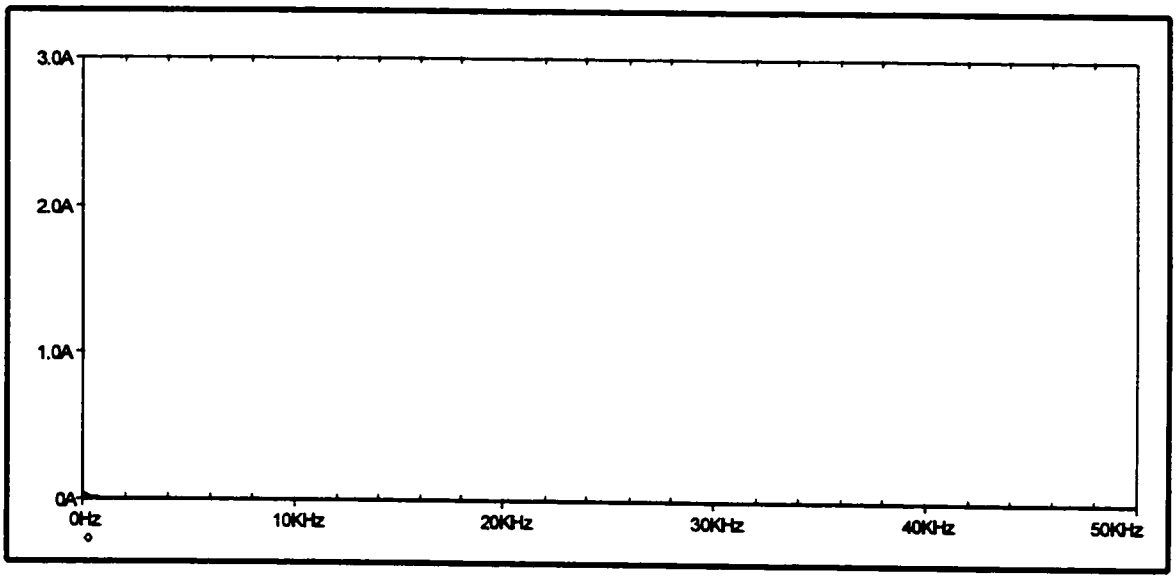

Figure 2-3.2.9. Frequency Spectrum of the dc Output voltage under Balanced Condition

Figures 2-3.2.8 and 2-3.2.9 shows the output dc current and its frequency spectrum. As can be seen, there are no harmonics present.

2.3.3. Analysis of the Boost Type PWM Rectifier under Unbalanced Operating Condition

As stated earlier, the advantages of the Boost Type PWM Rectifier are only realized when the input voltages are balanced. Under unbalanced operating conditions, harmonics of relatively low frequencies not present at the PWM switching functions appear at the dc bus voltage and at the input current. It was also shown in Chapter 2 that the output current I_o of the matrix converter is a function of the converter transfer function H and the input current vector I.

$$I_O = Hi \tag{2.3.3.1}$$

Where H is the vector of the three independent line-to-neutral switching function of the converter given as

$$H = \begin{bmatrix} Sw_1 & Sw_2 & Sw_3 \end{bmatrix} \tag{2.3.3.2}$$

and the input current vector is given by

$$i = \begin{bmatrix} i_a \\ i_b \\ i_c \end{bmatrix} \tag{2.3.3.3}$$

Therefore, the fundamental components of the phase-to-neutral switching functions (balanced) can be expressed as follows.

$$\begin{aligned} Sw_1(t) &= h_1 \sin(\omega t - \Phi) \\ Sw_2(t) &= h_2 \sin(\omega t - \Phi - 120^o) \\ Sw_3(t) &= h_3 \sin(\omega t - \Phi + 120^o) \end{aligned} \tag{2.3.3.4}$$

And the converter phase-to-neutral voltages are given by

$$V_{aln} = \frac{1}{2} V_{dc} h_1 \sin(\omega t - \Phi)$$

$$V_{bln} = \frac{1}{2} V_{dc} h_2 \sin(\omega t - \Phi - 120^o) \qquad (2.3.3.5)$$

$$V_{cln} = \frac{1}{2} V_{dc} h_3 \sin(\omega t - \Phi + 120^o)$$

Where h_1 h_2 and h_3 are the switching function and V_{dc} is the dc capacitor voltage. These equations indicate that the synthesized voltages of the rectifier are always balanced; therefore, there exist no negative sequence voltage components at its terminals. Figure 2.3.3.1 shows the negative sequence of the per phase equivalent circuits of the balanced input voltage.

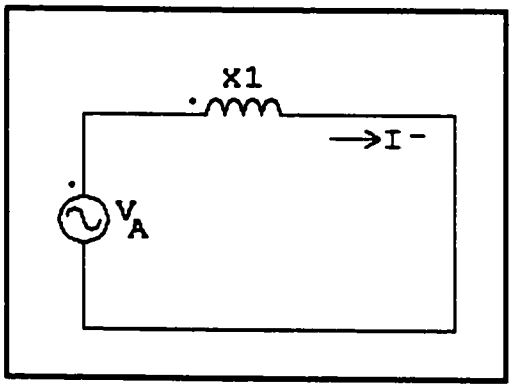

Figure 2-3.3.1. Negative Sequence Component Equivalent Circuit

As can be seen from Figure 2-3.3.1, it is apparent that the negative sequence components of the line current are limited only by the input line impedance X_l (equal to ωL) and the ac source impedance. Therefore the input currents are unbalanced and can be expressed as follow;

$$\begin{bmatrix} i_a \\ i_b \\ i_c \end{bmatrix} = \begin{bmatrix} 1 & 1 & 1 \\ 1 & a^2 & a \\ 1 & a & a^2 \end{bmatrix} \times \begin{bmatrix} I^0 \\ I^+ \\ I^- \end{bmatrix} \tag{2.3.3.6}$$

where a = $1\underline{/120^0}$ and $a^2 = 1\underline{/240^0}$ Where I^0, I^+, I^- are the zero, positive, and negative sequence input currents magnitudes. From Sarma and Glover [24], since $I_a + I_b + I_c = 0$, the negative sequence current will never flow in the circuit, i.e. $I^0 = 0$.

Similarly, the input unbalanced voltages are expressed as

$$\begin{bmatrix} V_a \\ V_b \\ V_c \end{bmatrix} = \begin{bmatrix} 1 & 1 & 1 \\ 1 & a^2 & a \\ 1 & a & a^2 \end{bmatrix} \times \begin{bmatrix} V^0 \\ V^+ \\ V^- \end{bmatrix} \tag{2.3.3.7}$$

Where V^0, V^+, V^- are the zero, positive and the negative sequence input voltages magnitudes. The fundamental components of the input currents to the rectifier in time-domain are given by

$$\begin{aligned} i_a(t) &= I_a \sin(\omega t - \alpha_1) \\ i_b(t) &= I_b \sin(\omega t - \alpha_2 - 120^o) \\ i_c(t) &= I_c \sin(\omega t - \alpha_3 + 120^o) \end{aligned} \tag{2.3.3.8}$$

From equation (2.3.3.1) the total output current is

$$I_0(t) = i_a(t)Sw_1 + i_b(t)Sw_2 + i_c(t)Sw_3$$

$$= \begin{aligned} &I_a \sin(\omega t - \alpha_1)h_1 \sin(\omega t - \Phi) + I_b \sin(\omega t - \alpha_2 - 120^0)h_2 \sin(\omega t - \Phi - 120^0) + \\ &I_c \sin(\omega t - \alpha_3 + 120^0)h_3 \sin(\omega t - \Phi + 120^0) \end{aligned}$$

From the trigonometric identity

$$\sin\beta \sin\delta = \frac{1}{2}[\cos(\beta - \delta) - \cos(\beta + \delta)]$$

$$I_0(t) = \frac{1}{2} I_a h_1 [\cos(\Phi - \alpha_1) - \cos(2\omega t - \Phi - \alpha_1)]$$
$$+ \frac{1}{2} I_b h_2 [\cos(\Phi - \alpha_2) - \cos(2\omega t - \Phi - \alpha_2 - 240)] \quad (2.3.3.9)$$
$$+ \frac{1}{2} I_c h_3 [\cos(\Phi - \alpha_3) - \cos(2\omega t - \Phi - \alpha_3 + 240)]$$

From equation (2.3.3.9) it is evident that the unbalanced input current will generate a dc fundamental and harmonics of second order. That is,

$$I_0(t) = I_{dc} + I_{2h}(2\omega t) \quad (2.3.3.10)$$

Where I_{dc} is the dc fundamental given by

$$I_{dc} = \frac{1}{2} I_a h_1 [\cos(\Phi - \alpha_1)] + \frac{1}{2} I_b h_2 [\cos(\Phi - \alpha_2)]$$
$$+ \frac{1}{2} I_c h_3 [\cos(\Phi - \alpha_3)] \quad (2.3.3.11)$$

and

$$I_{2h}(2\omega t) = -\frac{1}{2} I_a h_1 \cos(2\omega t - \Phi - \alpha_1)$$
$$-\frac{1}{2} I_b h_2 \cos(2\omega t - \Phi - \alpha_2 - 240) \quad (2.3.3.12)$$
$$-\frac{1}{2} I_c h_3 \cos(2\omega t - \Phi - \alpha_3 + 240)$$

Here we are concerned with the second order harmonic $2\omega t$, primarily for its low frequency and relatively large amplitude, which may increase significantly the ripple in the dc bus voltage. Because the second order harmonics are the result of the fundamental component of the switching function, it follows that the magnitude of this harmonic depends on the modulation index of the switching functions.

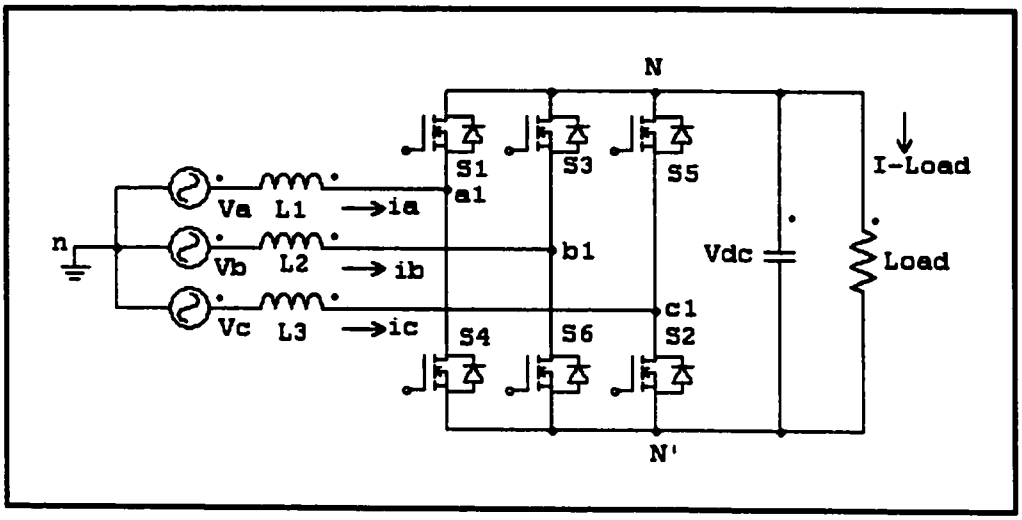

Figure 2-3.4.1. Boost Type PWM Rectifier under Unbalanced Input Voltage

2.3.4. Simulation Results

To show that unbalanced operating conditions results in harmonics at the output and the input, the Boost Type PWM rectifier Figure 2-3.4.1 was simulated using Pspice.

The parameters are as follows:

Input voltages (peak), $V_a = 100V$, $V_b = 105V$ *and* $V_c = 120V$

Line impedance (per phase), $L1 = L2 = L3 = 1mH$

Fundamental frequency, $f = 50hz$

Output capacitor, $C = 100\mu F$

Switching frequency, f_s = 5Khz

Output load (resistive), $R = 100$ *ohms*

Figures 2-3.4.2 and 2-3.4.3 shows the unbalanced input voltage and the output voltage and current. A harmonic analysis shows that, there is a second harmonic present in the output voltage of the converter and third harmonic present in the input current.

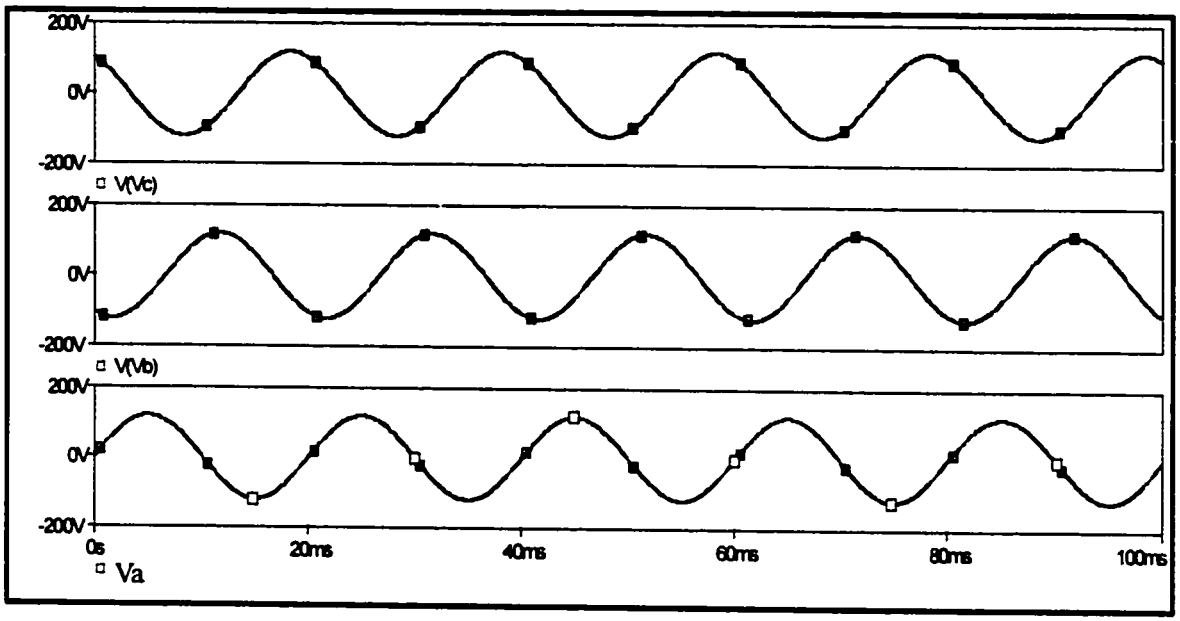

Figure 2-3.4.2. Unbalanced Input Voltages $V_a(t)$, $V_b(t)$ and $V_c(t)$

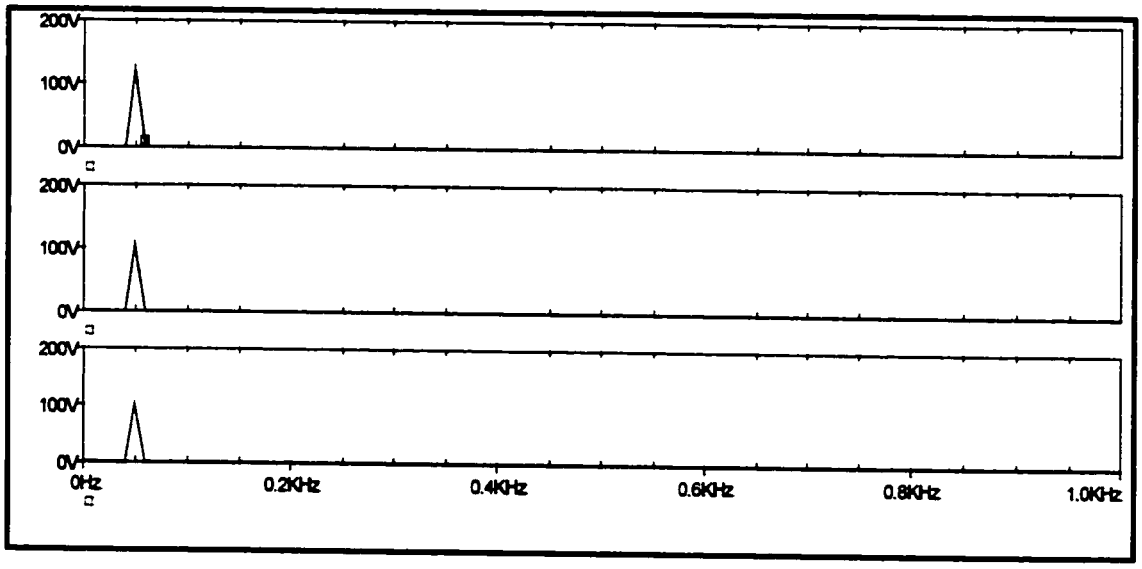

Figure 2-3.4.3. Frequency Spectrum of $V_a(t)$, $V_b(t)$ and $V_c(t)$ for Unbalanced Input Voltages

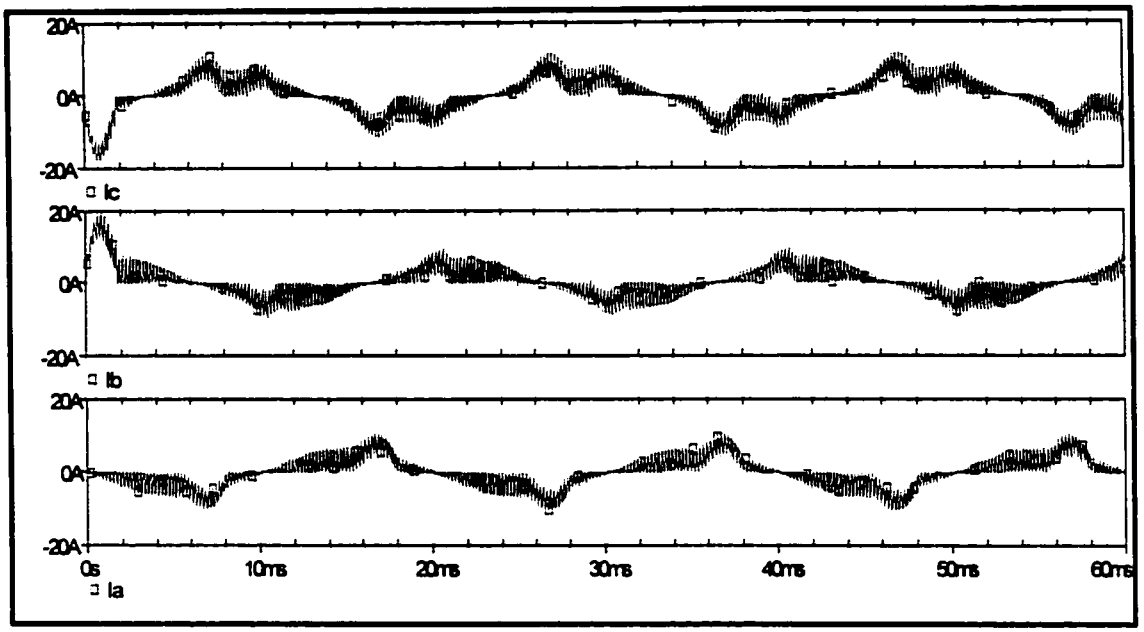

Figure 2-3.4.4 Input Line Current $I_a(t)$, $I_b(t)$ and $I_c(t)$ under Unbalanced Condition

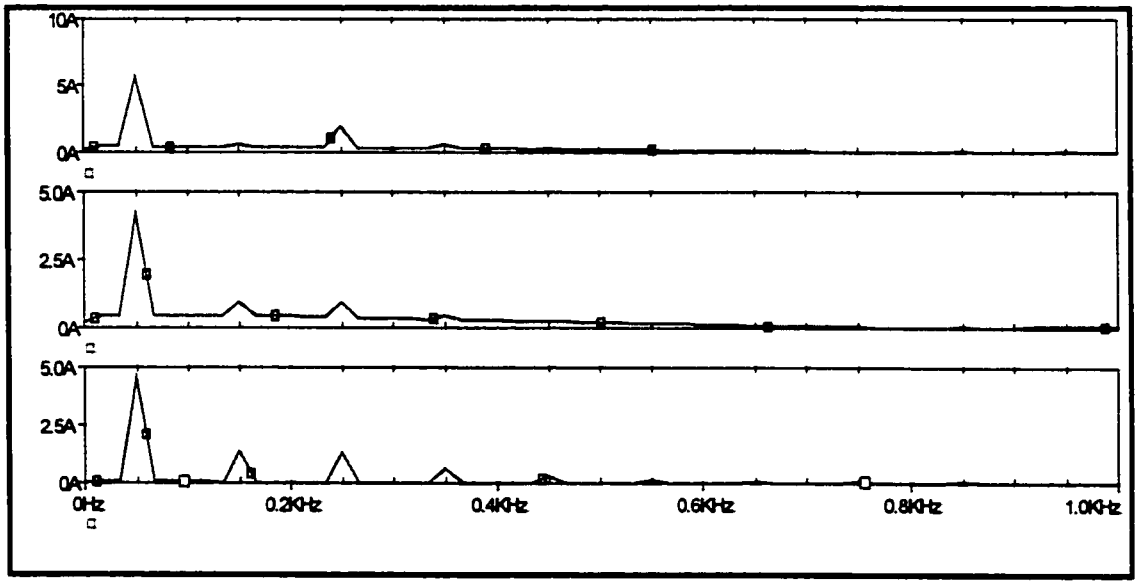

Figure 2-3.4.5 Frequency Spectrum of $I_a(t)$, $I_b(t)$ and $I_c(t)$ under Unbalanced Condition

Figures 2-3.4.4 and 2-3.4.5 represent the input current waveform under unbalanced operating conditions. The presence of the 3rd order harmonic in the frequency spectrum is a direct result of the reflected 2nd order harmonic in the output current back the input.

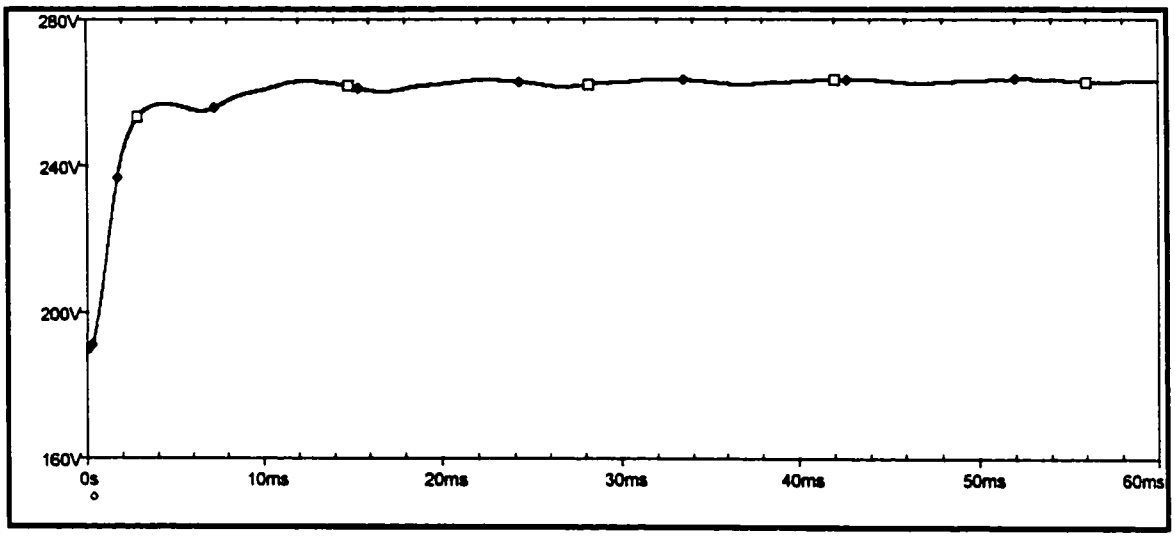

Figure 2-3.4.6. Output dc Voltage under Unbalanced Input Voltages

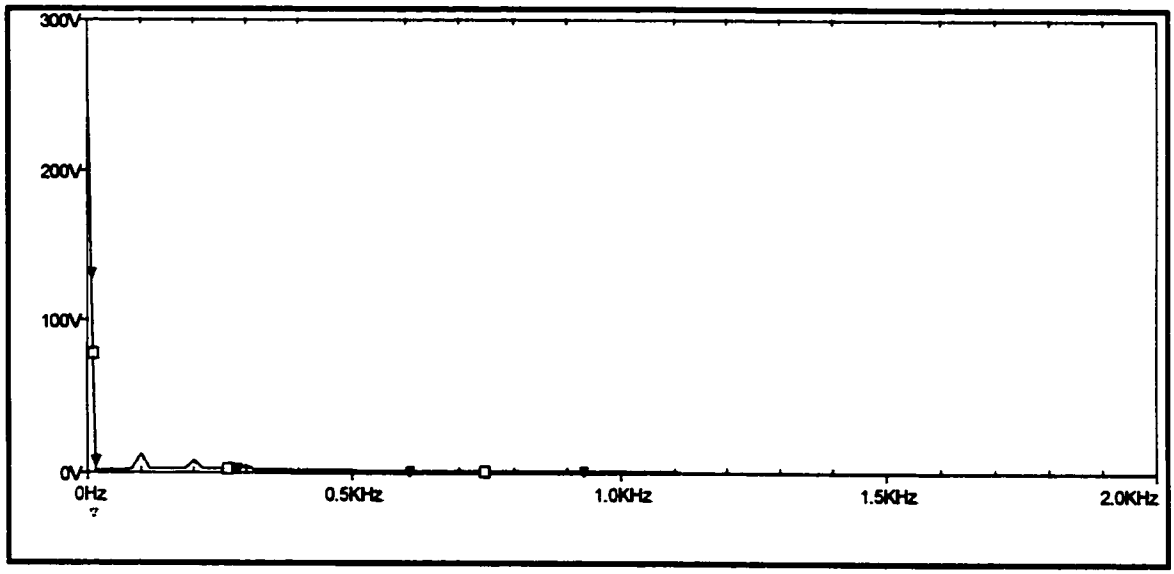

Figure 2-3.4.7. Frequency Spectrum of the dc Output Voltage under Unbalanced Input Voltages

Figure 2-3.4.6 and 2-3.4.7 shows the dc output voltage and its frequency spectrum under unbalanced operating condition. Indeed, it shows that there is 2nd harmonic present.

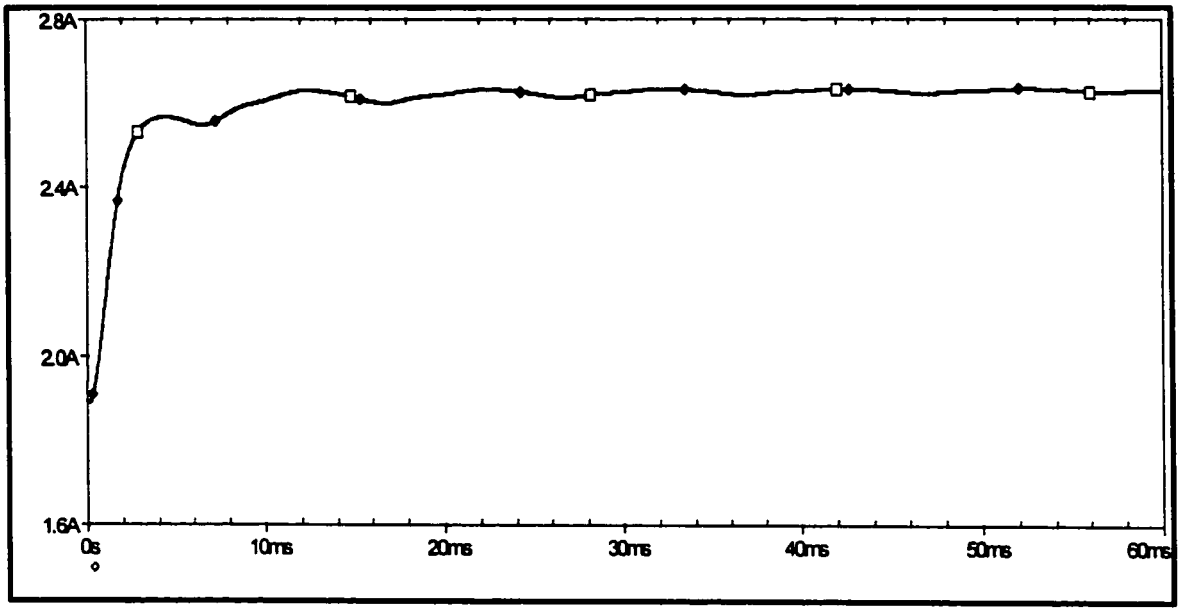

Figure 2-3.4.8 Output dc Current under Unbalanced Input Voltages

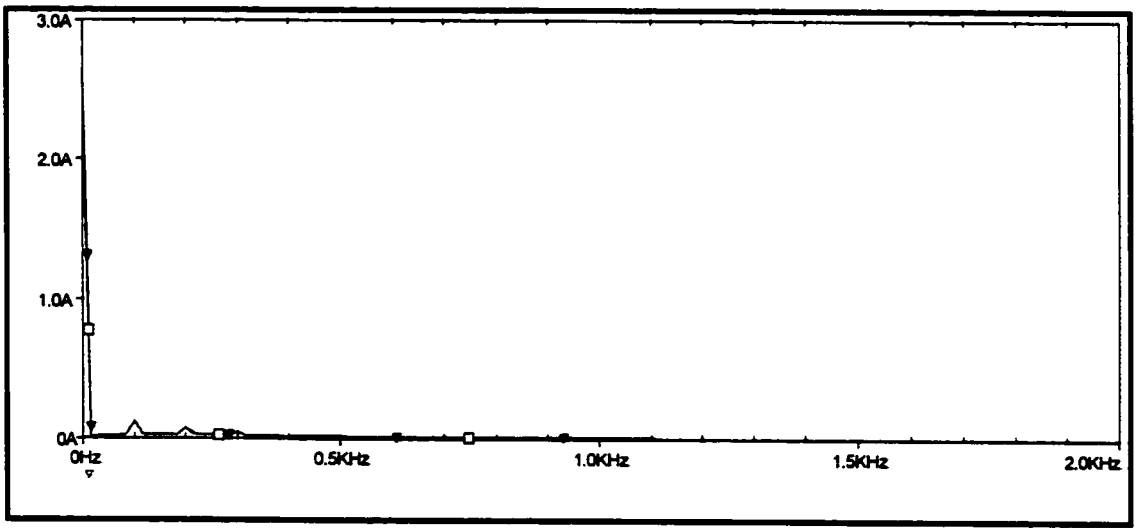

Figure 2-3.4.9. Frequency Spectrum of the dc Output Current under Unbalanced Input Voltages

Figure 2-3.4.8 and 2-3.4.9 shows the dc current output and its frequency spectrum under unbalanced operating conditions. The existence of the 2^{nd} order harmonic in the frequency spectrum is a result of the unbalanced input voltage.

CHAPTER III

METHODOLOGY AND MATHEMATICAL MODEL

Section 3.1 outlines the conditions for which the system is analyzed. These conditions are essential to the operation of the system and therefore must be observed. Section 3.2 gives the relationship between the output voltage, input voltage and the switches in a regenerative mode. Section 3.3 and 3.4 explains the relationship between the converter's input current and voltage as related to sequence components of the three-phase input voltage and the switches. Section 3.5 shows the equations for the converter phase to neutral voltage. Section 3.6 gives the input voltage and current in the stationary and the rotating frame. Section 3.7 gives the steady state analysis of the system and section 3.8 express the power equations.

3.1. Conditions for Mathematical Analysis

The system of Figure 3-1.1 is a voltage-source-type PWM rectifier. It is assumed that:

a) the system uses six bidirectional switches with capability of conducting in both direction.

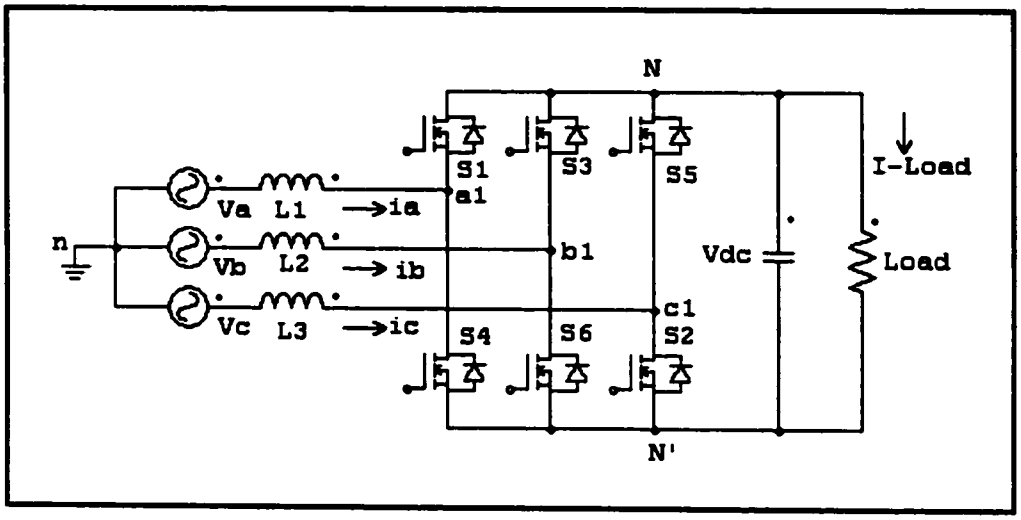

Figure 3-1.1. Voltage-Type PWM Rectifier

b) switches operate in continuous conduction mode and must be switched on and off such that the output voltage is never zero or shorted.

c) it is further assumed that the input voltages to the system are unbalanced and contain no zero sequence voltages.

3.2. Relationship between the Switches, Line-to-Neutral, and the Line-to-Line Voltages

From the dc side of the converter the relationship between the switches, line-to-neutral, and line-to-line voltages are as shown below. As shown there are eight (2^3) possible on and off switching patterns for the three Power MOSFETs that controls the output of the converter and act as feeders during regeneration (inverter). The states of the lower three Power MOSFETs are the exact opposite of the upper power MOSFETs. That is, once the switching states of the upper switches have been determined then the states of the lower switches are known.

From the dc side of the voltage in Figure 3-1.1 it follows that;

$$\begin{bmatrix} V_{ab} \\ V_{bc} \\ V_{ca} \end{bmatrix} = V_{dc} \begin{bmatrix} 1 & -1 & 0 \\ 0 & 1 & -1 \\ -1 & 0 & 1 \end{bmatrix} \times \begin{bmatrix} Sw_1 \\ Sw_2 \\ Sw_3 \end{bmatrix} \tag{3.2.1}$$

and

$$\begin{bmatrix} V_{aln} \\ V_{bln} \\ V_{cln} \end{bmatrix} = \frac{V_{dc}}{3} \begin{bmatrix} 2 & -1 & -1 \\ -1 & 2 & -1 \\ -1 & -1 & 2 \end{bmatrix} \times \begin{bmatrix} Sw_1 \\ Sw_2 \\ Sw_3 \end{bmatrix} \tag{3.2.2}$$

3.3. Converter Input Voltages

Application of symmetric component theory would shows that the line-to-neutral input voltages to the system are given by

$$\begin{bmatrix} V_{an} \\ V_{bn} \\ V_{cn} \end{bmatrix} = \begin{bmatrix} 1 & 1 & 1 \\ 1 & a^2 & a \\ 1 & a & a^2 \end{bmatrix} \times \begin{bmatrix} V^0 \\ V^p \\ V^n \end{bmatrix} \tag{3.3.1}$$

Where V^0, V^p, V^n are the zero, positive and the negative sequence input voltages.

Further simplification of equation (3.3.1) gives the following.

$$V_{an}(t) = |V^0| \sin(\omega t + \theta_v^0) + |V^p| \sin(\omega t + \theta_v^p) + |V^n| \sin(\omega t + \theta_v^n) \tag{3.3.2}$$

$$V_{bn}(t) = |V^0| \sin(\omega t + \theta_v^0) + |V^p| \sin(\omega t + \theta_v^p + \frac{4\pi}{3}) + |V^n| \sin(\omega t + \theta_v^n + \frac{2\pi}{3}) \tag{3.3.3}$$

$$V_{cn}(t) = |V^0| \sin(\omega t + \theta_v^0) + |V^p| \sin(\omega t + \theta_v^p + \frac{2\pi}{3}) + |V^n| \sin(\omega t + \theta_v^n + \frac{4\pi}{3}) \tag{3.3.4}$$

These equations will be used later to develop the space vector for the PWM.

3.4. Converter Input Current

The converter input current vector is given by,

$$\bar{I} = \begin{bmatrix} I_a \\ I_b \\ I_c \end{bmatrix} = \begin{bmatrix} 1 & 1 & 1 \\ 1 & a^2 & a \\ 1 & a & a^2 \end{bmatrix} \times \begin{bmatrix} I^0 \\ I^p \\ I^n \end{bmatrix} \tag{3.4.1}$$

Where I^0, I^p, I^n are the zero, positive, and negative sequence input current. As stated earlier in Chapter II, since the zero sequence current doesn't flow in the circuit, i.e. $I^0 = 0$. Equation (3.4.1) becomes

$$\begin{bmatrix} I_a \\ I_b \\ I_c \end{bmatrix} = \begin{bmatrix} 1 & 1 & 1 \\ 1 & a^2 & a \\ 1 & a & a^2 \end{bmatrix} \times \begin{bmatrix} 0 \\ I^p \\ I^n \end{bmatrix} \tag{3.4.2}$$

where a is as defined previously.

In this case the positive and negative sequence currents are

$$I_a(t) = |I^p| \sin(\omega t + \theta_i^p) + |I^n| \sin(\omega t + \theta_i^n) \tag{3.4.3}$$

$$I_b(t) = |I^p| \sin(\omega t + \theta_i^p - \frac{2\pi}{3}) + |I^n| \sin(\omega t + \theta_i^n + \frac{2\pi}{3}) \tag{3.4.4}$$

$$I_c(t) = |I^p| \sin(\omega t + \theta_i^p + \frac{2\pi}{3}) + |I^n| \sin(\omega t + \theta_i^n - \frac{2\pi}{3}) \tag{3.4.5}$$

As stated earlier, the output current I_0 of the converter is a function of the converter switching function H and the input current vector I i.e.,

$$I_O = Hi \tag{3.4.6}$$

Where H is the vector of the three independent line-to-neutral switching function of the converter given as,

$$H = [Sw_1 \quad Sw_2 \quad Sw_3] \tag{3.4.7}$$

$$\begin{bmatrix} Sw_1 \\ Sw_2 \\ Sw_3 \end{bmatrix} = \begin{bmatrix} 1 & 1 & 1 \\ 1 & a^2 & a \\ 1 & a & a^2 \end{bmatrix} \times \begin{bmatrix} 0 \\ h^p \\ h^n \end{bmatrix} \tag{3.4.8}$$

Where h^p and h^n, are the positive, and negative sequence of the switching function. An expansion of equation (3.4.8) gives the sequence components of the switching function as follows.

$$Sw_1(t) = |h^p|\sin(\omega t + \theta_h^p) + |h^n|\sin(\omega t + \theta_h^n) \tag{3.4.9}$$

$$Sw_2(t) = |h^p|\sin(\omega t + \theta_h^p - \frac{2\pi}{3}) + |h^n|\sin(\omega t + \theta_h^n + \frac{2\pi}{3}) \tag{3.4.10}$$

$$Sw_3(t) =) \ |h^p|\sin(\omega t + \theta_h^p + \frac{2\pi}{3}) + |h^n|\sin(\omega t + \theta_h^n + \frac{2\pi}{3}) \tag{3.4.11}$$

So, the total output current is

$$I_0(t) = I_a Sw_1 + I_b Sw_2 + I_c Sw_3 \tag{3.4.12}$$

$$=(h^p + h^n)\times(I^p + I^n) + (a^2 h^p + a h^n)$$

$$=(ah^p + a^2 h^n)\times(aI^p + aI^n) + (a^2 I^p + aI^n) = 3h^p I^n + 3h^n I^p \tag{3.4.13}$$

As it was shown earlier, equation (3.4.13) becomes;

$$I_0(t) = 3\times h^p \times e^{j\omega t} \times e^{j\theta_h^p} \times I^n \times e^{j\omega t} \times e^{j\theta_i^n} + 3\times h^n \times e^{j\omega t} \times e^{j\theta_h^n} \times I^n \times e^{j\omega t} \times e^{j\theta_i^p}$$

$$= 3|h^p||I^n|\cos(\omega t + \theta_h^p)\cos(\omega t + \theta_i^n) + 3|h^n||I^n|\cos(\omega t + \theta_h^n)\cos(\omega t + \theta_i^p) \tag{3.4.14}$$

An application of the trigonometric identity $\cos(\alpha)\cos(\beta) = \frac{1}{2}[\cos(\alpha+\beta) + \cos(\alpha-\beta)]$ to equation (3.4.14) gives a dc component and a second harmonic quantity as

$$I_0(2\omega t) = \frac{3}{2}|h^p||I^n|\cos(2\omega t + \theta_h^p + \theta_i^n) + \frac{3}{2}|h^n||I^p|\cos(2\omega t + \theta_h^n + \theta_i^p) \tag{3.4.15}$$

where $|h^p|,|h^n|,\theta_h^p,\theta_h^n$ are the magnitudes and phase angles of the switching functions and $|I^p|,|I^n|,\theta_i^p,\theta_i^n$ are the magnitudes and phase angles of sequence current components.

Similar calculations have been done in [2].

3.5. Converter Phase-to- Neutral Voltages

The converter phase-to-neutral voltages are given by,

$$\overline{V} = [V_{aln} \quad V_{bln} \quad V_{cln}]^T \tag{3.5.1}$$

The pole voltages at the input of the converter are given by

$$V_{a_1N} = \frac{1}{2}V_{dc}h_1 \sin(\omega t - \Phi) + \frac{1}{2}V_{dc}$$

$$= \frac{1}{2}[h_1 \sin(\omega t - \Phi) + 1]V_{dc} \tag{3.5.2}$$

$$V_{b_1N} = \frac{1}{2}V_{dc}h_1 \sin(\omega t - \Phi - 120^o) + \frac{1}{2}V_{dc}$$

$$= \frac{1}{2}[h_1 \sin(\omega t - \Phi - 120^o) + 1]V_{dc} \tag{3.5.3}$$

$$V_{c_1N} = \frac{1}{2}V_{dc}h_1 \sin(\omega t - \Phi + 120^o) + \frac{1}{2}V_{dc}$$

$$= \frac{1}{2}[h_1 \sin(\omega t - \Phi + 120^o) + 1]V_{dc} \tag{3.5.4}$$

These equations indicate that the synthesized voltages of the rectifier are always balanced; and therefore, no negative sequence voltage components exist at its terminals.

3.6. *d-q* Frame Transformation

Generally, for modeling and control design it very convenient to transform three-phase variables of the input voltage, current, and, switching functions to a ***d-q*** rotating frame. From Figure 3-1.1 an application of KVL to each phase shows that the voltage equations are

$$V_a = L_1 \frac{di_a}{dt} + V_{a_1 n} \tag{3.6.1}$$

$$V_b = L_2 \frac{di_b}{dt} + V_{b_2 n} \tag{3.6.2}$$

$$V_c = L_3 \frac{di_c}{dt} + V_{c_3 n} \tag{3.6.3}$$

In the stationary ***d-q*** reference frame the voltages are

$$V_d^S = L \frac{di_d^S}{dt} + V_d^S \tag{3.6.4}$$

$$V_q^S = L \frac{di_q^S}{dt} + V_q^S \tag{3.6.5}$$

In an unbalanced three-phase system, only the positive and the negative sequence fundamental components are present. This is because the presence of a negative sequence component would cause variation in both the magnitude and angular frequency in the input voltage vector. Without the zero sequence voltage the positive and the negative sequences can be written

$$V_{dqs} = V_{dq}^p e^{j\omega t} + V_{dq}^n e^{-j\omega t} \tag{3.6.6}$$

where

$$V_{dqs} = \frac{2}{3}\left[V_a + V_b e^{j2\pi/3} + V_c e^{-j2\pi/3}\right] \tag{3.6.7}$$

and

$$V_{dq}^{p} = V_{d}^{p} + jV_{q}^{p} \tag{3.6.8}$$

$$V_{dq}^{n} = V_{d}^{n} + jV_{q}^{n} \tag{3.6.9}$$

Similarly,

$$I_{dqs} = I_{dq}^{p} e^{j\omega t} + I_{dq}^{n} e^{-j\omega t} \tag{3.6.10}$$

The terms $V_{d}^{p} e^{j\omega t}$, $V_{q}^{p} e^{j\omega t}$ indicate counterclockwise rotation and represent the positive sequence and the terms $V_{d}^{p} e^{-j\omega t}$, $V_{q}^{p} e^{-j\omega t}$ indicate clockwise rotation and represent the negative sequence.

Generally, the terms $\omega LI_{d}^{n}, \omega LI_{q}^{p}, -\omega LI_{d}^{p}, -\omega LI_{q}^{n}$ are inserted to de-coupled *d-q* dynamics. In the synchronous reference frame equations (3.6.1 – 3.6.3)

$$V_{d}^{p} = L\frac{dI_{q}^{p}}{dt} + \omega LI_{q}^{p} + V_{pd}^{p} \tag{3.6.11}$$

$$V_{q}^{p} = L\frac{dI_{d}^{p}}{dt} - \omega LI_{d}^{p} + V_{pq}^{p} \tag{3.3.12}$$

$$V_{d}^{n} = L\frac{dI_{q}^{n}}{dt} - \omega LI_{q}^{n} + V_{pd}^{n} \tag{3.6.13}$$

$$V_{q}^{n} = L\frac{dI_{d}^{n}}{dt} + \omega LI_{d}^{n} + V_{pq}^{n} \tag{3.6.14}$$

Therefore, the differential equation for the dc side of the rectifier can be written as

$$C\frac{dv_{dc}}{dt} = I_{0} - I_{L} = \frac{3}{4}(h_{d}i_{d} + h_{q}i_{q}) - I_{L} \tag{3.6.17}$$

With the switching functions as control variables, equations (3.6.11), (3.6.12), (3.6.13), (3.6.14) and (3.6.17) are nonlinear function of the system.

3.7. Steady State Analysis

At steady state it is desired that a unity power factor be obtain, i.e, I_q should be equal to zero, implying that V_q is equal to zero. Controlling I_q to zero implies I_d equals line current $I_{(max)}$. Controlling I_q and V_q to zero implies that harmonics in the system must be eliminated. Harmonics can be eliminated in a system with unbalanced input voltage balanced line impedance by generating unbalanced switching functions of equal magnitude and phase but with a change in sign of the harmonics generated by the system.

The counter-action between the two unwanted component will cancel each other. Therefore bringing the system to steady state.

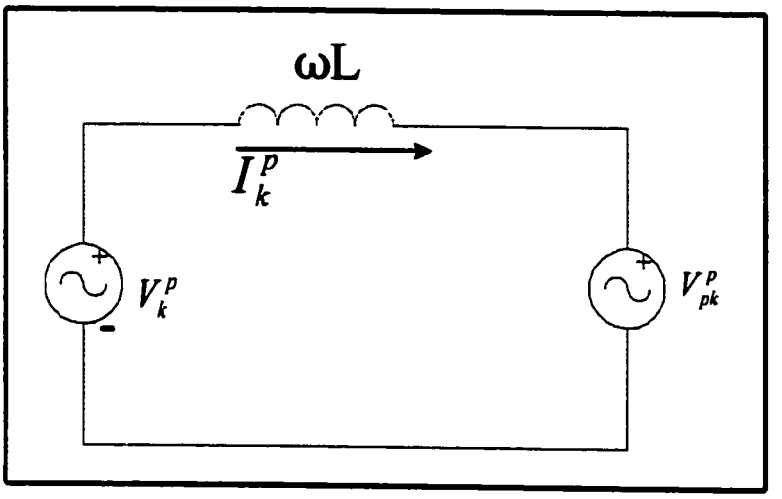

Figure 3-7.1. Per-Phase Representation of the positive Sequence Voltage

From Figure 3-7.1, let

$$\omega L = \frac{V_k^p - V_{pk}^p}{I_k^p} \text{ or } \omega L I_k^p = V_k^p - V_{pk}^p \qquad (3.7.1)$$

Where k = *input voltage phase a, b, or c,*

V_{pk}^{p} = the positive sequence phase converter pole voltage

Then in *d-q* frame

$$V_k^p = L\frac{di_q^p}{dt} + \omega L i_q^p + V_{pd}^p \tag{3.7.2}$$

and the positive sequences of pole voltages V_{pk}^{p} are

$$V_{pa}^p = \frac{1}{2} V_{dc} h_1^p \sin(\omega t - \theta_{h1}) \tag{3.7.4}$$

$$V_{pb}^p = \frac{1}{2} V_{dc} h_3^p \sin(\omega t - \theta_{h_2} - 120^0) \tag{3.7.5}$$

$$V_{pc}^p = \frac{1}{2} V_{dc} h_2^p \sin(\omega t - \theta_{h_1} + 120^0) \tag{3.7.6}$$

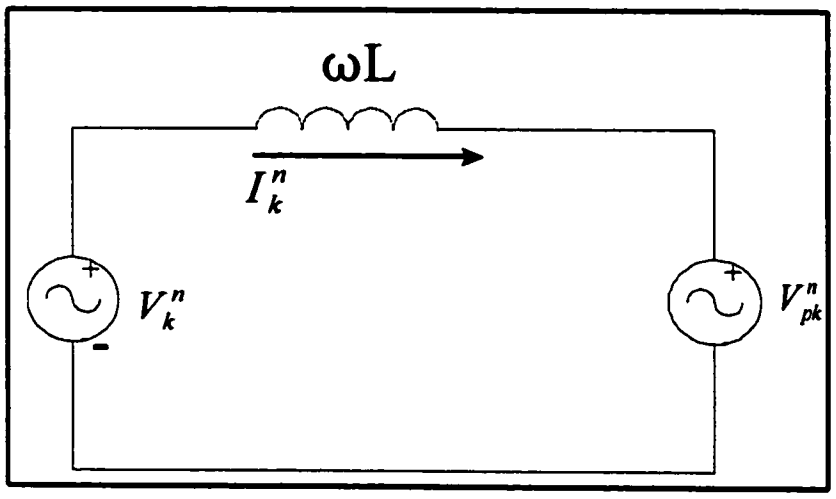

Figure 3-7.2. Per-Phase Representation of the Negative Sequence Voltage

From Figure 3-7.2, let

$$\omega L = \frac{V_k^n - V_{pk}^n}{I_k^n} \text{ or } \omega L I_k^n = V_k^n - V_{pk}^n \tag{3.7.6}$$

Where k =*input voltage phase a, b, or c*

V_{pk}^{n} = the negative sequence converter pole voltage

Then in *d-q* frame

$$V_k^n = L\frac{di_d^n}{dt} + \omega L i_d^n + V_{pd}^n \tag{3.7.7}$$

and the negative sequences of pole voltages V_p are

$$V_{pa}^n = \frac{1}{2}V_{dc}h_1^n \sin(\omega t - \theta_{h1}) \tag{3.7.8}$$

$$V_{pb}^n = \frac{1}{2}V_{dc}h_2^n \sin(\omega t - \theta_{h_2} - 120^0) \tag{3.7.9}$$

$$V_{pc}^n = \frac{1}{2}V_{dc}h_3^n \sin(\omega t - \theta_{h_3} + 120^0) \tag{3.7.10}$$

The input sequence voltages are given by equations (3.3.2,3.3.3, and 3.3.4).

Based on these equation and equation (3.4.3, 3.4.4 and 3.4.5) the average Dc power can be written as

$$P_{dc} = 3[V_a^p I_a^p + V_a^n I_a^n + V_b^p I_b^p + V_b^n I_b^n + V_c^p I_c^p + V_c^n I_c^n]$$

The controller that will be designed later will utilized a reference voltage V_{ref} to force the dc output voltage to stay at a constant value. At steady state let h_{q0} and h_{d0} be the value of the switching function.

Then equation (3.7.2), (3.7.7), and (3.6.17) can be written as follows.

$$V_k = \frac{1}{2}h_{d0}V_{ref}$$

$$2V_k = h_{d0}V_{ref} \tag{3.7.11}$$

$$0 = \omega L I_{\max} + \frac{1}{2}h_{q0}V_{ref}$$

$$0 = 2\omega L I_{\max} + h_{q0} V_{ref} \tag{3.7.12}$$

$$I_L = \frac{3}{4} h_{d0} I_{\max} \tag{3.7.13}$$

From equations (3.7.11) and (3.7.12),

$$h_{d0} = \frac{2V_k}{V_{ref}} \tag{3.7.14}$$

$$h_{q0} = \frac{-2\omega L I_{\max}}{V_{ref}} \tag{3.7.15}$$

Substituting (3.7.14) into (3.7.13),

$$I_L = \frac{3V_k I_{\max}}{2V_{ref}} \tag{3.7.16}$$

From equation (3.7.16),

$$I_{\max} = \frac{2V_{ref} I_L}{3V_k} \tag{3.7.17}$$

3.8. Power in Unbalanced Three-Phase Systems

With unbalanced input voltage, apparent power S is given by;

$$V_{dqs} \times I^*_{dqs} =$$

$$\left(V^p_{pd} e^{j\omega t} + V^n_{dq} e^{-j\omega t}\right) * \left(I^p_{dq} e^{j\omega t} + I^n_{dp} e^{-j\omega t}\right)^* \tag{3.8.1}$$

Thus for the apparent power $S = P + jQ$,

we can obtain real power P and reactive power Q such that [18]

$$P(t) = P_0 + P_1 \cos 2\omega t + P_2 \sin 2\omega t \tag{3.8.2}$$

$$Q(t) = Q_0 + Q_1 \cos 2\omega t + Q_2 \sin 2\omega t \tag{3.8.3}$$

Where

$$P_0 = \frac{3}{2}\left(V_d^p I_d^p + V_q^p I_q^p + V_d^n I_d^n + V_q^n I_q^n\right)$$

$$P_1 = \frac{3}{2}\left(V_d^n I_d^p + V_q^n I_q^p + V_d^p I_d^n + V_q^p I_q^n\right)$$

$$P_2 = \frac{3}{2}\left(V_d^n I_d^p - V_q^n I_q^p - V_d^p I_d^n + V_q^p I_q^n\right)$$

$$Q_0 = \frac{3}{2}\left(-V_d^p I_d^p + V_q^p I_q^p - V_d^n I_d^n + V_q^n I_q^n\right)$$

$$Q_1 = \frac{3}{2}\left(V_q^n I_d^p - V_d^n I_q^p + V_q^p I_d^n - V_d^p I_q^n\right)$$

$$Q_2 = \frac{3}{2}\left(-V_d^n I_d^p - V_q^n I_q^p + V_d^n I_d^n + V_q^p I_q^n\right)$$

It is quite obvious that the P_1, P_2, Q_1, and Q_2 components of equation (3.8.2) and (3.8.3) are due to unbalance in the rectifier. These terms represent the basic mutual interaction between the positive and negative sequence components that under normal circumstances does not exist in balanced three-phase systems. It is these components plus Q_0 that must be eliminated in order to maintain a constant dc voltage at the output of the rectifier. Q_0 must be eliminated to achieve unity power factor.

Writing (3.8.2) and (3.8.3) in matrix form we obtain

$$\begin{bmatrix} \frac{2}{3}P_0 \\ \frac{2}{3}Q_0 \\ \frac{2}{3}P_2 \\ \frac{2}{3}P_1 \end{bmatrix} = \begin{bmatrix} V_d^p & V_q^p & V_d^n & V_q^n \\ -V_d^p & V_q^p & -V_d^n & V_q^n \\ V_d^n & -V_q^n & -V_d^p & V_q^p \\ V_d^n & V_q^n & V_d^p & V_q^p \end{bmatrix} \begin{bmatrix} I_d^p(t) \\ I_q^p(t) \\ I_d^n(t) \\ I_q^n(t) \end{bmatrix} \tag{3.8.4}$$

Eliminating the dc ripple, voltage equation (3.8.4) becomes

$$\begin{bmatrix} I_d^p(t) \\ I_q^p(t) \\ I_d^n(t) \\ I_q^n(t) \end{bmatrix} = \begin{bmatrix} V_d^p & V_q^p & V_d^n & V_q^n \\ -V_d^p & V_q^p & -V_d^n & V_q^n \\ V_d^n & -V_d^n & -V_d^p & V_q^p \\ V_d^n & V_q^n & V_d^p & V_q^p \end{bmatrix}^{-1} \begin{bmatrix} \frac{2}{3}P_0 \\ 0 \\ 0 \\ 0 \end{bmatrix} \tag{3.8.5}$$

Further simplification of equation (3.8.5) shows that,

$$I_d^p(t) = \frac{2V_d^p P_0}{3\{[(V_d^p)^2 + (V_q^p)^2] - [(V_d^n)^2 + (V_q^n)^2]\}} \tag{3.8.6}$$

$$I_q^p(t) = \frac{2V_q^p P_0}{3\{[(V_d^p)^2 + (V_q^p)^2] - [(V_d^n)^2 + (V_q^n)^2]\}} \tag{3.8.7}$$

$$I_d^n(t) = -\frac{2V_d^n P_0}{3\{[(V_d^p)^2 + (V_q^p)^2] - [(V_d^n)^2 + (V_q^n)^2]\}} \tag{3.8.8}$$

$$I_q^n(t) = -\frac{2V_q^n P_0}{3\{[(V_d^p)^2 + (V_q^p)^2] - [(V_d^n)^2 + (V_q^n)^2]\}} \tag{3.8.9}$$

Equations (3.8.6-3.8.9) could be further simplified to as follows:

From equation (3.8.6)

$$(I_d^p(t))3\{[(V_d^p)^2 + (V_q^p)^2] - [(V_d^n)^2 + (V_q^n)^2]\} = 2V_d^p P_0$$

$$P_0 = \frac{3}{2} \times \frac{(I_d^p(t))((V_d^p)^2 + (V_q^p)^2 - (V_d^n)^2 - (V_q^n)^2)}{V_d^p} \tag{3.8.10}$$

From equation (3.8.7)

$$(I_q^p(t))3\{[(V_d^p)^2 + (V_q^p)^2] - [(V_d^n)^2 + (V_q^n)^2]\} = 2V_q^p P_0$$

$$P_0 = \frac{3}{2} \times \frac{(I_q^p(t))((V_d^p)^2 + (V_q^p)^2 - (V_d^n)^2 - (V_q^n)^2)}{V_q^p} \tag{3.8.11}$$

From equation (3.8.8)

$$P_0 = -\frac{3}{2}\frac{\left(I_d^n(t)\right)\left((V_d^p)^2 + (V_q^p)^2 - (V_d^n)^2 + (V_q^n)^2\right)}{V_d^n} \tag{3.8.12}$$

From equation (3.8.9)

$$P_0 = -\frac{3}{2}\frac{\left(I_q^n(t)\right)\left((V_d^p)^2 + (V_q^p)^2 - (V_d^n)^2 + (V_q^n)^2\right)}{V_q^n} \tag{3.8.13}$$

From the above equations (3.8.6) through (3.8.9) it is evident that not all of the reactive power can be eliminated because components of the reactive power are still present. However average reactive power is zero implying that ac reactive power is present. Also, it is evident from the equations above that the negative sequence current will flow if there is a negative sequence in the input voltage.

3.9. Harmonic Elimination using Symmetrical Components

From equation 3.4.15 it can be seen that the second order harmonics can be eliminated if

$\frac{3}{2}|h^p||I^n|\cos(2\omega t + \theta_h^p + \theta_i^n) = \frac{3}{2}|h^n||I^p|\cos(2\omega t + \theta_h^n + \theta_i^p)$ shifted at 180^0. That is,

$$|h^p||I^n|\cos(\theta_h^p + \theta_i^n) = |h^n||I^p|\cos(180^0 + \theta_h^n + \theta_i^p) \tag{3.9.1}$$

From the per phase equivalent circuits,

$$\omega L I_k^p = V_k^p - V_{pk}^p \tag{3.9.2}$$

$$\omega L I_k^n = V_k^n - V_{pk}^n \tag{5.9.3}$$

Recall that V_{pk}^p and V_{pk}^n are the pole voltages and are give by;

$$\frac{1}{2}V_{dc}h^p \text{ and } \frac{1}{2}V_{dc}h^n \tag{3.9.4}$$

It was shown earlier that considering only the per phase input voltage and the line impedance,

$$V^n = V_p^n \text{ and } V^p = V_p^p \tag{3.9.5}$$

From equation (3.9.1) and (3.9.5) we develop the following relationships

$$h^p V^n = h^n V^p \tag{3.9.6}$$

Equation (3.9.6) can be rewritten in a proportion form as follows

$\frac{|h^p|}{|h^n|} = \frac{|V^p|}{|V^n|}$ which gives rise to the following

$$\theta_V^p - \theta_h^p = \theta_V^n - \theta_h^n \tag{3.9.7}$$

From equation (3.8.2) and (3.8.3) it is easily shown that

$$h^+ = \frac{2V_k^p}{P_0}\cos(\theta_V^p - \theta_h^p) \tag{3.9.10}$$

and

$$2\sin(\theta_V^p - \theta_h^p) = \frac{2\omega L P_0}{3\{(V^p)^2 - (V^n)^2\}} \tag{3.9.11}$$

Equations [(3.9.7)-(3.9.11)] represent harmonics elimination in the PWM Boost Type Rectifier under unbalanced input voltage. Eliminating harmonics at the both the input and output of the Boost Type PWM Rectifier implies, the magnitudes and phase angles of the voltages and current have to be controlled. Using the dc bus error ($V_{ref} - V_{dc}$) both the magnitudes of the input voltage and current sequence component can be synthesized. These currents are then used as reference currents in the current control loop. The outputs from the current controller are then used as inputs to stability controller.

CHAPTER IV

SPACE-VECTOR PWM

4.1. Voltage vector for space-vector PWM

To effectively control any unbalance in the PWM boost type converter, it is absolute important that the magnitudes and the phase angles of the positive and negative component in the input voltage be known. Therefore, in this section the derivation of the equations for the magnitudes and the phase angle are carried out using the instantaneous value of the input voltages $V_1(t)$, $V_2(t)$, and $V_3(t)$. All voltage magnitudes are in rms; we could multiply by $\sqrt{2}$ to obtain peak values.

4.2. Derivation of the Positive Sequence magnitude and Phase angle

Generally, the voltage vector is given by

$$V_{sp} = (V_d^p + V_q^p)e^{i\omega t} + (V_d^n + V_q^n)e^{-i\omega t} \tag{4.2.1}$$

which represents the positive and the negative sequence voltages in real and imaginary parts.

The positive sequence space vector, V_{sp}^p, is expressed as

$$V_{sp}^p = \frac{2}{3}\left(V_a(t) + uV_b(t) + u^2V_c(t)\right), \text{ where } u = 1\underline{/120^0} \text{ and } u^2 = 1\underline{/240^0} \tag{4.2.2}$$

As shown earlier in Chapter III

$$V_a(t) = |V^0| \sin(\omega t + \theta_v^0) + |V^p| in(\omega t + \theta_v^p) + |V^n| \sin(\omega t + \theta_v^n)$$

$$V_b(t) = |V^0| \sin(\omega t + \theta_v^0) + |V^p| \sin(\omega t + \theta_v^p + \frac{4\pi}{3}) + |V^n| \sin(\omega t + \theta_v^n + \frac{2\pi}{3})$$

$$V_c(t) = |V^0| \sin(\omega t + \theta_v^0) + |V^p| \sin(\omega t + \theta_v^p + \frac{2\pi}{3}) + |V^n| \sin(\omega t + \theta_v^n + \frac{4\pi}{3})$$

Substituting the above equations for $V_a(t)$, $V_b(t)$, and $V_c(t)$ in equation (4.2.2) and simplify (see Appendix A) we get the real component of the space vector as

$$X = |V_{sp}^p| \cos(\theta_v^p) \tag{4.2.3}$$

and the imaginary component of the space vector as

$$Y = |V_{sp}^p| \sin(\theta_v^p) \tag{4.2.4}$$

It is clear from equation (4.2.3) and (4.2.4) that the magnitude of the positive sequence space vector is

$$\sqrt{2}|V_{sp}^p| = \sqrt{X^2 + Y^2} \tag{4.2.5}$$

and the phase angle is

$$\theta_v^p = \tan^{-1} \frac{Y}{X} \tag{4.2.6}$$

4.3. Derivation of the Negative Sequence magnitude and Phase angle

Generally, the voltage vector is given by

$$V_{sp} = (V_d^p + V_q^p)e^{i\omega t} + (V_d^n + V_q^n)e^{-i\omega t} \tag{4.3.1}$$

which represents the positive and the negative sequence voltages in real and imaginary parts.

The negative sequence space vector, V_{sp}^{n}, is expressed as

$$V_{sp}^{n} = \frac{2}{3}\left(V_a(t) + u^2 V_b(t) + u V_c(t)\right) \tag{4.3.2}$$

As shown earlier in Chapter III

$$V_a(t) = \left|V^0\right|\sin(\omega t + \theta_v^0) + \left|V^p\right|\sin(\omega t + \theta_v^p) + \left|V^n\right|\sin(\omega t + \theta_v^n)$$

$$V_b(t) = \left|V^0\right|\sin(\omega t + \theta_v^0) + \left|V^p\right|\sin(\omega t + \theta_v^p + \frac{4\pi}{3}) + \left|V^n\right|\sin(\omega t + \theta_v^n + \frac{2\pi}{3})$$

$$V_c(t) = \left|V^0\right|\sin(\omega t + \theta_v^0) + \left|V^p\right|\sin(\omega t + \theta_v^p + \frac{2\pi}{3}) + \left|V^n\right|\sin(\omega t + \theta_v^n + \frac{4\pi}{3})$$

Substituting the above equations for $V_a(t)$, $V_b(t)$, and $V_c(t)$ in equation (4.3.2) and simplifying (see Appendix A) we get the real component of space vector

$$X_1 = \left|V_{sp}^{n}\right|\sin(\theta_v^n) \tag{4.3.3}$$

and the imaginary component of the space vector as

$$Y_1 = \left|V_{sp}^{n}\right|\cos(\theta_v^n) \tag{4.3.4}$$

It is clear from equation (4.3.3) and (4.3.4) that the magnitude of the positive sequence space vector is

$$\sqrt{2}\left|V_{sp}^{n}\right| = \sqrt{X_1^2 + Y_1^2} \tag{4.3.5}$$

and the phase angle is

$$\theta_v^n = \tan^{-1}\frac{X_1}{Y_1} \tag{4.3.6}$$

4.4. PWM Switching Strategy

Of the PWM techniques described in Chapter I, the space-vector switching technique will be used to determine the switching states of the rectifier. This is because

In general,

$$h_n = \begin{cases} \frac{4}{3} e^{j(n-1)} & n = 1, 2, ..., 6 \\ 0 & n = 7, 8 \end{cases} \tag{4.4.7}$$

It has been shown [20] that at steady state

$$h_d^2 + h_q^2 \le \left(\frac{4}{3} \left(\cos 30^0 \right) \right)^2 = \frac{4}{3} \tag{4.4.8}$$

therefore the magnitude of the space vector of the switching function must be less or equal to $\frac{2}{\sqrt{3}}$. Let T equal the switching period and $\frac{T}{2}$ equal to half the switching period given by $\frac{1}{f_S}$ and $\frac{1}{2f_S}$ respectively, where f_S is the switching frequency of the rectifier.

Let T_n represents the on-times for h_n (switching function) for the space vector and T_{n+1} represent the off-times for h_{n+1}(switching function) of the space vector for

State $\begin{cases} n & \text{on} \\ n+1 & \text{off} \end{cases}$.

The switching function broken down to it various components are give by

$$h_1(t) = h^0 \sin(\omega t + \theta_h^u) + h^p \sin(\omega t + \theta_h^p) + h^n \sin(\omega t + \theta_h^n) \tag{4.4.9}$$

$$h_2(t) = h^0 \sin(\omega t + \theta_h^0) + h^p \sin(\omega t + \theta_h^p - \frac{2\pi}{3}) + h^n \sin(\omega t + \theta_h^n + \frac{2\pi}{3}) \tag{4.4.10}$$

$$h_3(t) = h^0 \sin(\omega t + \theta_h^0) + h^p \sin(\omega t + \theta_h^p + \frac{2\pi}{3}) + h^n \sin(\omega t + \theta_h^n + \frac{2\pi}{3}) \tag{4.4.11}$$

Since no zero sequence exist in the switching functions, the above equations reduce to

$$h_1(t) = h^p \sin(\omega t + \theta_h^p) + h^n \sin(\omega t + \theta_h^n) \tag{4.4.12}$$

$$h_2(t) = h^p \sin(\omega t + \theta_h^p - \frac{2\pi}{3}) + h^n \sin(\omega t + \theta_h^n + \frac{2\pi}{3}) \tag{4.4.13}$$

$$h_3(t) = h^p \sin(\omega t + \theta_h^p + \frac{2\pi}{3}) + h^n \sin(\omega t + \theta_h^n + \frac{2\pi}{3}) \quad (4.4.14)$$

Let $\frac{T_n}{T} = D$ (duty ratio) (4.4.15)

Then the switching function space vector can be written as follows

$$h_d^s = D\left(h_d^p T_n + h_q^p T_{n+1}\right) \quad (4.4.16)$$

$$h_q^s = D\left(h_d^n T_n + h_q^n T_{n+1}\right) \quad (4.4.17)$$

If we multiply equation (4.4.16) by h_d^n and equation (4.4.17) by h_d^p we get

$$h_d^n h_d^s = D\left(h_d^p T_n h_d^n + h_d^n h_q^p T_{n+1}\right) \quad (4.4.18)$$

$$h_d^p h_q^s = D\left(h_d^p h_d^n T_n + h_d^p h_q^n T_{n+1}\right) \quad (4.4.19)$$

Solving these two equations simultaneously, we get

$$h_d^n h_d^s - h_d^p h_q^s = DT_{n+1}\left(h_q^p h_d^n - h_d^p h_q^n\right)$$

$$\frac{h_d^n h_d^s - h_d^p h_q^s}{D(h_q^p h_d^n - h_d^p h_q^n)} = T_{n+1} \quad (4.4.20)$$

Similarly,

$$\frac{h_q^n h_d^s - h_q^p h_q^s}{D(h_d^p h_q^n - h_d^n h_q^p)} = T_n \quad (4.4.21)$$

Form reference [23], a positive solution for T_n and T_{n+1} always exist if the nearest vectors h_n and h_{n+1} adjacent to the vectors h_d^s and h_q^s are selected. Generally, the sum of the conduction times T_n and T_{n+1} is not equal the switching period T.

From Figure 4.4.2, for $T_n + T_{n+1} < T$ the PWM is in the zero switching stage (7 and 8) implying

$$T_0 = T - (T_n + T_{n+1})$$

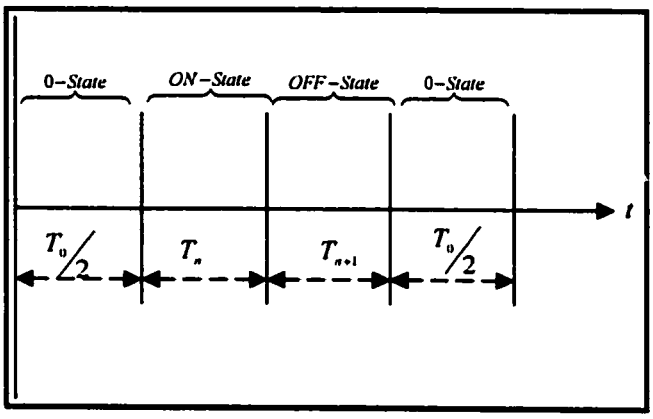

Figure 4.4.2. Switching Cycles and Times

For $T_n + T_{n+1} > T$ the positive squence of the switching function space vector can not be synthesized in time T and therefore, must be limited in magnitude. In such a case, the magnitude of the vector can be scaled by scaling the periods for T_n and T_{n+1} as follows;

$$T_n' = \frac{T_n}{T_n + T_{n+1}} T \text{ and } T_{n+1}' = \frac{T_{n+1}}{T_n + T_{n+1}} T \tag{4.4.23}$$

CHAPTER V

PROPOSED CONTROL METHOD

5.1. Introduction

The control strategy developed is based on Lyapunov's direct method that will make the system globally asymptotically stable. Under balanced operating conditions the open loop system general is asymptotically stable if the line impedance is greater than the input line reactance. However, under this condition the dynamics behavior in general is not acceptable. That is, as the input line resistance reduces (approaching zero) the system becomes more oscillatory and therefore not stable or only marginally stable. Instability in the system is even greater if the system in general is not balanced. Therefore, the objective of this new control strategy will be to make the system stable by driving the dc output voltage to a reference voltage, provide unity power factor with a near sinusoidal input line current.

Though a similar approach has been implemented by [23] the present approach is significantly different from their approach. In their approach they considered only the fact that the system becomes more oscillatory as the input line resistance(R) approaches zero and all other system parameters are balanced. In the present approach, the input line resistance is zero, and input voltages and input line impedances (in some cases) are

unbalanced making the system more unstable. In this case the harmonics have to filtered or eliminated prior to stabilizing the system. Several control methods as mentioned in the literature search have been developed to control or eliminate harmonics in an unbalanced system. However, none of the control method developed thus far gives a comprehensive approach to solving the harmonic and system stability problems. This dissertation offer such an approach.

5.2. Overview of Lyapunov Theory

Lyapunov stability analysis involves two methods since the solutions of nonlinear differential equations are not very easy to obtain;

a. The linearization method concerned with the small motion of nonlinear systems draws conclusions about a nonlinear system's local stability around equilibrium point from the stability properties of its linear approximation.

b. The direct method which is not limited or restricted to local motion, and applicable to all dynamic systems determines stability properties of a nonlinear system by constructing a scalar 'energy-like" function for the system and examining the variations in the function with time. Since there is no general effective approach in finding Lyapunov function, intuitions and trial-and-error are general employed in an attempt to find an appropriate Lyapunov function. Generally, the application of Lyapunov theory to control design is rewarding because it allows the design to deliberately modify the systems dynamic by designing a controller in such

a way that the chosen scalar function become a Lyapunov function for the closed-loop system.

A nonlinear dynamic system is normal represented by a set of nonlinear differential equation in the form of,

$$\dot{x} = f(x) \tag{5.2.1}$$

Where

f is an n x 1 nonlinear vector function

x is the n x 1 state vector

n is the order of the system

A particular value of the state vector is called a point because it corresponds to a point in the state-space. The solutions for x(t) of (5.2.1) usually correspond to the curve in state-space as t varies from zero to infinity. Generally, this curve is called "state trajectory or system trajectory". In general, (5.2.1) can also represent the closed-loop dynamics of a feedback control system with the control input being of a state x and time t, and therefor disappearing in the closed-loop dynamic. I.e. for,

$$\dot{x} = f(x, u) \tag{5.2.2}$$

where u is some control law given as

$$u = g(x) \tag{5.1.3}$$

then (5.2.2) can be written as

$$\dot{x} = f(x, g(x)) \equiv f(x)$$

The basic Lyapunov stability theorem states that if there exist a continuously differentiable function $V(x)$ such that;

a. $V(0) = 0$

b. $V(x) > 0$ for all $x \neq 0$

c. $\frac{dV}{dt} = \left(\frac{\partial V}{\partial x}\right)' f(x) = \sum_{i=1}^{n} \frac{\partial V}{\partial x_i} f_i(x) < 0$ for $x \neq 0$

Then the origin of the system $\dot{X} = f(x)$ is stable.

From the above stated conditions it follows that;

a. If a function *V(x)* satisfy conditions a and b, its "positive definite"

b. Condition c is the mathematical statement of the requirement that the function *V(x)* be decreasing for $x \neq 0$.

c. A function that meets all three condition of the Lyapunov stability theorem is a "Lyapunov function".

d. If *V(x)* is positive definite and $\dot{V}(x)$ is negative definite and $V(x) \rightarrow \infty$ as $\| x \| \rightarrow \infty$, then the equilibrium point at the origin is globally asymptotically stable.

Therefore, the stability of the origin of a dynamic system is certain if a Lyapunov function can be found. A different Lyapunov function will yield a different result for the same system. The advantage of using Lyapunov direct method is that, if the Lyapunov function is not negative definite the control law can be modified to make the function negative definite.

5.3. Existence of Lyapunov Functions

If the origin of a system is stable, there exist a positive definite function *V(x)* that satisfies the above condition with a non-negative derivative except at x = 0.

If the equilibrium point at the origin is uniformly asymptotically stable, there exist a positive definite and decrescent function $V(\mathbf{x})$ with a negative definite derivative.

A scalar function $V(\mathbf{x})$ is said to be decrescent if

$V(0) = 0$, and if $\forall t \geq 0$, $V(\mathbf{x}) \leq V_1(\mathbf{x})$

A scalar time-varying function V(**x**) is locally positive definite if V(0) = 0 and there exist a time-invariant positive definite function Vo(**x**) such that

$\forall t \geq t_0$, $V(\mathbf{x}) \geq V_0(\mathbf{x})$ That is, a time-variant function is locally positive if it dominates a time-invariant locally positive function.

5.4. Lyapunov Function for the PWM Boost Rectifier

Let $x_{1a} = i_{ad} - I_{max}$, $x_{1b} = i_{bd} - I_{max}$, $x_{1c} = i_{cd} - I_{max}$,

$x_{2a} = i_{aq}$, $x_{2b} = i_{bq}$, $x_{2c} = i_{cq}$ and $x_3 = V_{dc} - V_{ref}$ (5.4.1)

From Chapter III the general equations for the rotating *d-q* frame was as follows:

$$L\frac{di_d}{dt} = \omega L i_q - \frac{1}{2}V_{dc}h_d + V_n \tag{5.4.2}$$

$$L\frac{di_q}{dt} = -\omega L i_d - \frac{1}{2}V_{dc}h_q \tag{5.4.3}$$

From equations (5.4.2) and (5.4.3) we develop the following six equations

$$L_a\frac{di_{ad}}{dt} = \omega L_a i_{aq} - \frac{1}{2}V_{dc}h_{1d} + V_a \tag{5.4.4}$$

$$L_a\frac{di_{aq}}{dt} = -\omega L_a i_{ad} - \frac{1}{2}V_{dc}h_{1q} \tag{5.4.5}$$

$$L_b\frac{di_{bd}}{dt} = \omega L_b i_{bq} - \frac{1}{2}V_{dc}h_{2d} + V_b \tag{5.4.5}$$

$$L_b \frac{di_{bq}}{dt} = -\omega L_b i_{bd} - \frac{1}{2} V_{dc} h_{2q} \tag{5.4.7}$$

$$L_c \frac{di_{cd}}{dt} = \omega L_c i_{cq} - \frac{1}{2} V_{dc} h_{3d} + V_c \tag{5.4.8}$$

$$L_c \frac{di_{cq}}{dt} = -\omega L_c i_{cd} - \frac{1}{2} V_{dc} h_{3q} \tag{5.4.9}$$

Now, lets define a positive definite Lyapunov function candidate with x_1, x_2, and x_3 as state variables of the system under investigation as

$$V(x) = \frac{3}{2} L_a x_{1a}^2 + \frac{3}{2} L_b x_{1b}^2 + \frac{3}{2} L_c x_{1c}^2 + \frac{3}{2} L_a x_{2a}^2 + \frac{3}{2} L_b x_{2b}^2 + \frac{3}{2} L_c x_{2c}^2 + C x_3^2 \tag{5.4.10}$$

Taking the derivative of (5.4.10) we get

$$\begin{aligned} \dot{V}(\bar{x}) = {} & 3x_{1a} L_a \dot{x}_{1a} + 3x_{1b} L_b \dot{x}_{1b} + 3x_{1c} L_c \dot{x}_{1c} + 3x_{2a} L_a \dot{x}_{2a} + \\ & 3x_{2b} L_b \dot{x}_{2b} + 3x_{2c} L_c \dot{x}_{2b} + 2x_3 C \dot{x}_3 \end{aligned} \tag{5.4.11}$$

In Chapter III it was shown that without the zero sequence component,

$$i_0 = \frac{3}{4}(i_a h_1 + i_b h_2 + i_c h_3) \tag{5.4.12}$$

Transforming equation (5.4.12) in the *d-q* plane we have

$$i_0 = \frac{3}{4}\left[(i_{ad} h_{1d} + i_{aq} h_{1q}) + (i_{bd} h_{2d} + i_{bq} h_{2q}) + (i_{cd} h_{3d} + i_{cq} h_{3q})\right] \tag{5.4.13}$$

Therefore

$$C \frac{dv_{dc}}{dt} = i_0 - i_L = \frac{3}{4}\left[(i_{ad} h_{1d} + i_{aq} h_{1q}) + (i_{bd} h_{2d} + i_{bq} h_{2q}) + (i_{cd} h_{3d} + i_{cq} h_{3q})\right] - i_L \tag{5.4.14}$$

From Chapter IV,

$$h_d = h_{do} + \Delta h_d \tag{5.4.15}$$

$$h_q = h_{qo} + \Delta h_q \tag{5.4.16}$$

$$3x_{1c}L_c\dot{x}_{1c} = 3x_{1c}\omega L_b x_{2c} - 3\frac{V_c}{V_{ref}}x_{1c}x_3 - \frac{3\Delta h_{3d}}{2}x_{1c}x_3 - \frac{3}{2}\Delta h_{3d}x_{2c}V_{ref} \tag{5.4.19}$$

A similar procedure would show that equation (5.4.5), (5.4.7) and (5.4.9) become

$$L_a\dot{x}_{2a} = -\omega L_a(x_{1a} + I_{\max}) - \frac{1}{2}(x_3 + V_{ref})\left(\frac{-2\omega L_a I_{\max}}{V_{ref}} + \Delta h_{1q}\right)$$

$$= -\omega L_a x_{1a} + \frac{\omega L_a I_{\max}}{V_{ref}}x_3 - \frac{\Delta h_{1q}}{2}x_3 - \frac{1}{2}V_{ref}\Delta h_{1q}$$

$$3x_{2a}L_a\dot{x}_{2a} = 3\left(-\omega L_a x_{1a} + \frac{\omega L_a I_{\max}}{V_{ref}}x_3 - \frac{\Delta h_{1q}}{2}x_3 - \frac{1}{2}V_{ref}\Delta h_{1q}\right)x_{2a}$$

$$= -3\omega L_a x_{2a}x_{1a} + 3\frac{\omega L_a I_{\max}}{V_{ref}}x_{2a}x_3 - \frac{3\Delta h_{1q}}{2}x_{2a}x_3 - \frac{3}{2}V_{ref}x_{2a}\Delta h_{1q} \tag{5.4.20}$$

$$L_b\dot{x}_{2b} = -\omega L_b(x_{1b} + I_{\max}) - \frac{1}{2}(x_3 + V_{ref})\left(\frac{-2\omega L_b I_{\max}}{V_{ref}} + \Delta h_{2q}\right)$$

$$3x_{2b}L_b\dot{x}_{2b} = 3\left(-\omega L_b x_{1b} + \frac{\omega L_b I_{\max}}{V_{ref}}x_3 - \frac{\Delta h_{2q}}{2}x_3 - \frac{1}{2}V_{ref}\Delta h_{2q}\right)x_{2b}$$

$$= -3\omega L_b x_{2b}x_{1b} + 3\frac{\omega L_b I_{\max}}{V_{ref}}x_{2b}x_3 - \frac{3\Delta h_{2q}}{2}x_{2b}x_3 - \frac{3}{2}V_{ref}x_{2b}\Delta h_{2q} \tag{5.4.21}$$

$$L_c\dot{x}_{2c} = -\omega L_c(x_{1c} + I_{\max}) - \frac{1}{2}(x_3 + V_{ref})\left(\frac{-2\omega L_c I_{\max}}{V_{ref}} + \Delta h_{3q}\right)$$

$$3x_{2c}L_c\dot{x}_{2c} = 3\left(-\omega L_c x_{1c} + \frac{\omega L_c I_{\max}}{V_{ref}}x_3 - \frac{\Delta h_{3q}}{2}x_3 - \frac{1}{2}V_{ref}\Delta h_{3q}\right)x_{2c}$$

$$= -3\omega L_c x_{2c}x_{1c} + 3\frac{\omega L_c I_{\max}}{V_{ref}}x_{2c}x_3 - \frac{3\Delta h_{3q}}{2}x_{2c}x_3 - \frac{3}{2}V_{ref}x_{2c}\Delta h_{3q} \tag{5.4.22}$$

$$C\dot{x}_3 = \frac{3}{4}(x_{1a} + I_{\max})\left(\frac{2V_a}{V_{ref}} + \Delta h_{1d}\right) + \frac{3x_{2a}}{4}\left(\frac{-2\omega L_a I_{\max}}{V_{ref}} + \Delta h_{1q}\right) - \frac{3I_{\max}V_a}{V_{ref}} +$$

$$\frac{3}{4}(x_{1b}+I_{\max})\left(\frac{2V_b}{V_{ref}}+\Delta h_{2d}\right)+\frac{3x_{2b}}{4}\left(\frac{-2\omega L_b I_{\max}}{V_{ref}}+\Delta h_{2q}\right)-\frac{3I_{\max}V_b}{V_{ref}}+$$

$$\frac{3}{4}(x_{1c}+I_{\max})\left(\frac{2V_c}{V_{ref}}+\Delta h_{3d}\right)+\frac{3x_{2c}}{4}\left(\frac{-2\omega L_c I_{\max}}{V_{ref}}+\Delta h_{3q}\right)-\frac{3I_{\max}V_c}{V_{ref}}$$

$$2x_3C\dot{x}_3=2\left[\frac{3}{4}(x_{1a}+I_{\max})\left(\frac{2V_a}{V_{ref}}+\Delta h_{1d}\right)+\frac{3x_{2a}}{4}\left(\frac{-2\omega L_a I_{\max}}{V_{ref}}+\Delta h_{1q}\right)-\frac{3I_{\max}V_a}{V_{ref}}\right.$$

$$\frac{3}{4}(x_{1b}+I_{\max})\left(\frac{2V_b}{V_{ref}}+\Delta h_{2d}\right)+\frac{3x_{2b}}{4}\left(\frac{-2\omega L_b I_{\max}}{V_{ref}}+\Delta h_{2q}\right)-\frac{3I_{\max}V_b}{V_{ref}}$$

$$\left.\frac{3}{4}(x_{1c}+I_{\max})\left(\frac{2V_c}{V_{ref}}+\Delta h_{3d}\right)+\frac{3x_{2c}}{4}\left(\frac{-2\omega L_c I_{\max}}{V_{ref}}+\Delta h_{3q}\right)-\frac{3I_{\max}V_c}{V_{ref}}\right]x_3$$

$$=\frac{3x_{1a}x_3V_a}{V_{ref}}+\frac{3}{2}x_3x_{1a}\Delta h_{1d}-\frac{3x_3I_{\max}V_a}{V_{ref}}+\frac{3}{2}x_3I_{\max}\Delta h_{1d}-\frac{3I_{\max}x_3x_{2a}}{V_{ref}}+\frac{3x_3x_{2a}\,\Delta h_{1q}}{2}$$

$$+\frac{3x_{1b}x_3V_b}{V_{ref}}+\frac{3}{2}x_3x_{1b}\Delta h_{2d}-\frac{3x_3I_{\max}V_b}{V_{ref}}+\frac{3}{2}x_3I_{\max}\Delta h_{2d}-\frac{3I_{\max}x_3x_{2a}}{V_{ref}}+\frac{3x_3x_{2b}\,\Delta h_{2q}}{2}$$

$$+\frac{3x_{1c}x_3Vc_a}{V_{ref}}+\frac{3}{2}x_3x_{1c}\Delta h_{3d}-\frac{3x_3I_{\max}V_c}{V_{ref}}+\frac{3}{2}x_3I_{\max}\Delta h_{3d}-\frac{3I_{\max}x_3x_{2c}}{V_{ref}}+\frac{3x_3x_{2c}\,\Delta h_{3q}}{2}$$

(5.4.23)

Equations (5.4.17-5.4.23) are combined to obtain $\dot{V}(\bar{x})$ i.e.,

$$\dot{V}(\bar{x})=3x_{1a}\omega L_a x_{2a}-3\frac{V_a}{V_{ref}}x_{1a}x_3-\frac{3\Delta h_{1d}}{2}x_{1a}x_3-\frac{3}{2}\Delta h_{1d}x_{1a}V_{ref}+$$

$$+3x_{1b}\omega L_b x_{2b} - 3\frac{V_b}{V_{ref}}x_{1b}x_3 - \frac{3\Delta h_{2d}}{2}x_{1b}x_3 - \frac{3}{2}\Delta h_{2d}x_{2a}V_{ref} +$$

$$3x_{1c}\omega L_b x_{2c} - 3\frac{V_c}{V_{ref}}x_{1c}x_3 - \frac{3\Delta h_{3d}}{2}x_{1c}x_3 - \frac{3}{2}\Delta h_{3d}x_{2c}V_{ref}$$

$$-3\omega L_a x_{2a}x_{1a} + 3\frac{\omega L_a I_{\max}}{V_{ref}}x_{2a}x_3 - \frac{3\Delta h_{1q}}{2}x_{2a}x_3 - \frac{3}{2}V_{ref}x_{2a}\Delta h_{1q}$$

$$-3\omega Lbx_{2b}x_{1b} + 3\frac{\omega L_b I_{\max}}{V_{ref}}x_{2b}x_3 - \frac{3\Delta h_{2q}}{2}x_{2b}x_3 - \frac{3}{2}V_{ref}x_{2b}\Delta h_{2q}$$

$$-3\omega L_c x_{2c}x_{1c} + 3\frac{\omega L_c I_{\max}}{V_{ref}}x_{2c}x_3 - \frac{3\Delta h_{3q}}{2}x_{2c}x_3 - \frac{3}{2}V_{ref}x_{2c}\Delta h_{3q}$$

$$\dot{V}(\bar{x}) =$$

$$-3\frac{x_3V_a I_{\max}}{V_{ref}} - 3\frac{x_3V_b I_{\max}}{V_{ref}} - 3\frac{x_3V_c I_{\max}}{V_{ref}} + \frac{3}{2}x_3 I_{\max}\Delta h_{1d}\,\frac{3}{2}x_3 I_{\max}\Delta h_{2d} + \frac{3}{2}x_3 I_{\max}\Delta h_{3d}$$
$$-\frac{3}{2}x_{2a}V_{ref}\Delta h_{1q} - \frac{3}{2}x_{2b}V_{ref}\Delta h_{2q} - \frac{3}{2}x_{2c}V_{ref}\Delta h_{3q} - \frac{3}{2}x_{1a}V_{ref}\Delta h_{1d} - \frac{3}{2}x_{1b}V_{ref}\Delta h_{2d} - \frac{3}{2}x_{1c}V_{ref}\Delta h_{3d}$$

$$-3\frac{x_3V_a I_{\max}}{V_{ref}} - 3\frac{x_3V_b I_{\max}}{V_{ref}} - 3\frac{x_3V_c I_{\max}}{V_{ref}} + \frac{3}{2}x_3 I_{\max}\Delta h_{1d} + \frac{3}{2}x_3 I_{\max}\Delta h_{2d} + \frac{3}{2}x_3 I_{\max}\Delta h_{3d}$$
$$-\frac{3}{2}x_{2a}V_{ref}\Delta h_{1q} - \frac{3}{2}x_{2b}V_{ref}\Delta h_{2q} - \frac{3}{2}x_{2c}V_{ref}\Delta h_{3q} - \frac{3}{2}x_{1a}V_{ref}\Delta h_{1d} - \frac{3}{2}x_{1b}V_{ref}\Delta h_{2d} - \frac{3}{2}x_{1c}V_{ref}\Delta h_{3d}$$

Further simplification yields

$$\dot{V}(\bar{x}) = -\frac{3}{2}\left[(V_{ref}x_{1a} - x_3 I_{\max})\Delta h_{1d} + (V_{ref}x_{1b} - x_3 I_{\max})\Delta h_{2d} + (V_{ref}x_{1c} - x_3 I_{\max})\Delta h_{3d}\right]$$

$$-\frac{3}{2}\left[(V_{ref}x_{2a}\Delta h_{1q} + V_{ref}x_{2b}\Delta h_{2q} + V_{ref}x_{2c}\Delta h_{3q}\right] \qquad (5.4.25)$$

5.5. Proposed Control Strategy

From the above Lyapunov function the values for $\Delta h_{1d}, \Delta h_{2d}, \Delta h_{3d}$, $\Delta h_{1q}, \Delta h_{2q}$, and Δh_{3q}, (control law) will be determined such that $\dot{V}(\bar{x})$ along any trajectory would be negative definite.

This law(s) will be examined and modified if necessary to make sure that the switching functions are not saturated. As it was mentioned in Chapter 4, at steady-state sinusoidal operation of the rectifier, the switching functions must be

$$h_d^2 + h_q^2 \le \left(\frac{4}{3}\cos 30\right)^2 = \frac{4}{3} \tag{5.5.1}$$

indicating that the switching functions would remain unsaturated if the magnitude of the switching function space-vector is equal or less than $\frac{2}{\sqrt{3}}$. That is, we must calculate new values for Δh_d and Δh_q such that the magnitude of switching function space vector must remain within it limit else there will be no synthesizing. The newly calculated switching functions from (5.4.25) will be examined to ascertain if they guarantee a negative definite for the Lyapunov function $\dot{V}(\bar{x})$. This is not an easy case as has been determined by [23] in a related research dealing with stability of a balanced three-phase rectifier. From equations (5.4.15) and (5.4.16)

$$h_d = h_{do} + \Delta h_d$$

$$h_q = h_{qo} + \Delta h_q$$

Substituting into equation (5.5.1) we get

$$(h_{d0} + \Delta h_d)^2 + (h_{q0} + \Delta h_q)^2 \le \frac{4}{3} \tag{5.5.2}$$

From equation (5.4.25) it can be seen that $\dot{V}(\bar{x})$ along any trajectory would be negative definite if

$$\Delta h_{1d} = \psi_1 (x_{1a} V_{ref} - x_3 I_{\max}), \quad \text{for } \psi_1 > 0 \tag{5.5.3}$$

$$\Delta h_{1q} = \xi_1 (x_{2a} V_{ref}), \quad \text{for } \xi_1 > 0 \tag{5.3.4}$$

$$\Delta h_{2d} = \psi_2 (x_{1b} V_{ref} - x_3 I_{\max}), \quad \text{for } \psi_2 > 0 \tag{5.5.5}$$

$$\Delta h_{2q} = \xi_2 (x_{2b} V_{ref}), \quad \text{for } \xi_2 > 0 \tag{5.5.6}$$

$$\Delta h_{3d} = \psi_3 (x_{1c} V_{ref} - x_3 I_{\max}), \quad \text{for } \psi_3 > 0 \tag{5.5.7}$$

$$\Delta h_{3q} = \xi_3 (x_{2c} V_{ref}), \quad \text{for } \xi_3 > 0 \tag{5.5.8}$$

Where ξ and ψ are real constants.

From (5.5.1) the maximum possible steady state value for the switching function ($(h_d)_{\max}$ and $(h_q)_{\max}$) are determined. This equation will be used to develop control law(s) governing the limits for switching function saturation.

Let,

$$h_{1d\max} = h_{1d} + \Delta h_{1d\max} \tag{5.5.9}$$

$$h_{2d\max} = h_{2d} + \Delta h_{2d\max} \tag{5.5.10}$$

$$h_{3d\max} = h_{3d} + \Delta h_{3d\max} \tag{5.5.11}$$

$$h_{1q\max} = h_{1q} + \Delta h_{1q\max} \tag{5.5.12}$$

$$h_{2q\max} = h_{2q} + \Delta h_{2q\max} \tag{5.5.13}$$

$$h_{3q\max} = h_{3q} + \Delta h_{3q\max} \tag{5.5.14}$$

Substituting equation (5.5.9) and (5.5.12) into equation (5.5.1) we get

$$|\Delta h_{1d\max}| \le \sqrt{\frac{4}{3} - (h_{1q\max})^2} - |h_{1d}| \equiv \mathrm{h}_{1\mathrm{d}}(\max) \tag{5.5.16}$$

Similarly, substituting equation (5.5.10) and (5.5.13) into (5.5.1) we obtain

$$|\Delta h_{2d\max}| \le \sqrt{\frac{4}{3} - (h_{2q\max})^2} - |h_{2d}| \equiv \mathrm{h}_{2\mathrm{d}}(\max) \tag{5.3.17}$$

Substituting equation (5.5.11) and (5.5.14) into (5.5.1) and simplifying we obtain

$$|\Delta h_{3d\max}| \le \sqrt{\frac{4}{3} - (h_{3q\max})^2} - |h_{3d}| \equiv \mathrm{h}_{3\mathrm{d}}(\max) \tag{5.5.18}$$

Substituting equation (5.5.9) into (5.5.22) and simplifying we get

$$|\Delta h_{1q\max}| \le \sqrt{\frac{4}{3} - (h_{1d\max})^2} - |h_{1q}| \equiv \mathrm{h}_{1\mathrm{q}}(\max) \tag{5.5.19}$$

Similarly, substituting equation (5.5.10) and (5.5.13) into (5.5.1) and simplify we obtain

$$|\Delta h_{2q\max}| \le \sqrt{\frac{4}{3} - (h_{2\max})^2} - |h_{2q}| \equiv \mathrm{h}_{2\mathrm{q}}(\max) \tag{5.5.20}$$

Substituting equation (5.5.11) and (5.5.14) into (5.5.1) and simplifying we obtain

$$|\Delta h_{3q\max}| \le \sqrt{\frac{4}{3} - (h_{3d\max})^2} - |h_{3q}| \equiv \mathrm{h}_{3\mathrm{q}}(\max) \tag{5.5.21}$$

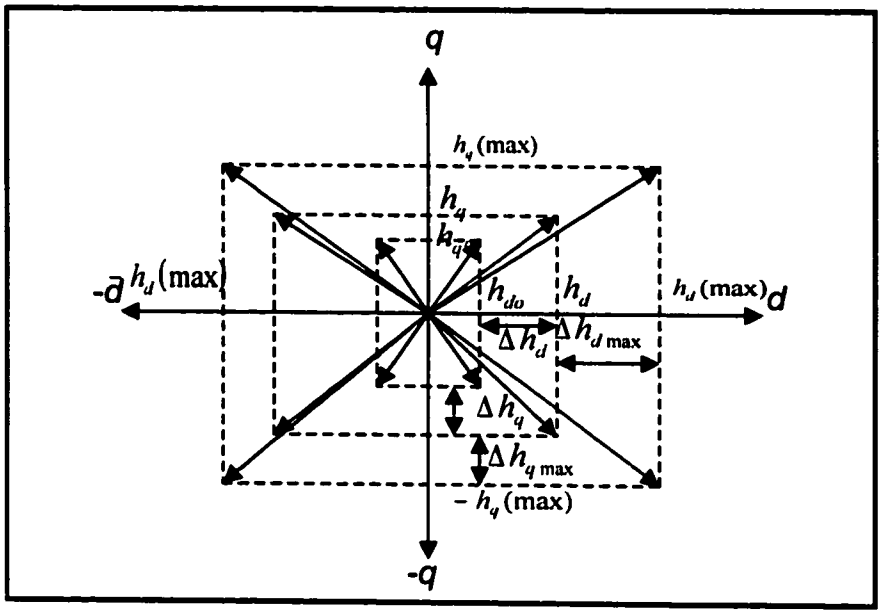

Figure 5-5.1. Switching constraints space vector.

From the above equations it is clear that the new switching functions are within the limits as required by equation (5.5.2). To ensure that $\dot{V}(\bar{x})$ is negative definite we determine a range (constraints Figure 5-5.1) in which the switching functions must stay unsaturated. To accomplish this we examine what happen when the system is either controlled by h_d or h_q. Let the system be control by h_{1d}, h_{2d} or h_{3d} which implies $\Delta h_{1q} = \Delta h_{2q} = \Delta h_{3q} = 0$, then the possible values that h_{1d}, h_{2d} or h_{3d} can take are between $h_{1d}(\max)$ and $-h_{1d}(\max)$, $h_{2d}(\max)$ and $-h_{2d}(\max)$, or $h_{3d}(\max)$ and $-h_{3d}(\max)$. This means, the range in which h_{1d}, h_{2d} or h_{3d} could change is;

$$
\begin{aligned}
-[h_{1d}(\max) + h_{1d0}] \le \Delta h_{1d} \le [h_{1d}(\max) - h_{1d0}] \\
-[h_{2d}(\max) + h_{2d0} \le \Delta h_{2d} \le [h_{2d}(\max) - h_{2d0}] \\
-[h_{3d}(\max) + h_{3d0} \le \Delta h_{3d} \le [h_{3d}(\max) - h_{3d0}]
\end{aligned}
\qquad (5.5.22)
$$

Similarly, let the system be control by h_{1q}, h_{2q} or h_{3q} which implies $\Delta h_{1d} = \Delta h_{2d} = \Delta h_{3d} = 0$, then the possible values that h_{1q}, h_{2q} or h_{3q} can take are between $h_{1q}(\max)$ and $-h_{1q}(\max)$, $h_{2q}(\max)$ and $-h_{2q}(\max)$, or $h_{3q}(\max)$ and $-h_{3q}(\max)$, . This means, the range in which h_{1q}, h_{2q} or h_{3q} could change is;

$$\begin{aligned} -[h_{1q}(\max) + h_{1q0}] \le \Delta h_{1q} \le [h_{1q}(\max) - h_{1q0}] \\ -[h_{2q}(\max) + h_{2q0}] \le \Delta h_{2q} \le [h_{2q}(\max) - h_{2q0}] \\ -[h_{3q}(\max) + h_{3q0}] \le \Delta h_{3q} \le [h_{3q}(\max) - h_{3q0}] \end{aligned} \tag{5.5.23}$$

It follows that equations (5.5.3-5.5.8) can be rewritten based on the saturation constraints as follows

$$\Delta h_{1d} = -[h_{1d}(\max) - h_{1d0}] \text{ if } \psi_1(x_{1a}V_{ref} + x_3 I_{\max}) < -[h_{1d}(\max) + h_{1d0}] \tag{5.5.24}$$

$$\begin{aligned} \Delta h_{1d} &= \psi_1(x_{1a}V_{ref} - x_3 I_{\max}) \\ &\text{if } -[h_{1d}(\max) + h_{1d0}] \le \psi_1(x_{1a}V_{ref} - x_3 I_{\max}) \le [h_{1d}(\max) - h_{1d0}] \end{aligned} \tag{5.5.25}$$

$$\Delta h_{1d} = [h_{1d}(\max) - h_{1d0}] \text{ if } \psi_1(x_1 V_{ref} - x_3 I_{\max}) > [h_{1d}(\max) - h_{1d0}] \tag{5.5.26}$$

$$\Delta h_{2d} = -[h_{2d}(\max) + h_{2d0}] \text{ if } \psi_2(x_{1b}V_{ref} - x_3 I_{\max}) < -[h_{2d}(\max) + h_{2d0}] \tag{5.5.27}$$

$$\begin{aligned} \Delta h_{2d} &= \psi_2(x_{1b}V_{ref} - x_3 I_{\max}) \\ &\text{if } -[h_{2d}(\max) + h_{2d0}] \le \psi_2(x_{1b}V_{ref} - x_3 I_{\max}) \le [h_{2d}(\max) + h_{2d0}] \end{aligned} \tag{5.5.28}$$

$$\Delta h_{2d} = [h_{2d}(\max) - h_{2d0}] \text{ if } \psi_2(x_{1b}V_{ref} - x_3 I_{\max}) > [(h_{2d}(\max) - h_{2d0}] \tag{5.5.29}$$

$$\Delta h_{3d} = -[h_{3d}(\max) + h_{3d0}] \text{ if } \psi_3(x_{1c}V_{ref} - x_3 I_{\max}) < -[h_{3d}(\max) + h_{3d0}] \tag{5.5.30}$$

$$\begin{aligned} \Delta h_{3d} &= \psi_3(x_{1c}V_{ref} - x_3 I_{\max}) \\ &\text{if-}[h_{3d}(\max) + h_{3d0}] \le \psi_3(x_{1c}V_{ref} - x_3 I_{\max}) \le -[h_{3d}(\max) + h_{3d0}] \end{aligned} \tag{5.5.31}$$

$$\Delta h_{3d} = [h_{3d}(\max) - h_{1d0}] \text{ if } \psi_3(x_{1c}V_{ref} - x_3 I_{\max}) > [h_{3d}(\max) - h_{3d0}] \tag{5.5.32}$$

$$\Delta h_{1q} = -[h_{1q}(\max) + h_{1q0}] \text{ if } \xi_1(x_{2a}V_{ref}) > -[h_{1q}(\max) + h_{1q0}] \tag{5.5.33}$$

$$\Delta h_{1q} = \xi_1(x_{2a}V_{ref}) \quad \text{if } [h_{1q}(\max) + h_{1q0}] \le \xi_1(x_{2a}V_{ref}) \le -[h_{1q}(\max) + h_{1q0}] \tag{5.5.34}$$

$$\Delta h_{1q} = [h_{1q}(\max) - h_{1q0}] \text{ if } \xi_1(x_{2a}V_{ref}) < [h_{1q}(\max) - h_{1q0}] \tag{5.5.35}$$

$$\Delta h_{2q} = -[h_{2q}(\max) + h_{2q0}] \text{ if } \xi_2(x_{2b}V_{ref}) > -[(h_{2q}(\max) + h_{2q0}] \tag{5.5.36}$$

$$\Delta h_{2q} = \xi_2(x_{2b}V_{ref}) \quad \text{if } [h_{2q}(\max) - h_{2q0}] \le \xi_2(x_{2b}V_{ref}) \le -[(h_{2q}(\max) + h_{2q0}] \tag{5.5.37}$$

$$\Delta h_{2q} = [h_{2q}(\max) - h_{2q0}] \text{ if } \xi_2(x_{2b}V_{ref}) < [h_{2q}(\max) - h_{2q0}] \tag{5.5.38}$$

$$\Delta h_{3q} = -[h_{3q}(\max) + h_{3q0}] \text{ if } \xi_3(x_{2c}V_{ref}) > -[h_{3q}(\max) + h_{3q0}] \tag{5.5.39}$$

$$\Delta h_{3q} = \xi_3(x_{2c}V_{ref}) \quad \text{if } [h_{3q}(\max) - h_{3q0}] \le \xi_3(x_{2c}V_{ref}) \le -[(h_{3q}(\max) + h_{3q0}] \tag{5.5.40}$$

$$\Delta h_{3q} = [h_{3q}(\max) - h_{3q0}] \text{ if } \xi_3(x_{2c}V_{ref}) < [h_{3q}(\max) - h_{3q0}] \tag{5.5.41}$$

During the simulation process, the value for ξ and ψ will selected by trial and error method since ξ and ψ are real constants and can not be easily calculated. Alternatively, they could be chosen by some optimization process to increase system stability and reduce overshoot.

CHAPTER VI

COMPUTER SIMULATION

6.1. Introduction

The design of electronics and electrical circuits in most cases require some method or methods by which the performance of the circuits could be measured. Given the complexity of modern integrated circuits (IC), utilizing computers to simulate electronics circuit in many ways offer critical information about the circuit that would have other wise been very difficulty to obtain in laboratory setting. In power electronics the combination of passive electronics components such as MOSFET, thyistors and other solid state electronics switches causes the topology of the a circuit to change as they open and close under the influence of some type of control. With the frequent changes in the circuit topology, it is very difficult and in most cases not advisable to try to determine current or voltage in such a circuit as a function of time. Therefore, computer simulation can be used to model such circuits and at the same time, investigate influence of certain circuit parameters. Generally, computer simulation are used in the industries today to shorten the design process and in most cases provide an easier way to study the influence of a parameter or parameters in a design. Basically, there are two types of computer simulation [24].

a. circuit oriented simulations

b. equation solving simulations

Under the circuit oriented simulation, a circuit topology and component value are provided. The simulator in turn, generated equations internally and in some cases offer a means of selecting the details of the component model. Depending on the simulator the controller can be implemented by means of a transfer function or models such as operational amplifiers (OPAM), comparators, etc. Pspice, SPICE (Simulated Program with Integrated Circuit Emphasis), EMTP (Electro-Magnetic Transient Program), and Electronics Workbench are just a few of the many circuit oriented simulators. The equation solver on the order hand describes the circuit and the controller by means of algebraic and or differential equations. With this type of simulator it is important that all the state equations at which the circuit will operate be developed. MATLAB and MATHCAD are two examples of these types of Simulators. Some other advantages associated with computer simulations are [25]:

a. Evaluating the effect of variations in circuit components

b. Assessment for performance improvement

c. Evaluating the effect of disturbance without the need of very expensive measuring devices

d. Perform Fourier analysis without the need for expensive waveform analyzer

e. Evaluation of the effect of nonlinear elements to system performance

f. Perform Sensitivity analysis to determine system performance limits and tolerance.

g. Design optimization.

For this dissertation a simulator that utilizes both the circuit-oriented and the solver is used. However, there are inherent advantages and disadvantages with combining both methods. These advantages and disadvantage include but not limited to:

a. Changes in the circuit topology and control can easily be made.
b. Built-in models for analog and digital component and controller are usually include in the library.
c. Initial setup time is very lengthy.
d. The focus is on both circuit and mathematical solution
e. Segments of the circuit could be simulated independently prior to building a comprehensive system.

PSIM was chosen over several available simulators because it offers both the advantages and disadvantages listed above. Most of the available simulator are either circuit-oriented or equation solver, not a combination of both. See Appendix F for some of PSIM features.

As stated in Chapter I, there are basically three types of PWM switching techniques; sinusoidal PWM switching technique, hysteresis PWM switching technique, and the space vector switching technique. Traditionally, the space vector PWM has been considered the better of the three given the fact it generally generate less harmonic distortion in the converter output voltage and current. The space vector PWM was selected for this research for this reason.

Under the space vector PWM control technique the output voltage and current are approximated by using a combination of approximately eight switching patterns. Generally, there are five stages to be considered when implementing the digital space

vector PWM control scheme; vector calculation, vector location, time interval calculation, the switching state selection and the digital stage which determine which switch to be turned on-of given the information stored in the Lookup Table (Table 6-1.1).

Table 6-1.1 Switching Logic for the Lookup Tables

	Sw-1	Sw-2	Sw-3	Sw-4	Sw-5	Sw-6
Step 1	1	1	0	0	0	1
Step 2	1	1	1	0	0	0
Step 3	1	0	1	0	1	0
Step 4	1	1	1	0	0	0
Step 5	1	1	0	0	0	1
Step 6	1	1	1	0	0	0
Step 7	0	1	1	1	0	0
Step 8	0	1	0	1	0	1
Step 9	0	1	1	1	0	0
Step 10	1	1	1	0	0	0
Step 11	0	1	1	1	0	0
Step 12	0	0	1	1	1	0
Step 13	1	0	1	0	1	0
Step 14	0	0	1	1	1	0
Step 15	0	1	1	1	0	0
Step 16	0	0	1	1	1	0
Step 17	0	0	0	1	1	1
Step 18	0	1	0	1	0	1
Step 19	0	0	0	1	1	1
Step 20	0	0	1	1	1	0
Step 21	0	0	0	1	1	1
Step 22	1	0	0	0	1	1
Step 23	1	0	1	0	1	0
Step 24	1	0	0	0	1	1
Step 25	0	0	0	1	1	1
Step 26	1	0	0	0	1	1
Step 27	1	1	0	0	0	1
Step 28	0	1	0	1	0	1
Step 29	1	1	0	0	0	1
Step 30	1	0	0	0	1	1
Step 31	0	0	0	0	0	0

For more information on most of the components and their functions used in implementing the digital space vector PWM, see Appendix F.

Generally, unbalanced in a three-phase converter generate a second harmonic at the dc bus. The second harmonic could be eliminated using different methods. Reference [19] uses a notch filter to eliminate the second harmonic prior to controlling the output voltage. In implementing reference [19], the positive sequence current is measured in the positive synchronous reference frame by using a notch filter (120Hz) to eliminate the negative sequence current. Using the same procedure, the negative sequence current is measured in the negative synchronous reference frame. These two measured currents are used for two feedback proportional plus integral (PI) controllers. One of the controllers is used to regulate the positive sequence current and the other controller is used to regulate the negative sequence current. This method of control facilitates the control of the negative sequence current in synchronous reference frame as a dc signal, thereby eliminating the need to increase the gain since it may cause the system to oscillate or become unstable.

6.2. Simulation of the PWM Boost Type Rectifier

In this section simulations are conducted to verify the theory and the validity of the system under unbalanced operating conditions.

Section 6.2.1 shows the simulations results under unbalanced input voltage and balanced input line impedance. In section 6.2.1.1 the PWM is simulated using open loop control. The results show that there exist 2^{nd} harmonics at the out of the converter and the presents of 3^{rd} harmonics at the input of the converter. Section 6.2.1.2 shows the

simulation of a proportional plus integral feedback control method by reference [19] under the unbalanced input voltage and balanced input line impedance. Section 6.2.1.3 shows the results of the system using the proposed Lyapunov control method.

Section 6.2.2 shows the simulation results under balanced input voltage and unbalanced input line impedance. In section 6.2.2.1 the PWM rectifier is simulated using open loop control. Section 6.2.2.2 the simulation of a proportional plus integral feedback control method by reference [19] under balanced input voltage and unbalanced input line impedance. Section 6.2.2.3 shows the results of the PWM rectifier under balanced input voltage and unbalanced input line impedance using the proposed Lyapunov control method.

Section 6.2.3 discusses the simulation results of the proposed Lyapunov control method and reference [19] when given a wider input voltage and input line impedance range.

Section 6.3, discusses the comparison between the proposed Lyapunov control method and the proportion plus integral control method by reference [19]. In comparing the two control methods, the parameters of the Lyapunov controller are adjusted to obtained the same rise time as with reference [19]. This allows for a fair comparison of Ripple. Rise time is the time the system output takes to reach steady state. The results are presented in Table 6-3.1. Also, in this section calculations are performed to determine the amount of Error in the waveforms.

6.2.1 Unbalance Input Voltage and Balanced Input Line Impedance

In this section we simulate the PWM rectifier under unbalanced input voltage and balanced input line impedance. The PWM is simulated first by using open loop control then by reference [19] closed loop control method and finally by the proposed Lyapunov closed loop control method.

6.2.1.1 Unbalanced Input Voltage and Balanced Input Line Impedance (Open Loop)

To show that unbalanced operating conditions due to imbalance in the input voltage will result in harmonics at the converters output and input, the Boost Type PWM rectifier Figure 6-2.1 was simulated using PSIM.

The parameters are as follows:

Input voltages, $V_a = 165V$, $V_b = 170V$ and $V_c = 160V$

Line impedance (per phase), L1 = L2 = L3 = 10mH

Fundamental frequency, $f = 60hz$

Output capacitor, C = 10000μF

Switching frequency, $f_s = 10Khz$

Output load (resistive), R = 100 ohms

Reference voltage 270 Volts

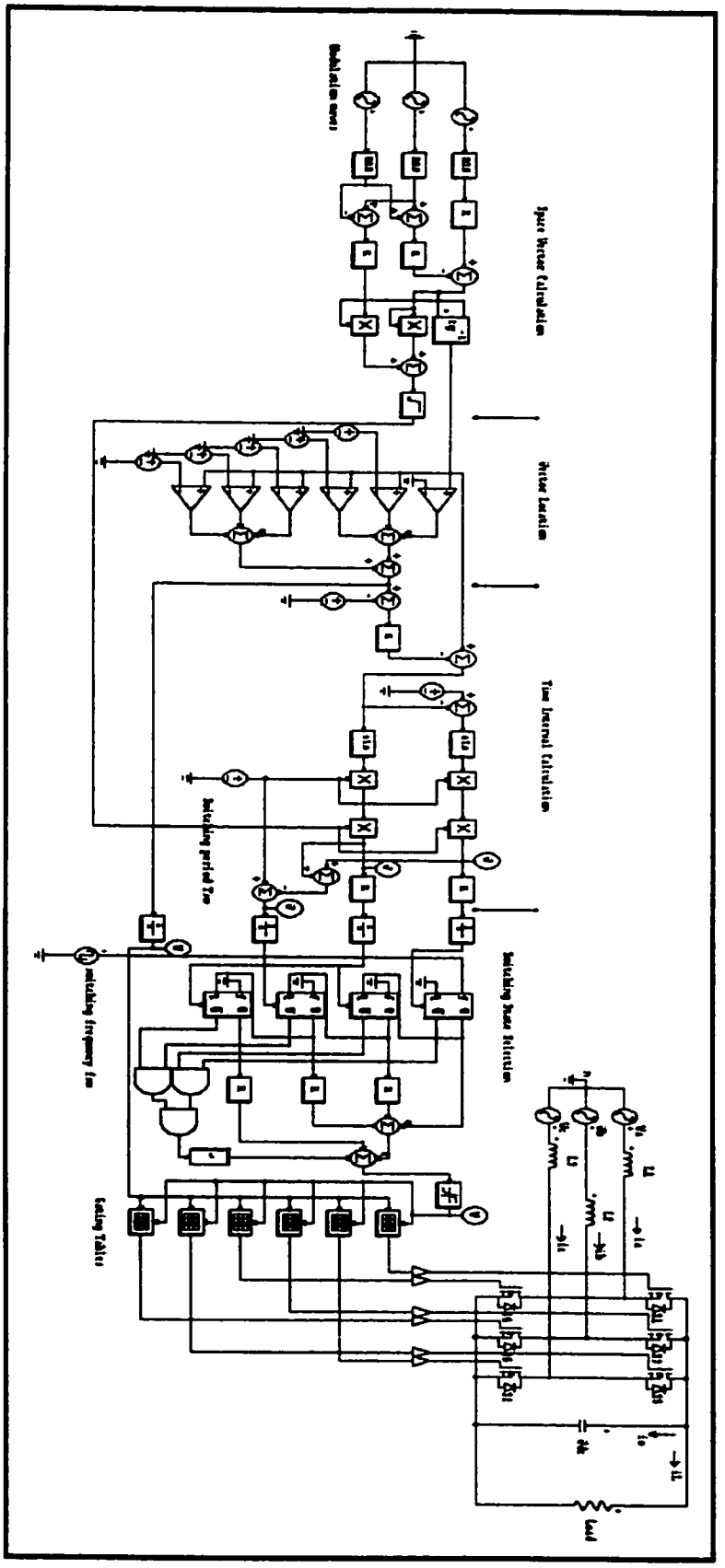

Figure 6-2.1. Digital Implementation of the Space Vector PWM 3-PhaseRectifier under Balanced Input Voltage and Unbalanced Input Line Impedance Open Loop.

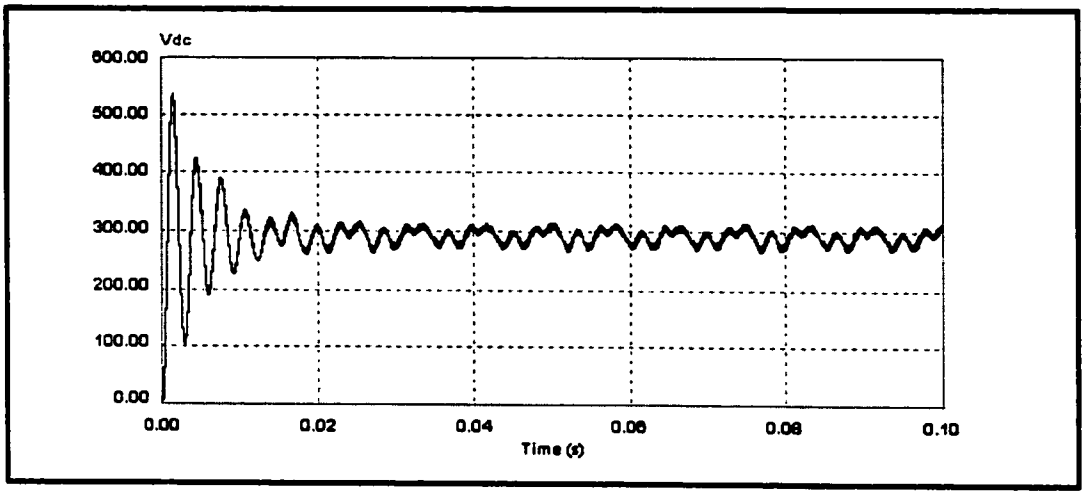

Figure 6-2.1.1.2. Output Voltage under Unbalanced Input Voltage and Balanced Input Line Impedance Open Loop

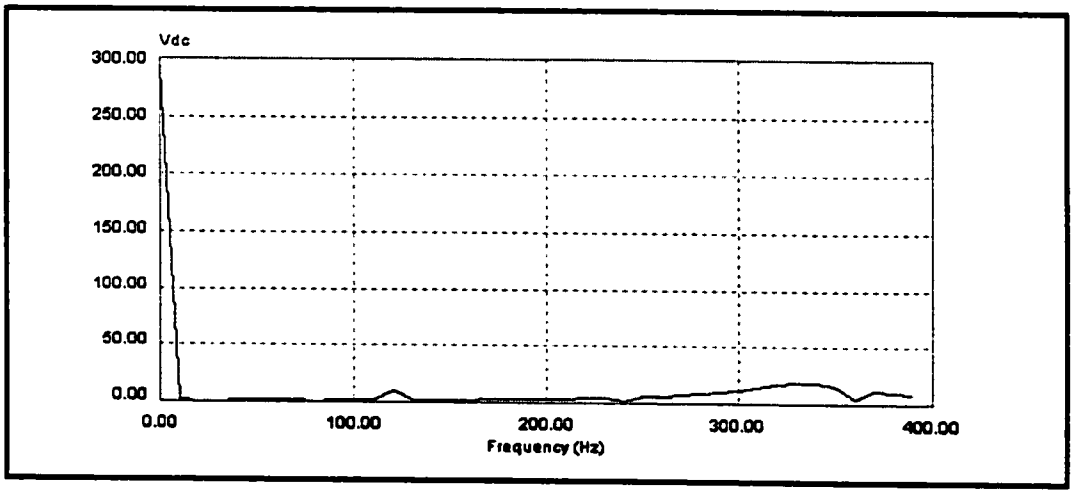

Figure 6-2.1.1.3. Frequency Spectrum of the Output Voltage under Unbalanced Input Voltage and Balanced Input Line Impedance Open Loop

Figures 6-2.1.1.2 and 6-2.1.1.3 show the output dc voltage and its frequency spectrum. As can be seen, there are harmonics (2^{nd} order) present at the output of the converter. The steady-state error, average output voltage and the ripple content are as shown below.

$$V_{output,ripple} = \Delta V_{max,min} = 310 - 283.00 = 27V$$

$$\%Ripple = \frac{\Delta V_{max,min}}{V_{avg}} \times 100\% = \frac{27}{291.5} \times 100\% = 9.1\%$$

Average output Voltage = 291.5 giving rise to an 9.8 % steady - state error

Rise Time = 0.001 - Sec

6.2.1.2 Unbalanced Input Voltage and Balanced Input Line Impedance using Reference [19] Control Method (closed Loop)

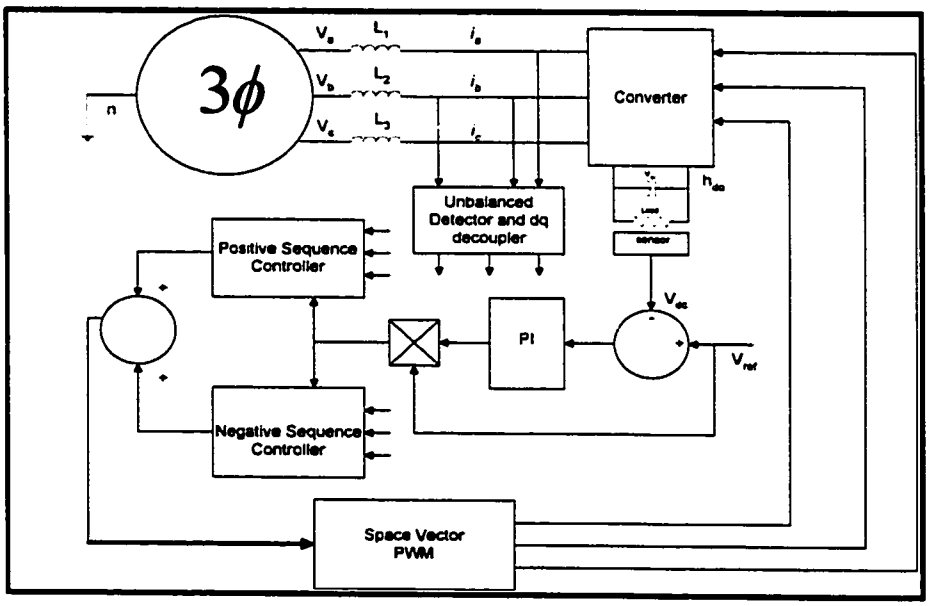

Figure 6-2.1.2.1. Reference [19]'s Unbalanced Input Voltage and Balanced Input Line Impedance (Closed Loop)

To show that unbalanced operating conditions do not result in harmonics, the PWM rectifier Figure 6-2.1.2.1 was simulated using PSIM.

The parameters are as follows:

Input voltages, $V_a = 165V$, $V_b = 170V$ and $V_c = 160V$

Line impedance (per phase), L1 = L2 = L3 = 3.5mH

Fundamental frequency, $f = 60hz$

Output capacitor, $C = 10000\mu F$

Switching frequency, $f_s = 10Khz$

Output load (resistive), R = 100 ohms

Reference voltage (set point) = 270 Voltage

Gain = 0.5

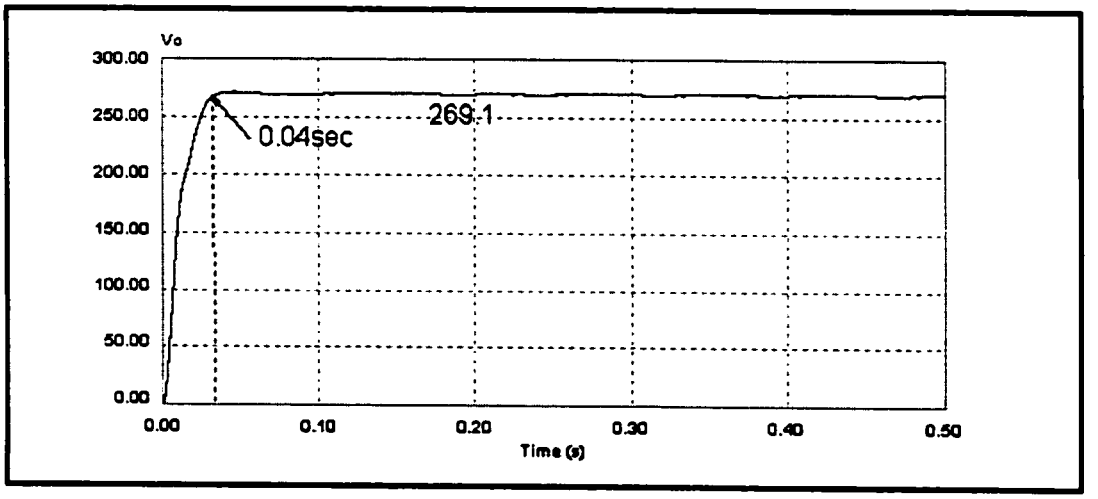

Figure 6-2.1.2.2. Reference [19]'s Output Voltage under Unbalanced Input Voltage and Balanced Input Line Impedance (Control loop)

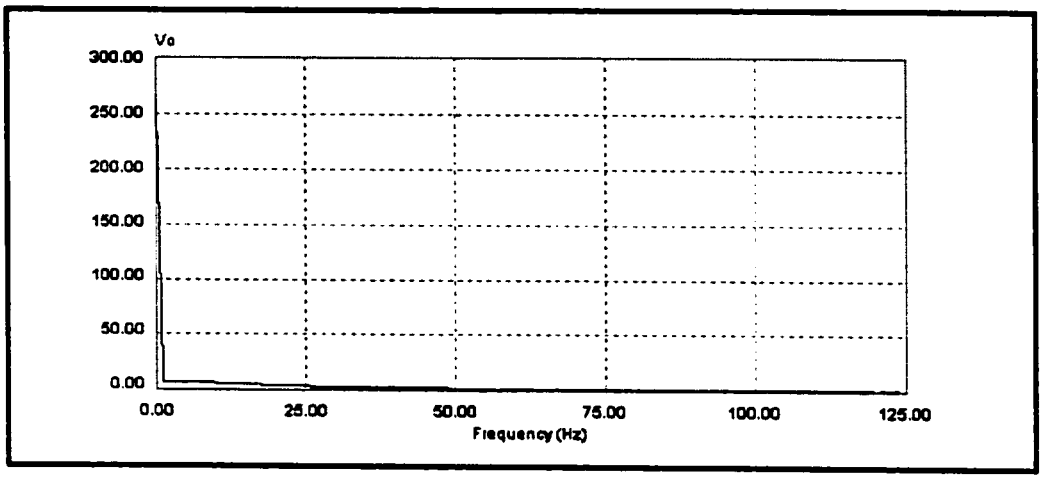

Figure 6-2.1.2.3. Reference [19]'s Frequency Spectrum Output Voltage under Unbalanced Input Voltage and Balanced Input Line Impedance (Control loop)

As can be seen from the output waveform Figures 6.2.1.2.2 and 6.2.1.2.3 there are no harmonics. The steady-state error and ripple content are as shown below.

$$V_{output,ripple} = \Delta V_{max,min} = 270 - 269.1 = 0.9V$$

$$\%Ripple = \frac{\Delta V_{max,min}}{V_{avg}} \times 100\% = \frac{0.9}{269.5} \times 100\% = 0.33\%$$

Average output Voltage = 269.5 giving rise to a 0.17 % steady - state error

Rise Time = 0.04 - Sec

6.2.1.3 Unbalanced Input Voltage and Balanced Input Line Impedance Lyapunov Control Method - Closed Loop.

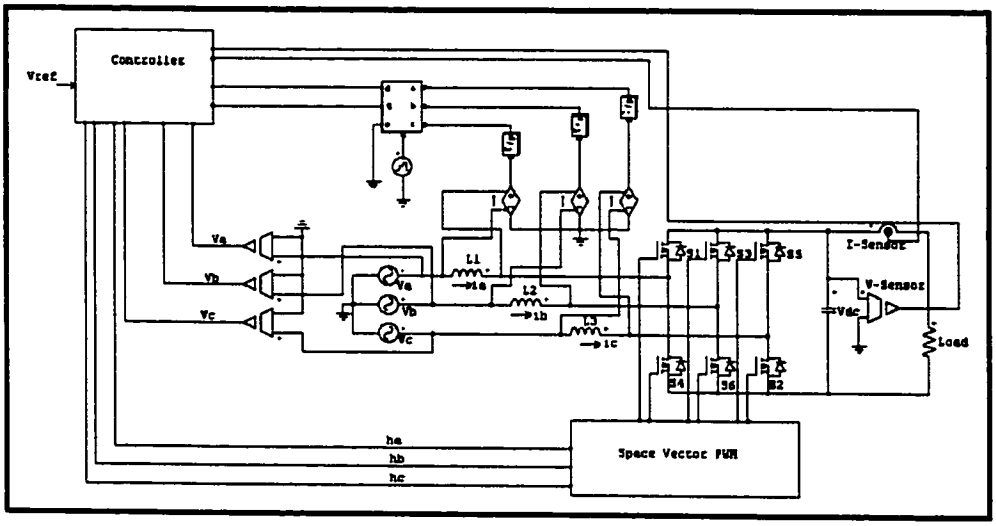

Figure 6-2.1.3.1. Unbalanced Input Voltage and Balanced Line Impedance Lyapunov Control Method (Closed Loop).

To show that unbalanced operating conditions do not result in harmonics given a wider range of unbalanced in input voltage, the Boost Type PWM rectifier Figure 6-2.1.3.1 was simulated using PSIM.

The parameters are as follows:

Input voltages, $V_a = 165V$, $V_b = 170V$ and $V_c = 160V$

Line impedance (per phase), L1 = L2 = L3 = 3.8mH

Fundamental frequency, $f = 60hz$

Output capacitor, $C = 10000\mu F$

Switching frequency, $f_s = 10Khz$

Output load (resistive), R = 100 ohms

Reference voltage (set point) = 270 Voltage

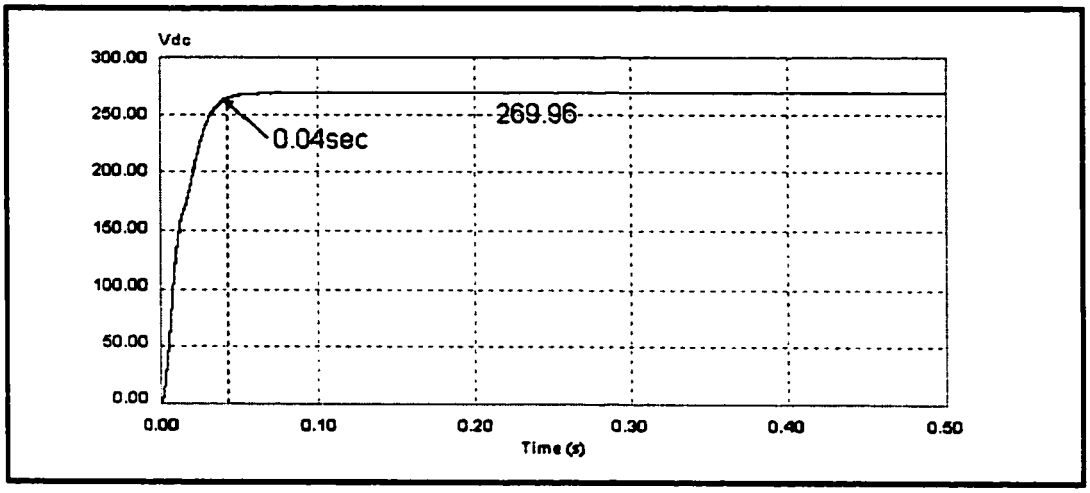

Figure 6-2.1.3.2. Output Voltage under Unbalance Input Voltage and Balanced Line Impedance using Lyapunov Based Control

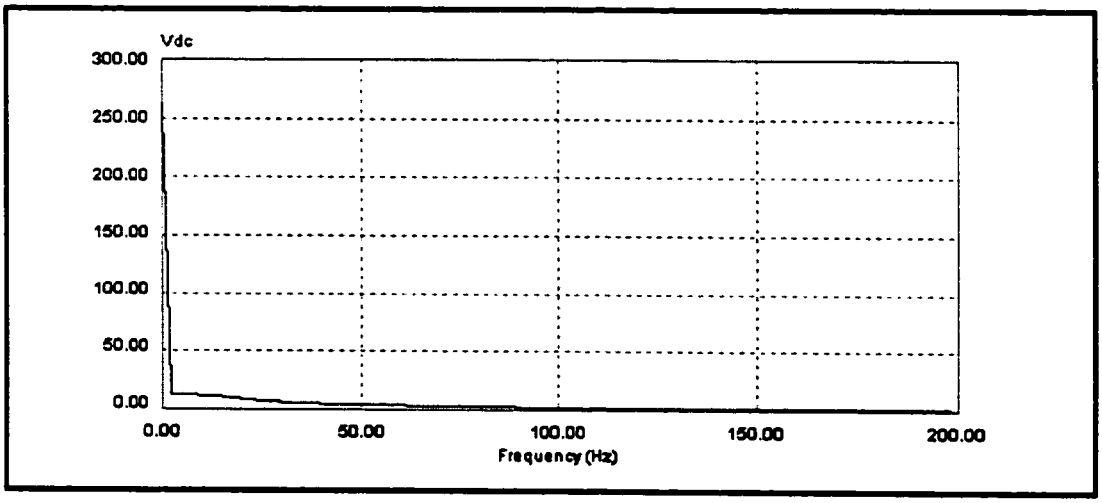

Figure 6-2.1.3.3. Frequency Spectrum of the Output Voltage under Unbalanced Input Voltage and Balanced Line Impedance using Lyapunov Based Control

As can be seen from the output waveform Figures 6.2.1.3.2 and 6.2.1.3.3 there are no harmonics.

$$V_{output,ripple} = \Delta V_{max,min} = 270 - 269.96 = 0.04V$$

$$\%Ripple = \frac{\Delta V_{max,min}}{V_{avg}} \times 100\% = \frac{0.04}{269.98} \times 100\% = 0.0148\%$$

Average output Voltage = 269.98 giving rise to a 0.007 % steady - state error
Rise Time = 0.04 - Sec

6.2.2 Balanced Input Voltage and Unbalanced Input Line Impedance

In this section we simulate the PWM rectifier under balanced input voltage and unbalanced input line impedance. The PWM is simulated first by using open loop control then by reference [19] closed loop control method and finally by the proposed Lyapunov closed loop control method.

6.2.2.1 Balanced Input Voltage and Unbalanced Input Line Impedance (Open Loop)

To show that unbalanced operating conditions due to imbalance in the impedance will result in harmonics at the converters output and input, the Boost Type PWM rectifier Figure 6-2.1.1.1 was simulated using PSIM.

The parameters are as follows:

Input voltages, V_a = 170V, V_b = 170V and V_c = 170V

Line impedance (per phase), L1 = 1m,L2 = 5mH and L3 = 10mH

Fundamental frequency, f = 60hz

Output capacitor, C = 10000μF

Switching frequency, f_s = 10Khz

Output load (resistive), R = 100 ohms

Reference Voltage = 270 Volts

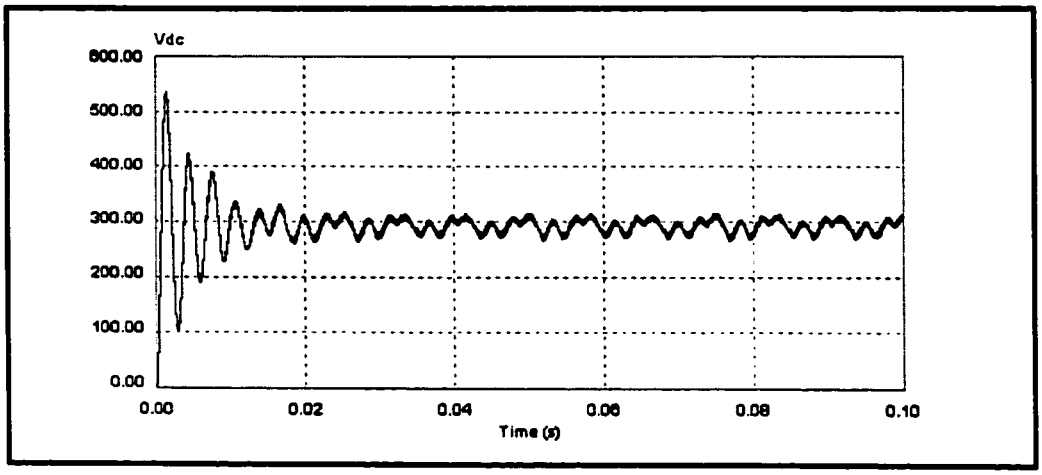

Figure 6-2.2.1.1. Output Voltage under Balanced Input Voltage and Unbalanced Input Line Impedance (Open Loop)

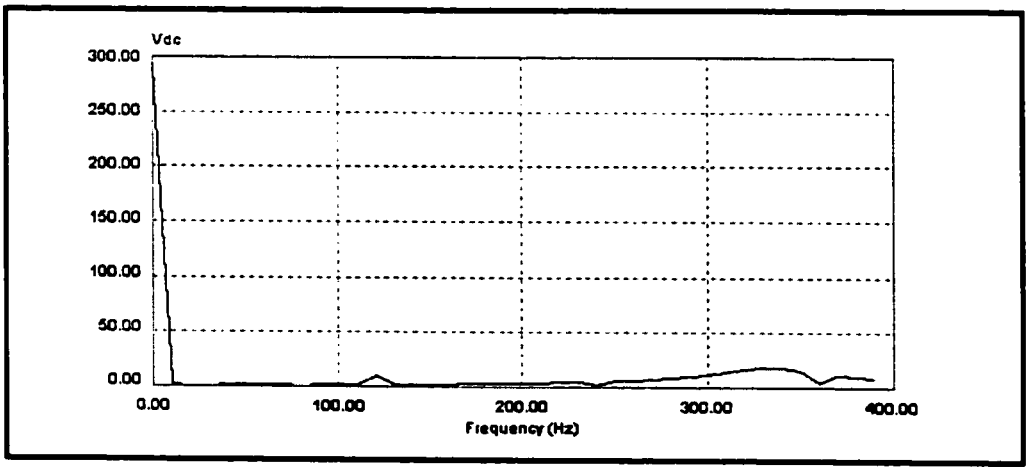

Figure 6-2.2.1.2. Frequency Spectrum of the Output Voltage under Balanced Input Voltage and Unbalanced Input Line Impedance (Open Loop)

Figures 6-2.2.1.1 and 6-2.2.1.2 show the output dc voltage and its frequency spectrum. As can be seen, there are harmonics (2^{nd} order) present at the output of the converter. The steady-state error and ripple content are as shown below including the rise time.

$$V_{output,ripple} = \Delta V_{max,min} = 310 - 283.00 = 17V$$

$$\%Ripple = \frac{\Delta V_{max,min}}{V_{avg}} \times 100\% = \frac{27}{291.5} \times 100\% = 9.1\%$$

Average output Voltage = 296.5 giving rise to an 9.8 % steady - state error

Rise Time = 0.001 - Sec

6.2.2.2 Balanced Input Voltage and Unbalanced Input Line Impedance using Reference [19] Control Method (closed Loop)

To show that unbalanced operating conditions due to imbalance in the input line impedance will not result in harmonics at the converter output and input, the Boost Type PWM rectifier reference [19] was simulated using PSIM.

The parameters are as follows:

Input voltages, V_a =170V, V_b = 170V and V_c = 170V

Line impedance (per phase), L1 =7mH, L2 = 5mH, and L3 = 10mH

Fundamental frequency, f = 60hz

Output capacitor, C = 10000μF

Switching frequency, f_s = 10Khz

Output load (resistive), R = 100 ohms

Reference voltage (set point) = 270 Voltage

Gain = 0.5

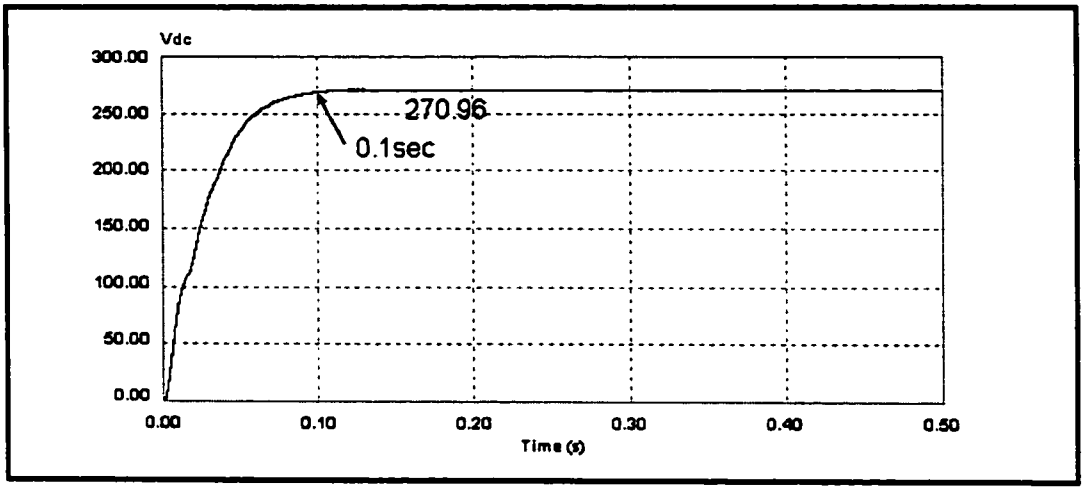

Figure 6-2.2.1.1 Reference [19]'s Output Voltage under Balanced Input Voltage and Unbalanced Input Line Impedance (closed Loop)

Figures 6-2.2.2.1 and 6-2.2.2.2 show the output dc voltage and its frequency spectrum. As can be seen, there are no harmonics present. The steady-state error and ripple content are as shown below including the rise time.

$$V_{output,ripple} = \Delta V_{max,min} = 270.96 - 270 = 0.96V$$

$$\%Ripple = \frac{\Delta V_{max,min}}{V_{avg}} \times 100\% = \frac{0.96}{270.48} \times 100\% = 0.35\%$$

Average output Voltage = 270.48 giving rise to a = 0.17% steady - state error

Rise Time = 0.1 - Sec

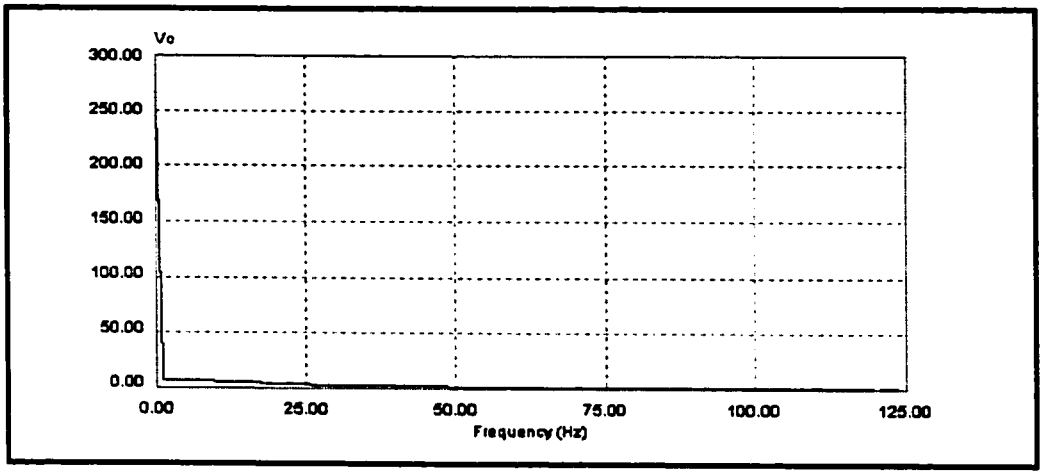

Figure 6-2.2.2.2 Reference [19]'s Frequency Spectrum Output Voltage under Balanced Input Voltage and Unbalanced Input Line Impedance (closed Loop)

6.2.2.3 Balanced Input Voltage and Unbalanced Input Line Impedance using Lyapunov Control Method (closed Loop)

To show that balanced operating conditions do not result in harmonics, the Boost Type PWM rectifier was simulated using PSIM.

The parameters are as follows:

Input voltages, $V_a = 170V$, $V_b = 170V$ and $V_c = 170V$

Line impedance (per phase), L1 = 10m,L2 = 8mH and L3 = 10mH

Fundamental frequency, $f = 60hz$

Output capacitor, C = 10000μF

Switching frequency, $f_s = 10Khz$

Output load (resistive), R = 100 ohms

Reference voltage (set point) = 270 V

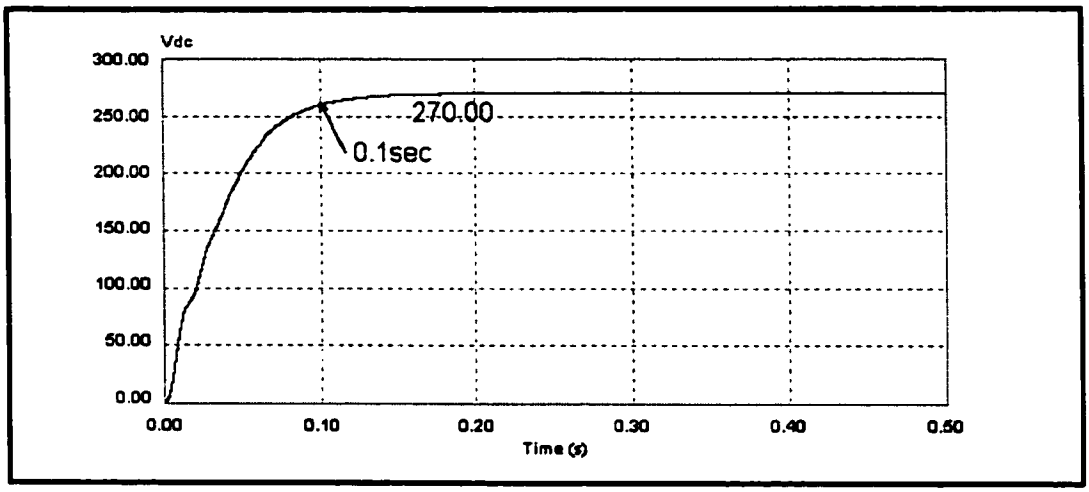

Figure 6-2.2.3.1. Output Voltage under Balance Input

Voltage and Unbalanced Line Impedance using Lyapunov Based Control

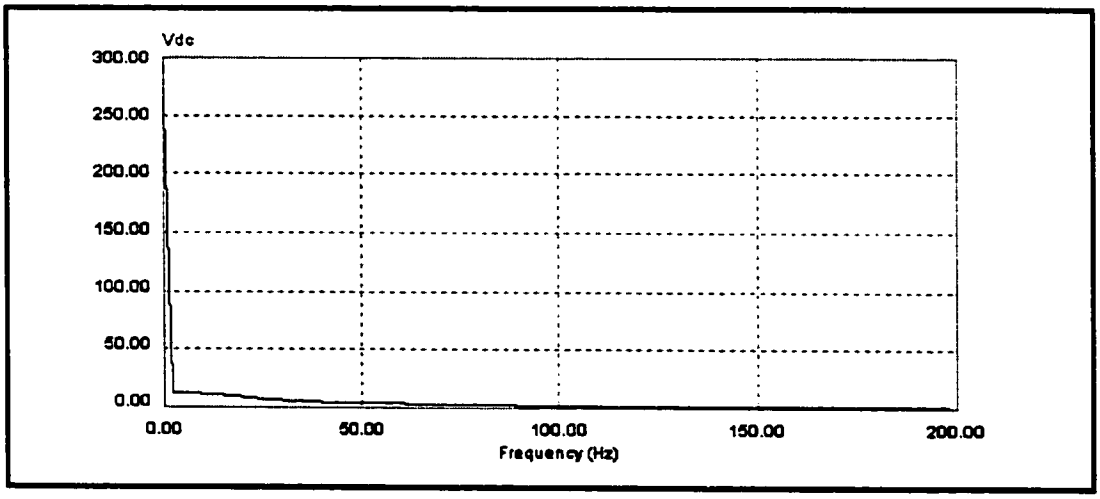

Figure 6-2.2.3.2. Frequency Spectrum of the Output Voltage under Balanced Input

Voltage and Unbalanced Line Impedance using Lyapunov Based Control

Figures 6-2.2.3.1 and 6-2.2.3.2 show the output dc voltage and its frequency spectrum. As can be seen, there are no harmonics present. The steady-state error and the ripple content are as shown below including the rise time.

$$V_{output,ripple} = \Delta V_{max,min} = 270 - 270 = 0V$$

$$\%Ripple = \frac{\Delta V_{max,min}}{V_{avg}} \times 100\% = \frac{0}{270} \times 100\% = 0\%$$

Average output Voltage = 270 giving rise to a 0% steady - state error

Rise Time = 0.1 - Sec

6.2.3 Robustness (Severe Unbalanced in Input Voltage and Balanced Input Line Impedance and Severe Unbalanced in Input Line Impedance and Balanced Input Voltage)

In this section we simulate the PWM rectifier under severe unbalanced input voltage and balanced input line impedance and under severe unbalanced input line impedance and balanced input voltage. The PWM is simulated first by using open loop control then by reference [19] closed loop control method and finally by the proposed Lyapunov closed loop control method.

6.2.3.1 Unbalanced Input Voltage and Balanced Input Line Impedance (Severe case)

To show that unbalanced operating conditions do not result in harmonics given a wider range of unbalanced in input voltage and input line impedance, the Boost Type PWM rectifier was simulated using PSIM. The parameters are as follows:

Input voltages, $V_a = 60V$, $V_b = 170V$ and $V_c = 60V$ (severe unbalanced condition)

Line impedance, L1 = L2 = L3 = 3.8mH (balanced condition)

Fundamental frequency, $f = 60hz$

Output capacitor, C = 10000μF

Switching frequency, f_s = 10Khz

Output load (resistive), R = 100 ohms

Reference voltage (set point) = 270 Voltage

From the open loop simulation result, the 2nd harmonic is present at the output of the converter where as, the third harmonic is present at the input of converter. In the closed loop configuration both reference [19] and the Lyapunov control method offer good results at the same rise time (0.06-sec). The results are as shown below.

$$V_{output,ripple} = \Delta V_{\max,\min} = 270 - 269.1 = 0.9V$$

$$\%Ripple = \frac{\Delta V_{\max,\min}}{V_{avg}} \times 100\% = \frac{0.9}{269.5} \times 100\% = 0.33\%$$

Average output voltage = 269.5 giving rise to a 0.17 % steady - state error

Rise Time = 0.06 - Sec

} Reference [19]

$$V_{output,ripple} = \Delta V_{\max,\min} = 270 - 269.98 = 0.04V$$

$$\%Ripple = \frac{\Delta V_{\max,\min}}{V_{avg}} \times 100\% = \frac{0.04}{269.995} \times 100\% = 0.0148\%$$

Average output Voltage = 269.995 giving rise to a 0.007 % steady - state error

Rise Time = 0.06 - Sec

} Lyapunov control

6.2.3.2 Balanced Input Voltage and Unbalanced Input Line Impedance (Severe case)

To show that unbalanced operating conditions do not result in harmonics given a wider range of unbalanced in input voltage and input line impedance, the Boost Type PWM rectifier was simulated using PSIM. The parameters are as follows:

Input voltages, $V_a = 170V$, $V_b = 170V$ and $V_c = 170V$ (balanced condition)

Line impedance, L1 =1mH, L2 = 5mH and L3 = 8mH (severe unbalanced condition)

Fundamental frequency, $f = 60hz$

Output capacitor, C = 10000μF

Switching frequency, $f_s = 10Khz$

Output load (resistive), R = 100 ohms

Reference voltage (set point) = 270 Voltage

From the open loop simulation result, the 2nd harmonic is present at the output of the converter where as, the third harmonic is present at the input of converter. In the closed loop configuration both reference [19] and the Lyapunov control method offer good results at the same rise time (0.06-sec).

$$V_{output,ripple} = \Delta V_{max,min} = 270.96 - 270 = 0.96V$$
$$\%Ripple = \frac{\Delta V_{max,min}}{V_{avg}} \times 100\% = \frac{0.96}{269.48} \times 100\% = 0.35\%$$
Average output voltage = 269.48 giving rise toa 0.17 % steady - state error
Rise Time = 0.06 - Sec

} Reference [19]

$$V_{output,ripple} = \Delta V_{max,min} = 270 - 269.96 = 0.04V$$
$$\%Ripple = \frac{\Delta V_{max,min}}{V_{avg}} \times 100\% = \frac{0.04}{269.98} \times 100\% = 0.0148\%$$
Average output Voltage = 296.8 giving rise t a 0.007% steady - state error
Rise Time = 0.06 - Sec

} Lyapunov control

However, the Lyapunov control method gives an output closer to the desired value as the calculations of the percent ripple and steady-state error show. Under severer unbalanced input line impedance and balanced input voltage, both systems again offer good results with the Lyapunov control method offering an output closer to the desired value. Both systems exhibit stability with little or no significant change in percent error as compare to smaller range in unbalanced input voltage or unbalanced input line impedance.

6.3 Comparison of Lyapunov Based Controlled Method and Reference [19] Controlled Method

In this section we perform a comparative analysis between the proposed Lyapunov based control method and the proportional plus integral control method by reference [19]. Basically, we examine the amount of error in the output voltage and current waveforms. The waveforms are further examined for other factors such as rise time, dynamic response, stability and harmonic content.

6.3.1 Error in Output Voltage and Current under Proposed Lyapunov Control Method

The following is the computation of the amount of Error in the output voltage and current observed from the simulation results. The presence of Error in these waveforms is due primarily to the high switching frequency 10KHz switching operation.

Under minimum unbalanced input voltage (165V, 170V, 160V) and balanced input line impedance the percent error in the output voltage is,

$$V_{Error} = V_{ref} - V_{dc} = 270 - 269.98 = 0.02V$$
$$\%Error = \frac{V_{Error}}{V_{ref}} \times 100\% = \frac{0.02}{270} \times 100\% = 0.007\%$$

Under severe unbalanced input voltage (60V, 170V, 60V) and balanced input line impedance the percent error in the output voltage is,

$$V_{Error} = V_{ref} - V_{dc} = 270 - 269.98 = 0.02V$$
$$\%Error = \frac{V_{Error}}{V_{ref}} \times 100\% = \frac{0.02}{270} \times 100\% = 0.007\%$$

Under balanced input voltage (170V, 170V, 170V) and minimum unbalanced input line impedance (1mH, 2mH, 1mH) the percent error in the output voltage is,

$$V_{Error} = V_{ref} - V_{dc} = 270 - 270 = 0.0V$$
$$\%Error = \frac{V_{Error}}{V_{ref}} \times 100\% = \frac{0.0}{270} \times 100\% = 0.0\%$$

Under balanced input voltage (170V, 170V, 170V) and severe unbalanced input line impedance (1mH, 5mH, 10m) the percent error in the output voltage is,

$$V_{Error} = V_{ref} - V_{dc} = 270 - 270 = 0.0V$$
$$\%Error = \frac{V_{Error}}{V_{ref}} \times 100\% = \frac{0.0}{270} \times 100\% = 0.0\%$$

6.3.2. Error in Output Voltage under Reference [19] Control Method

Under minimum unbalanced input voltage (165V, 170V, 160V) and balanced input line impedance the percent error in the output voltage is,

$$V_{Error} = V_{ref} - V_{dc} = 270 - 269.55 = 0.45V$$
$$\%Error = \frac{V_{Error}}{V_{ref}} \times 100\% = \frac{0.45}{270} \times 100\% = 0.17\%$$

Under severe unbalanced input voltage (60V, 170V, 60V) and balanced input line impedance the percent error in the output voltage is,

$$V_{Error} = V_{ref} - V_{dc} = 270 - 269.55 = 0.45V$$

$$\%Error = \frac{V_{Error}}{V_{ref}} \times 100\% = \frac{0.45}{270} \times 100\% = 0.17\%$$

Under balanced input voltage (170V, 170V, 170V) and minimum unbalanced input line impedance (1mH, 2mH, 1m) the percent error in the output voltage is,

$$V_{Error} = V_{\max} - V_{dc} = 270.96 - 270. = 0.96V$$

$$\%Error = \frac{V_{Error}}{V_{\max}} \times 100\% = \frac{0.48}{270} \times 100\% = 0.17\%$$

Under balanced input voltage (170V, 170V, 170V) and severe unbalanced input line impedance (1mH, 5mH, 10mH) the percent error in the output voltage is,

$$V_{Error} = V_{ref} - V_{dc} = 270 - 269.55 = 0.45V$$

$$\%Error = \frac{V_{Error}}{V_{ref}} \times 100\% = \frac{0.45}{270} \times 100\% = 0.17\%$$

Looking at these values of percent error, it is fair to say that the proposed Lyapunov closed loop control method generally, has a smaller percent error in the output voltage as compare to the proportional integral feedback control method by Reference [19]. This is evident from the output waveforms of Lyapunov control method Figures 6-2.3.2 and the output waveform of the proportional control method by Reference 19 Figures 6-2.2.2. This case is further strengthened by their subsequent error calculations.

Under unbalanced input voltage and balanced input line impedance the waveforms from both control methods are shown in Figures 6-2.1.1– 6-2.2.1 above. As can be seen from the waveforms, there are no harmonics present at the output of the converters, however, further examination of the waveforms indicate that under Reference

[19] the converter has a lower output voltage percentage wise as indicated by the calculation of the amount of error in the output voltage under magnification. That is, the output value of the proposed Lyapunov control method is closer to the desired value than the out value from reference's [19] control method. The phenomenon observed under unbalanced input voltage and balanced input line impedance was also present under balanced input voltage and unbalanced input line impedance. This is also true when the converter operates under severe unbalanced conditions. Under both simulated conditions, dynamic responses for both systems are good. There are no noticeable overshoots in both system response curves. Neglecting designing both system to achieve equal rise time, reference [19] generally has a smaller rise time leading to faster response as compared to the proposed Lyapunov control method. However, the Lyapunov control technique leads to slower response, increased stability, and is more robust as compare to the Proportional Integral closed loop control method. This is supported by the fact that a small increase in gain under reference [19] throws the system into oscillation. Also, the Lyapunov control method gives great flexibility in the choice of selecting Lyapunov parameters. Advantages of reference [19] control method include, simple control loop and easy of implementation. Disadvantages include but not limited to oscillation as the gain of the controller is increased. Table 6-3.2.1 and 6-3.2.2 shows the comparison between the two control methods.

Table 6-3.2.1. Comparisons Between Proposed Control Method And Reference [19] Control Method Unbalanced Input Voltage and Balanced Input Line Impedance

	Reference [19]	Lyapunov
Minimum Unbalanced	Input Voltage(165V,170V,160V)	Input Voltage(165V,170V,160V)
Rise Time	0.04-Sec	0.04 -Sec
Error	0.17%	0.007%
Ripple	0.33%	0.0148%
Overshoot	None	None
Severe Unbalanced	Input Voltage (60V,170V,160V)	Input Voltage(60V,170V,160V)
Rise Time	0.06-Sec	0.06-Sec
Error	0.17%	0.0148%
Ripple	0.33%	0.007%
Overshoot	None	None

Table 6-3.2.2. Comparison between Lyapunov and Reference [19] Control under Balanced Input Voltage and Unbalanced Input Line Impedance.

	Reference [19]	Lyapunov
Minimum Unbalanced	Input Line Impedance (1mH, 5mH, 8mH)	Input Line Impedance (1mH, 5mH, 8mH)
Rise Time	0.1-Sec	0.1-Sec
Error	0.35%	0.0%
Ripple	0.17%	0.0%
Overshoot	None	None
Severe Unbalanced	Input Line Impedance (1mH, 10mH, 1H)	Input Line Impedance (1mH, 10mH, 1mH)
Rise Time	0.06-Sec	0.06-Sec
Error	0.17%	0.007%
Ripple	0.33%	0.0148%
Overshoot	None	None

CHAPTER VII

CONCLUSION AND FUTURE RESEARCH

In this section, a summary of the research and recommendations for future work are presented.

7.1 Summary and Conclusion

The main objective of this research was to develop a controller based on Lyapunov direct method that could be used to increase the performance of the Boost Type PWM Rectifier when subjected to unbalanced input voltages and unbalanced line impedance. Steady state equations to the system are obtained. Based on the open loop steady state solution, a closed loop solution is proposed based on Lyapunov's method. Specifically, a Lyapunov function for the Pulse Width Modulation Boost Type rectifier is constructed.

Simulation results show very good response and stable operation of the Boost Type PWM Rectifier under unbalanced operating conditions when the proposed control technique is applied. The proposed solution utilizes the space vector Pulse Width Modulation technique along with a Lyapunov based controller. The desired output

voltage is obtained by utilizing a reference voltage V_{ref} to force the output voltage to the desired levels by comparing the dc output to the V_{ref} and using the difference to adjust the duty ratio of the space vector Pulse Width Modulator.

This research presents a proof of the proposed control technique to cancel harmonics and at the same time maintain system stability. Computer simulations are developed using PSIM. System stability and harmonic cancellation were verified by using several different models representing several different levels of imbalance in the system. These models include

a. Balanced input voltage and unbalanced line impedance.

b. Unbalanced line impedance and balanced input voltage.

Simulation results prove that both harmonics and stability can be achieved at the same time when the PWM Boost Type Rectifier operates under unbalanced conditions. This proposed control method can be very useful in the application of the Pulse Width Modulation Inverter for variable speed drives where second harmonics at the DC bus can cause significant harm to the electric machine.

Earlier research based on Lyapunov's direct method addresses disturbance such as step change in reference voltage and load current in balanced system These parameters are independent of the system dynamics. Therefore, the two methods yield different results.

7.2 Suggestions for Future Research

Naturally, an extension of the research presented should include but not be limited to the following:

1. The hardware implementation of the Lyapunov based control of the PWM Boost Type Rectifier under unbalanced operating condition to verify system feasibility.
2. Improve control technique so as to allow the system to operate from a single voltage source.
3. The system could be simulated and implemented using other Sinusoidal PWM control techniques.
4. Though the control technique presented in this work is for AC-DC converters, the general idea could be used to implement DC – AC converters.
5. The study could be extended to AC-DC-AC converters.

REFERENCES

[1] T. Wildi, **Electrical machines, drives, and power system**, 4th edition, Prentice-Hall, Inc. 2000.

[2] A. Stankovic, "**Input-Out Harmonic Elimination of the PWM boost type rectifier under unbalanced operating condition,**" Ph.D. Dissertation, University of Wisconsin-Madison, 1998

[3] J. W. Wilson, "The forced-commutated inverter as a regenerative rectifier" **IEEE Transactions on Industrial Application,** Volume 1A-14, no. 4, July/August 1978.

[4] L. Moran, P. D. Ziogas and G. Joos, "Design aspects of synchronous PWM rectifier-inverter systems under unbalanced Input voltage conditions", **IEEE Transactions on Industrial Application,** Volume 28, no. 6, Nov/Dec 1992.

[5] P. D. Ziogas, Y. Kang, and V. R. Stefanovic,"Rectifier-inverter Frequency Changers with suppressed dc link components," **IEEE Transactions on Industrial Application,** Volume 1A-14, no. 4, July/August 1978.

[6] X. Liang MA, "High-performance PWM frequency changers " IEEE Transactions on Industrial Application, Volume 1A-22, no. 2, March/April 1986.

[7] J.W. Dixon and B.T. Ooi, "Indirect current control of a unity power factor sinusoidal current boost type three-phase rectifier," **IEEE Transactions on Power Electronics,** Volume 35, no. 4. pp. 508-515, 1988.

[8] R.Wu. S.B. Dewan, and G.R. Slemon, "Analysis of an ac-to-dc voltage source converter using PWM with phase and amplitude control," **IEEE Transactions on Industrial Application,** Volume 27, no. 2. pp. 355-364, 1991.

[9] J. Choi and S. Sul, "Fast current controller in three-phase ac/dc boost converter using d-q axis crosscoupling" **IEEE Transactions on Power Electronics,** Volume 13, no. 1, January 1998.

[10] J.W. Dixon, A. B. Kulkarni, M. Nishimoto, and B.T. Ooi, "Characteristics of a control-current PWM rectifier-inverter link." **IEEE Transactions on Industrial Application,** Volume 1A-23, no. 6. pp. 1022-1028, 1987.

[11] J.W. Dixon, J. C. Salmon, A. B. Kulkarni, and B.T. Ooi, "A three-phase controlled-current PWM rectifier with leading power factor." **IEEE Transactions on Industrial Application,** Volume 1A-23, no. 1. pp. 78-84, 1987.

[12] D.R. Veas, J.W. Dixon and B.T. Ooi, "A novel load current control method for leading power factor voltage source PWM rectifier," **IEEE Transactions on Power Electronics,** Volume 9, no.2. pp. 153-159, 1994.

[13] H. Komurcugil and O. Kukrer," Novel current-control method for three-phase PWM ac/dc voltage source converters," **IEEE Transactions on Industrial Electronics,** Volume 46, no.3. pp. 544-553, 1999.

[14] S. R. Sanders and G. C. verghese, " Lyapunov-based control for switching power converters, **IEEE Transactions on Power Electronics,** Volume 7, no.1. pp. 17-24, 1992.

[15] N. Kawasaki, H. Nomura, and M. Masuhiro, " A new control law of bilinear dc-dc converters developed by direct application of Lyapunov," **IEEE Transactions on Power Electronics,** Volume 10, no.3. pp. 318-325, 1995.

[16] A. Draou, Y. Sato, and T. Kataoka, " A new state feedback based transient control of PWM ac to dc voltage type converter," **IEEE Transactions on Power Electronics,** Volume 10, no.6. pp. 716-724, 1995.

[17] P. N. Enjeti and S. A. Choudhenry, " A new control strategy to improve the performance of a PWM AC to DC converter under unbalanced operating conditions," **IEEE Transactions on Power Electronics,** Volume 8, October 1993.

[18] P. Rioual, H. Pouliquen, and J. Louis, "Regulation of a PWM rectifier in the unbalanced network state using a generalized model," **IEEE Transactions on Power Electronics,** Volume 11,pp, 495-502, May 1996.

[19] H. Song and K. Nam, " Dual current control scheme for PWM converter under unbalanced input voltage conditions", **IEEE Transactions on Power Electronics,** Volume 46, no. 5, October 1999.

[20] T. G. Habetler, " A space vector-based rectifier regulator for ac/dc/dc converter," **IEEE Transactions on Power Electronics,** Volume 8, no.1. pp. 30-36, 1993.

[21] T. Ohnuki, O. Miyashita, P. Lataire, and G. Maggetto, "Control of a three-phase rectifier using estimated ac-side and dc-side voltages", **IEEE Transactions on Power Electronics,** Volume 14, no. 2, March 1999.

[22] I. Panahi, Z. Yu, and M. Arefeen,"**Generate advanced PWM signals using DSPs**", Electronics Design, pp. 83-90, 1998.

[23] H. Komurcugil and O. Kukrer," Lyapunov-based control for three-phase PWM ac/dc voltage-source converters," **IEEE Transactions on Industrial Electronics,** Volume 12, no.5. pp. 801-813, 1998.

[24] J. Duncan Glover and Mulukuta Sama, **Power System Analysis and Design** 2nd edition, PWS Publishing Company, 1987.

[25] Mohan, N., T.M. Undeland, W.P. Robbins, **Power Electronics**, Wiley, New York, 1995.

[26] Rashid, M.H., **SPICE For Circuits And Electronics Using Pspice**, Prentice Hall, New Jersey, 1990.

APPENDIX A

Derivation of the Sequence Components

Derivation of the Positive Sequence magnitude and Phase angle

Generally, the voltage vector is given by

$$V_{sp} = (V_d^p + V_q^p)e^{i\omega t} + (V_d^n + V_q^n)e^{-i\omega t} \quad \text{(A1)}$$

which represents the positive and the negative sequence voltages in real and imaginary parts.

The positive sequence space vector, V_{sp}^p, is expressed as

$$V_{sp}^p = \frac{2}{3}\left(V_a(t) + uV_b(t) + u^2V_c(t)\right), \text{ where } u = 1\underline{/120^0} \text{ and } u^2 = 1\underline{/240^0} \quad \text{(A2)}$$

As shown earlier in Chapter III

$$V_a(t) = |V^0|\sin(\omega t + \theta_v^0) + |V|^p \sin(\omega t + \theta_v^p) + |V^n|\sin(\omega t + \theta_v^n)$$

$$V_b(t) = |V^0|\sin(\omega t + \theta_v^0) + |V^p|\sin(\omega t + \theta_v^p + \frac{4\pi}{3}) + |V^n|\sin(\omega t + \theta_v^n + \frac{2\pi}{3})$$

$$V_c(t) = |V^0|\sin(\omega t + \theta_v^0) + |V^p|\sin(\omega t + \theta_v^p + \frac{2\pi}{3}) + |V^n|\sin(\omega t + \theta_v^n + \frac{4\pi}{3})$$

Substituting the above equations for $V_a(t)$, $V_b(t)$, and $V_c(t)$ in equation (A2) we get,

$$\frac{2}{3}[|V^0|\sin(\omega t+\theta_v^0)+|V^p|\sin(\omega t+\theta_v^p)+|V^n|\sin(\omega t+\theta_v^n)$$

$$-\frac{1}{2}|V^0|\sin(\omega t+\theta_v^0)-\frac{1}{2}|V^p|\sin(\omega t+\theta_v^p+\frac{4\pi}{3})-\frac{1}{2}|V^n|\sin(\omega t+\theta_v^n+\frac{2\pi}{3})$$

$$-\frac{1}{2}|V^0|\sin(\omega t+\theta_v^0)-\frac{1}{2}|V^p|\sin(\omega t+\theta_v^p+\frac{2\pi}{3})-\frac{1}{2}|V^n|\sin(\omega t+\theta_v^n+\frac{4\pi}{3})] \qquad \text{(A3)}$$

Simplification of (A3) gives

$$\mathrm{Re}(V_{sp})=\frac{2}{3}|V^p|[\sin(\omega t+\theta_v^p)-\frac{1}{2}\sin(\omega t+\theta_v^p+\frac{4\pi}{3})-\frac{1}{2}\sin(\omega t+\theta_v^p+\frac{2\pi}{3})]$$

$$+\frac{2}{3}|V^n|[\sin(\omega t+\theta_v^p)-\frac{1}{2}\sin(\omega t+\theta_v^n+\frac{2\pi}{3})-\frac{1}{2}\sin(\omega t+\theta_v^n+\frac{4\pi}{3})]$$

$$=|V^p|[\sin(\omega t+\theta_v^p)+|V^n|[\sin(\omega t+\theta_v^n) \qquad \text{(A4)}$$

Where Re (V_{sp}) indicates the real part of equation (A1)

By the same token,

$$\mathrm{Im}(V_{sp})=\frac{2}{3}|V^p|[\frac{\sqrt{3}}{2}\sin(\omega t+\theta_v^p+\frac{4\pi}{3})-\frac{\sqrt{3}}{2}\sin(\omega t+\theta_v^p+\frac{2\pi}{3})]$$

$$-\frac{2}{3}|V^n|[\frac{\sqrt{3}}{2}\sin(\omega t+\theta_v^n+\frac{2\pi}{3})-\frac{\sqrt{3}}{2}\sin(\omega t+\theta_v^n+\frac{4\pi}{3})]$$

$$=-|V^p|\cos(\omega t+\theta_v^p)+|V^n|\cos(2\omega t+\theta_v^n) \qquad \text{(A5)}$$

Where Im (V_{sp}) indicates the imaginary part of equation (A1)

Therefore

$$V_{sp}^p=\mathrm{Re}(V_{sp})+j\,\mathrm{Im}(V_{sp})$$

$$=[|V^p|\sin(\omega t+\theta_v^p)+|V^n|\sin(\omega t+\theta_v^n)]+[|V^p|\cos(\omega t+\theta_v^p)+|V^n|\cos(2\omega t+\theta_v^n)]j \qquad \text{(A6)}$$

Equation (A6) can be simplified by multiplying the real part of the positive sequence vector by $\sin\omega t$ and the imaginary part of the positive sequence vector by $\cos\omega t$.

That is,

$$V_{sp}^{p} = \mathrm{Re}|V_{sp}|\sin(\omega t) + \mathrm{Im}|V_{sp}|\cos(\omega t)$$

$$= [|V^{p}|\sin(\omega t + \theta_v^{p}) + |V^{n}|\sin(\omega t + \theta_v^{n})]\sin\omega t$$

$$- [|V^{p}|\cos(\omega t + \theta_v^{p}) + |V^{n}|\cos(2\omega t + \theta_v^{n})]\cos\omega t$$

$$= \frac{1}{2}|V^{p}|[\sin(\omega t + \theta_v^{p}) + \frac{1}{2}\sin\theta_v^{p} + \frac{1}{2}\sin(2\omega t + \theta_v^{p}) + \frac{1}{2}\sin\theta_v^{p}]$$

$$+ \frac{1}{2}|V^{n}|[\sin(2\omega t + \theta_v^{n}) + \frac{1}{2}\sin\theta_v^{n} + \frac{1}{2}\sin(2\omega t + \theta_v^{n}) + \frac{1}{2}\sin\theta_v^{n}]$$

$$= |V^{p}|\cos(\theta_v^{p}) - |V^{n}|\cos(2\omega t + \theta_v^{n}) \qquad \text{(A7)}$$

It is obvious that there is a second harmonic present and most be eliminated so as to be able to calculate the magnitude and phase angle of the vector. Taking the mean of equation (A7) we get the real component of the space vector as

$$X = \textbf{\textit{mean}}\{V^{p}\cos(\theta_v^{p}) - V^{n}\cos(2\omega t + \theta_v^{n})\}$$

$$= |V_{sp}^{p}|\cos(\theta_v^{p}) \qquad \text{(A8)}$$

Similarly, equation (A6) can again be simplified by multiplying the real part of the positive sequence vector by $\cos\omega t$ and the imaginary part of the positive sequence vector by $\sin\omega t$ and taking the sum.

That is,

$$V_{sp}^{p} = \mathrm{Re}|V_{sp}|\sin(\omega t) + \mathrm{Im}|V_{sp}|\cos(\omega t)$$

$$= [|V^{p}|\sin(\omega t + \theta_v^{p}) + |V^{n}|\sin(\omega t + \theta_v^{n})]\cos\omega t$$

$$+ [|V^p|\cos(\omega t + \theta_v^p) - |V^n|\cos(\omega t + \theta_v^n)]\sin \omega t$$

$$= \frac{1}{2}|V^p|[\sin(2\omega t + \theta_v^p) + \frac{1}{2}\sin\theta_v^p - \frac{1}{2}\sin(2\omega t + \theta_v^p) + \frac{1}{2}\sin\theta_v^p]$$

$$+ \frac{1}{2}|V^n|[\sin(2\omega t + \theta_v^n) + \frac{1}{2}\sin\theta_v^n + \frac{1}{2}\sin(2\omega t + \theta_v^n) + \frac{1}{2}\sin\theta_v^n]$$

$$= |V^p|\sin(\theta_v^p) + |V^n|\sin(2\omega t + \theta_v^n) \tag{A9}$$

Similarly, the imaginary component of the space vector is given by

$$Y = \textit{mean}\{|V^p|\sin(\theta_v^p) + |V^n|\sin(2\omega t + \theta_v^n)\}$$

$$= |V_{sp}^p|\sin(\theta_v^p) \tag{A10}$$

It is clear from equation (A8) and (A10) that the magnitude of the positive sequence space vector is

$$\sqrt{2}|V_{sp}^p| = \sqrt{X^2 + Y^2} \tag{A11}$$

and the phase angle is

$$\theta_v^p = \tan^{-1}\frac{Y}{X} \tag{A12}$$

Derivation of the Negative Sequence magnitude and Phase angle

Generally, the voltage vector is given by

$$V_{sp} = (V_d^p + V_q^p)e^{i\omega t} + (V_d^n + V_q^n)e^{-i\omega t} \tag{A13}$$

which represents the positive and the negative sequence voltages in real and imaginary parts. The positive sequence space vector, V_{sp}^n, is expressed as

$$V_{sp}^n = \frac{2}{3}\left(V_a(t) + u^2 V_b(t) + u V_c(t)\right) \tag{A14}$$

As shown earlier in Chapter III

$$V_a(t) = |V^0| \sin(\omega t + \theta_v^0) + |V^p| \sin(\omega t + \theta_v^p) + |V^n| \sin(\omega t + \theta_v^n)$$

$$V_b(t) = |V^0| \sin(\omega t + \theta_v^0) + |V^p| \sin(\omega t + \theta_v^p + \frac{4\pi}{3}) + |V^n| \sin(\omega t + \theta_v^n + \frac{2\pi}{3})$$

$$V_c(t) = |V^0| \sin(\omega t + \theta_v^0) + |V^p| \sin(\omega t + \theta_v^p + \frac{2\pi}{3}) + |V^n| \sin(\omega t + \theta_v^n + \frac{4\pi}{3})$$

Substituting the above equations for $V_a(t)$, $V_b(t)$, and $V_c(t)$ in equation (A14) we get

$$V_{sp}^n = \frac{2}{3}[|V^0| \sin(\omega t + \theta_v^0) + |V^p| \sin(\omega t + \theta_v^p) + |V^n| \sin(\omega t + \theta_v^n)$$

$$-\frac{1}{2}|V^0| \sin(\omega t + \theta_v^0) - \frac{1}{2}|V^p| \sin(\omega t + \theta_v^p + \frac{4\pi}{3}) - \frac{1}{2}|V^n| \sin(\omega t + \theta_v^n + \frac{2\pi}{3})$$

$$-\frac{1}{2}|V^0| \sin(\omega t + \theta_v^0) - \frac{1}{2}|V^p| \sin(\omega t + \theta_v^p + \frac{2\pi}{3}) - \frac{1}{2}|V^n| \sin(\omega t + \theta_v^n + \frac{4\pi}{3})]$$

Simplification of the above equation gives

$$\mathrm{Re}(V_{sp}) = \frac{2}{3}|V^p|[\sin(\omega t + \theta_v^p) - \frac{1}{2}\sin(\omega t + \theta_v^p + \frac{4\pi}{3}) - \frac{1}{2}\sin(\omega t + \theta_v^p + \frac{2\pi}{3})]$$

$$-\frac{2}{3}|V^n|[\sin(\omega t + \theta_v^n) - \frac{1}{2}\sin(\omega t + \theta_v^n + \frac{2\pi}{3}) - \frac{1}{2}\sin(\omega t + \theta_v^n + \frac{4\pi}{3})]$$

$$= |V^p| \sin(\omega t + \theta_v^p) + |V^n| \sin(\omega t + \theta_v^n) \qquad \text{(A15)}$$

By the same token,

$$\mathrm{Im}(V_{sp}) = \frac{2}{3}|V^p|[\frac{\sqrt{3}}{2}\sin(\omega t + \theta_v^p + \frac{4\pi}{3}) - \frac{\sqrt{3}}{2}\sin(\omega t + \theta_v^p + \frac{2\pi}{3})]$$

$$+\frac{2}{3}|V^n|[\frac{\sqrt{3}}{2}\sin(\omega t + \theta_v^n + \frac{2\pi}{3}) - \frac{\sqrt{3}}{2}\sin(\omega t + \theta_v^n + \frac{4\pi}{3})]$$

$$= |V^p| \cos(\omega t + \theta_v^p) + |V^n| \cos(2\omega t + \theta_v^n)$$

Therefore

$$V_{sp}^{p} = \mathrm{Re}\left|V_{sp}^{p}\right| - j\,\mathrm{Im}\left|V_{sp}^{p}\right|$$

$$= [\left|V^{p}\right|\sin(\omega t + \theta_{v}^{p}) + \left|V^{n}\right|\sin(\omega t + \theta_{v}^{n})] - [\left|V^{p}\right|\cos(\omega t + \theta_{v}^{p}) + \left|V^{n}\right|\cos(\omega t + \theta_{v}^{n})] \quad \text{(A16)}$$

Equation (A16) can be simplified by multiplying the real part of the positive sequence vector by $\sin\omega t$ and the imaginary part of the positive sequence vector by $\cos\omega t$.

That is,

$$V_{sp}^{p} = \mathrm{Re}\left|V_{sp}\right|\sin(\omega t) - \mathrm{Im}\left|V_{sp}\right|\cos(\omega t)$$

$$= [\left|V^{p}\right|\sin(\omega t + \theta_{v}^{p}) + \left|V^{p}\right|\sin(\omega t + \theta_{v}^{p})]\sin\omega t$$

$$-[\left|V^{p}\right|\cos(\omega t + \theta_{v}^{p}) + \left|V^{n}\right|\cos(\omega t + \theta_{v}^{n})]\cos\omega t$$

$$= \frac{1}{2}\left|V^{p}\right|[\sin(\omega t + \theta_{v}^{p}) + \frac{1}{2}\sin\theta_{v}^{p} + \frac{1}{2}\sin(2\omega t + \theta_{v}^{p}) + \frac{1}{2}\sin\theta_{v}^{p}]$$

$$+ \frac{1}{2}\left|V^{n}\right|[\sin(2\omega t + \theta_{v}^{n}) + \frac{1}{2}\sin\theta_{v}^{n} + \frac{1}{2}\sin(2\omega t + \theta_{v}^{n}) + \frac{1}{2}\sin\theta_{v}^{n}]$$

$$= \left|V^{n}\right|\sin(\theta_{v}^{n}) - \left|V^{p}\right|\sin(2\omega t + \theta_{v}^{p}) \quad \text{(A17)}$$

It is obvious that there is a second harmonic present and most be eliminated so as to be able to calculate the magnitude and phase angle of the vector. Taking the mean of equation (A17) we get the real component of the space vector as

$$X_{l} = \textbf{\textit{mean}}\{\left|V^{n}\right|\sin(\theta_{v}^{n}) + \left|V^{p}\right|\sin(2\omega t + \theta_{v}^{p})\}$$

$$= \left|V_{sp}^{n}\right|\sin(\theta_{v}^{n}) \quad \text{(A18)}$$

Similarly, equation (A18) can again be simplified by multiplying the real part of the positive sequence vector by $\cos\omega t$ and the imaginary part of the positive sequence vector by $\sin\omega t$ and taking the difference.

That is,

$$V_{sp}^{n} = \mathrm{Re}|V_{sp}|\sin(\omega t) + \mathrm{Im}|V_{sp}|\cos(\omega t)$$

$$= [|V^{p}|\sin(\omega t + \theta_v^{p}) + |V^{n}|\sin(\omega t + \theta_v^{n})]\cos\omega t$$

$$+ [|V^{p}|\cos(\omega t + \theta_v^{p}) - |V^{n}|\cos(\omega t + \theta_v^{n})]\sin\omega t$$

$$= \frac{1}{2}|V^{p}|[\sin(2\omega t + \theta_v^{p}) + \frac{1}{2}\sin\theta_v^{p} - \frac{1}{2}\sin(2\omega t + \theta_v^{p}) + \frac{1}{2}\sin\theta_v^{p}]$$

$$+ \frac{1}{2}|V^{n}|[\sin(2\omega t + \theta_v^{n}) + \frac{1}{2}\sin\theta_v^{n} + \frac{1}{2}\sin(2\omega t + \theta_v^{n}) + \frac{1}{2}\sin\theta_v^{n}]$$

$$= |V^{n}|\sin(\theta_v^{n}) + |V^{p}|\cos(2\omega t + \theta_v^{p}) \qquad \text{(A19)}$$

Similarly, the imaginary component of the space vector is give by

$$Y_1 = \textbf{\textit{mean}}\{|V^{n}|\cos(\theta_v^{n}) + |V^{p}|\cos(2\omega t + \theta_v^{p})\}$$

$$= |V_{sp}^{n}|\cos(\theta_v^{n}) \qquad \text{(A20)}$$

It is clear from equation (A18) and (A19) that the magnitude of the positive sequence space vector is

$$\sqrt{2}|V_{sp}^{n}| = \sqrt{X_1^2 + Y_1^2} \qquad \text{(A21)}$$

and the phase angle is

$$\theta_v^{n} = \tan^{-1}\frac{X_1}{Y_1} \qquad \text{(A22)}$$

Similar calculations have performed by [2,13,19].

APPENDIX B

MAPLE CODE FOR LYPUNOV CONTROL

This Appendix shows the Maple code that was used to solve for the Lyapunov equations shown in chapter V. Form Chapter III, the steady state equations for the control variable, switching function, maximum line current and the dc side voltage were developed. By substituting these equations and the state variable into the dynamic equations in the *dp* form, the Lyapunov function was obtained by the using the code listed below.

MAPLE CODE:

```
> eqn:=(omega*(L[1])*x[2]-((1/2)*(x[3]+V[r])*(2*(V[a])/V[r]+Delta*(h1[d]
> )))+V[a])*3*x[1];expand(");eqn1:=(omega*(L[2])*x[2]-((1/2)*(x[3]+V[r])
> *(2*(V[b])/V[r]+Delta*(h2[d])))+V[b])*3*x[1];expand(");eqn2:=(omega*(L
> [3])*x[2]-((1/2)*(x[3]+V[r])*(2*(V[c])/V[r]+Delta*(h3[d])))+V[c])*3*x[
> 1];expand(");eq1:=-(omega*(L[1])*(x[1]+I[max])+((1/2)*(x[3]+V[r])*((-2
> *omega*(L[1])*I[max]/V[r])+Delta*(h1[q])))*3*x[2];expand(");eq2:=-(om
> ega*(L[2])*(x[1]+I[max])+((1/2)*(x[3]+V[r])*((-2*omega*(L[2])*I[max]/V
> [r])+Delta*(h2[q])))*3*x[2];expand(");eq3:=-(omega*(L[3])*(x[1]+I[max
```

```
> ])+((1/2)*(x[3]+V[r])*((-2*omega*(L[3])/V[r])*I[max]+Delta*(h3[q])))*
> 3*x[2];expand('');eq4:=((3/4)*(((x[1]+I[max])*((2*V[a]/V[r])+Delta*h1[d
> ])+(((-2*omega*L[1]*I[max])/V[r])+Delta*h1[q])*x[2]))-(3*V[a]*I[max]/V
> [r]))*2*x[3];expand('');eq5:=(((((3/2)*(x[1]+I[max]))*(((2*V[b])/V[r])+
> Delta*h2[d]))+(3/4)*(((-2*omega*L[2])*I[max]/V[r])+Delta*(h2[q]))*x[2]
> )-(3*V[b]*I[max]/V[r]))*2*x[3];expand('');eq6:=(((((3/4)*((x[1]+I[max])
> )*((2*V[c]/V[r])+Delta*h3[d])))+(3/4)*((-2*omega*(L[3])*I[max]/V[r])+D
> elta*(h3[q]))*x[2])-(3*V[c]*I[max]/V[r]))*2*x[3];expand('');Ans3:=expan
> d((eq1)+(eq2)+(eq3));Ans4:=expand((Ans2)+(Ans3));Ans5:=expand((eq4)+(e
> q5)+(eq6));Ans6:=expand((Ans4)+(Ans5));

      /
eqn := 3 |
      \
                              /  V[a]           \
   omega L[1] x[2] - 1/2 (x[3] + V[r]) |2 ---- + Delta h1[d]| + V[a]
                              \  V[r]           /
   \
   | x[1]
   /
                    x[3] x[1] V[a]
3 x[1] omega L[1] x[2] - 3 -------------- - 3/2 x[3] x[1] Delta h1[d]
                         V[r]

    - 3/2 x[1] V[r] Delta h1[d]

      /
eqn1 := 3 |
      \
                              /  V[b]           \
   omega L[2] x[2] - 1/2 (x[3] + V[r]) |2 ---- + Delta h2[d]| + V[b]
                              \  V[r]           /
   \
   | x[1]
   /
```

```
                    x[3] x[1] V[b]
3 x[1] omega L[2] x[2] - 3 ---------- - 3/2 x[3] x[1] Delta h2[d]
                           V[r]

   - 3/2 x[1] V[r] Delta h2[d]

       /
eqn2 := 3 |
       \
                                 /  V[c]           \
   omega L[3] x[2] - 1/2 (x[3] + V[r]) |2 ---- + Delta h3[d]| + V[c]
                                 \  V[r]           /
   \
   | x[1]
   /

                    x[1] x[3] V[c]
3 x[1] omega L[3] x[2] - 3 ---------- - 3/2 x[1] x[3] Delta h3[d]
                           V[r]

   - 3/2 x[1] V[r] Delta h3[d]

       /
eq1 := -3 |omega L[1] (x[1] + I[max])
       \
                   /  omega L[1] I[max]          \\
   + 1/2 (x[3] + V[r]) |-2 ---------- + Delta h1[q]|| x[2]
                   \        V[r]                 //

                    x[2] x[3] omega L[1] I[max]
-3 x[1] omega L[1] x[2] + 3 ----------------------
                           V[r]

   - 3/2 x[2] x[3] Delta h1[q] - 3/2 x[2] V[r] Delta h1[q]

       /
eq2 := -3 |omega L[2] (x[1] + I[max])
       \

                   /  omega L[2] I[max]          \\
   + 1/2 (x[3] + V[r]) |-2 ---------- + Delta h2[q]|| x[2]
                   \        V[r]                 //


                    x[2] x[3] omega L[2] I[max]
-3 x[1] omega L[2] x[2] + 3 ----------------------
```

```
                                V[r]

    - 3/2 x[2] x[3] Delta h2[q] - 3/2 x[2] V[r] Delta h2[q]

       /
eq3 := -3 |omega L[3] (x[1] + I[max])
       \
                  /  omega L[3] I[max]          \\
    + 1/2 (x[3] + V[r]) |-2 ----------------- + Delta h3[q]|| x[2]
                  \       V[r]                  //

                        x[2] x[3] omega L[3] I[max]
-3 x[1] omega L[3] x[2] + 3 --------------------------
                                V[r]

    - 3/2 x[2] x[3] Delta h3[q] - 3/2 x[2] V[r] Delta h3[q]

      /               / V[a]          \
eq4 := 2 |3/4 (x[1] + I[max]) |2 ---- + Delta h1[d]|
      \               \ V[r]          /

        /  omega L[1] I[max]          \        V[a] I[max]\
    + 3/4 |-2 ----------------- + Delta h1[q]| x[2] - 3 ----------|
        \       V[r]                /          V[r]   /

   x[3]

  x[3] x[1] V[a]                          x[3] V[a] I[max]
3 -------------- + 3/2 x[3] x[1] Delta h1[d] - 3 ----------------
     V[r]                                 V[r]

                              x[2] x[3] omega L[1] I[max]
    + 3/2 x[3] I[max] Delta h1[d] - 3 --------------------------
                                   V[r]

    + 3/2 x[2] x[3] Delta h1[q]

      /               / V[b]          \
eq5 := 2 |3/2 (x[1] + I[max]) |2 ---- + Delta h2[d]|
      \               \ V[r]          /

        /  omega L[2] I[max]          \        V[b] I[max]\
    + 3/4 |-2 ----------------- + Delta h2[q]| x[2] - 3 ----------|
        \       V[r]                /          V[r]   /

   x[3]
```

$$6\,\frac{x[3]\,x[1]\,V[b]}{V[r]} + 3\,x[3]\,x[1]\,\text{Delta}\,h2[d] + 3\,x[3]\,I[max]\,\text{Delta}\,h2[d] - 3\,\frac{x[2]\,x[3]\,\text{omega}\,L[2]\,I[max]}{V[r]} + \frac{3}{2}\,x[2]\,x[3]\,\text{Delta}\,h2[q]$$

$$eq6 := 2\left|\frac{3}{4}\,(x[1] + I[max])\left|2\,\frac{V[c]}{V[r]} + \text{Delta}\,h3[d]\right|\right.$$

$$+ \frac{3}{4}\left|-2\,\frac{\text{omega}\,L[3]\,I[max]}{V[r]} + \text{Delta}\,h3[q]\right|\left.x[2] - 3\,\frac{V[c]\,I[max]}{V[r]}\right|\,x[3]$$

$$3\,\frac{x[1]\,x[3]\,V[c]}{V[r]} + \frac{3}{2}\,x[1]\,x[3]\,\text{Delta}\,h3[d] - 3\,\frac{x[3]\,V[c]\,I[max]}{V[r]} + \frac{3}{2}\,x[3]\,I[max]\,\text{Delta}\,h3[d] - 3\,\frac{x[2]\,x[3]\,\text{omega}\,L[3]\,I[max]}{V[r]} + \frac{3}{2}\,x[2]\,x[3]\,\text{Delta}\,h3[q]$$

$$Ans3 := -3\,x[1]\,\text{omega}\,L[1]\,x[2] + 3\,\frac{x[2]\,x[3]\,\text{omega}\,L[1]\,I[max]}{V[r]} - \frac{3}{2}\,x[2]\,x[3]\,\text{Delta}\,h1[q] - \frac{3}{2}\,x[2]\,V[r]\,\text{Delta}\,h1[q] - 3\,x[1]\,\text{omega}\,L[2]\,x[2] + 3\,\frac{x[2]\,x[3]\,\text{omega}\,L[2]\,I[max]}{V[r]} - \frac{3}{2}\,x[2]\,x[3]\,\text{Delta}\,h2[q] - \frac{3}{2}\,x[2]\,V[r]\,\text{Delta}\,h2[q] - 3\,x[1]\,\text{omega}\,L[3]\,x[2] + 3\,\frac{x[2]\,x[3]\,\text{omega}\,L[3]\,I[max]}{}$$

V[r]

- 3/2 x[2] x[3] Delta h3[q] - 3/2 x[2] V[r] Delta h3[q]

x[2] x[3] omega L[1] I[max]
Ans4 := Ans2 - 3 x[1] omega L[1] x[2] + 3 ----------
V[r]

- 3/2 x[2] x[3] Delta h1[q] - 3/2 x[2] V[r] Delta h1[q]

x[2] x[3] omega L[2] I[max]
- 3 x[1] omega L[2] x[2] + 3 ----------
V[r]

- 3/2 x[2] x[3] Delta h2[q] - 3/2 x[2] V[r] Delta h2[q]

x[2] x[3] omega L[3] I[max]
- 3 x[1] omega L[3] x[2] + 3 ----------
V[r]

- 3/2 x[2] x[3] Delta h3[q] - 3/2 x[2] V[r] Delta h3[q]

x[3] x[1] V[a]
Ans5 := 3 ---------- + 3/2 x[3] x[1] Delta h1[d]
V[r]

x[3] V[a] I[max]
- 3 ---------- + 3/2 x[3] I[max] Delta h1[d]
V[r]

x[2] x[3] omega L[1] I[max]
- 3 ---------- + 3/2 x[2] x[3] Delta h1[q]
V[r]

x[3] x[1] V[b]
+ 6 ---------- + 3 x[3] x[1] Delta h2[d]
V[r]

x[2] x[3] omega L[2] I[max]
+ 3 x[3] I[max] Delta h2[d] - 3 ----------
V[r]

x[1] x[3] V[c]
+ 3/2 x[2] x[3] Delta h2[q] + 3 ----------
V[r]

```
                                  x[3] V[c] I[max]
    + 3/2 x[1] x[3] Delta h3[d] - 3 ----------------
                                      V[r]

                                  x[2] x[3] omega L[3] I[max]
    + 3/2 x[3] I[max] Delta h3[d] - 3 --------------------------
                                      V[r]

    + 3/2 x[2] x[3] Delta h3[q]

                                  x[3] V[a] I[max]
Ans6 := Ans2 + 3/2 x[3] I[max] Delta h1[d] - 3 ----------------
                                      V[r]

                                  x[3] x[1] V[a]
    + 3/2 x[3] x[1] Delta h1[d] + 3 --------------
                                      V[r]

    - 3 x[1] omega L[1] x[2] - 3 x[1] omega L[2] x[2]

                                  x[1] x[3] V[c]
    - 3 x[1] omega L[3] x[2] + 3 --------------
                                      V[r]

    + 3/2 x[1] x[3] Delta h3[d] - 3/2 x[2] V[r] Delta h1[q]

    - 3/2 x[2] V[r] Delta h2[q] + 3 x[3] I[max] Delta h2[d]

                                  x[3] x[1] V[b]
    + 3 x[3] x[1] Delta h2[d] + 6 --------------
                                      V[r]

                                  x[3] V[c] I[max]
    - 3/2 x[2] V[r] Delta h3[q] - 3 ----------------
                                      V[r]

    + 3/2 x[3] I[max] Delta h3[d]

       /
eqn1 := 3 |
       \
                                  /  V[b]            \
   omega L[2] x[2] - 1/2 (x[3] + V[r]) |2 ---- + Delta h2[d]| + V[b]
                                  \  V[r]            /

   \
```

```
   | x[1]
   /


                    x[1] x[3] V[b]
3 x[1] omega L[2] x[2] - 3 -------------- - 3/2 x[1] x[3] Delta h2[d]
                         V[r]

    - 3/2 x[1] V[r] Delta h2[d]


        /
eqn2 := 3 |
        \

                                / V[c]           \
   omega L[3] x[2] - 1/2 (x[3] + V[r]) |2 ---- + Delta h3[d]| + V[c]
                                \ V[r]           /
   \
   | x[1]
   /

                    x[1] x[3] V[c]
3 x[1] omega L[3] x[2] - 3 -------------- - 3/2 x[1] x[3] Delta h3[d]
                         V[r]

    - 3/2 x[1] V[r] Delta h3[d]

        /
eq1 := -3 |omega L[1] (x[1] + I[max])
        \

                  /  omega L[1] I[max]           \\
    + 1/2 (x[3] + V[r]) |-2 ----------------- + Delta h1[q]|| x[2]
                  \       V[r]                 //


                    x[2] x[3] omega L[1] I[max]
-3 x[1] omega L[1] x[2] + 3 --------------------------
                              V[r]

    - 3/2 x[2] x[3] Delta h1[q] - 3/2 x[2] V[r] Delta h1[q]


        /
eq2 := -3 |omega L[2] (x[1] + I[max])
```

```
      \

                  /  omega L[2] I[max]          \\
   + 1/2 (x[3] + V[r]) |-2 ----------------- + Delta h2[q]|| x[2]
                  \       V[r]                  //


                     x[2] x[3] omega L[2] I[max]
-3 x[1] omega L[2] x[2] + 3 --------------------------
                               V[r]

   - 3/2 x[2] x[3] Delta h2[q] - 3/2 x[2] V[r] Delta h2[q]


      /
eq3 := -3 |omega L[3] (x[1] + I[max])
      \

                  /  omega L[3] I[max]          \\
   + 1/2 (x[3] + V[r]) |-2 ----------------- + Delta h3[q]|| x[2]
                  \       V[r]                  //

                     x[2] x[3] omega L[3] I[max]
-3 x[1] omega L[3] x[2] + 3 --------------------------
                               V[r]

   - 3/2 x[2] x[3] Delta h3[q] - 3/2 x[2] V[r] Delta h3[q]

     /              / V[a]          \
eq4 := 2 |3/4 (x[1] + I[max]) |2 ---- + Delta h1[d]||
     \              \ V[r]          /

       /  omega L[1] I[max]          \       V[a] I[max]\
   + 3/4 |-2 ----------------- + Delta h1[q]| x[2] - 3 ----------|
       \       V[r]                /          V[r]   /

  x[3]


 x[1] x[3] V[a]                          x[3] V[a] I[max]
3 ------------- + 3/2 x[1] x[3] Delta h1[d] - 3 ---------------
    V[r]                                 V[r]

                              x[2] x[3] omega L[1] I[max]
   + 3/2 x[3] I[max] Delta h1[d] - 3 --------------------------
                                        V[r]
```

```
   + 3/2 x[2] x[3] Delta h1[q]


     /              / V[b]          \
eq5 := 2 |3/2 (x[1] + I[max]) |2 ---- + Delta h2[d]|
     \              \ V[r]          /

       /  omega L[2] I[max]          \        V[b] I[max]\
   + 3/4 |-2 ----------------- + Delta h2[q]| x[2] - 3 ----------|
       \       V[r]                /          V[r]   /

  x[3]


 x[1] x[3] V[b]
6 -------------- + 3 x[1] x[3] Delta h2[d]
    V[r]

                          x[2] x[3] omega L[2] I[max]
   + 3 x[3] I[max] Delta h2[d] - 3 --------------------------
                                  V[r]

   + 3/2 x[2] x[3] Delta h2[q]


     /              / V[c]          \
eq6 := 2 |3/4 (x[1] + I[max]) |2 ---- + Delta h3[d]|
     \              \ V[r]          /

       /  omega L[3] I[max]          \        V[c] I[max]\
   + 3/4 |-2 ----------------- + Delta h3[q]| x[2] - 3 ----------|
       \       V[r]                /          V[r]   /

  x[3]


 x[1] x[3] V[c]                          x[3] V[c] I[max]
3 -------------- + 3/2 x[1] x[3] Delta h3[d] - 3 ---------------
    V[r]                                 V[r]

                          x[2] x[3] omega L[3] I[max]
   + 3/2 x[3] I[max] Delta h3[d] - 3 --------------------------
                                  V[r]

   + 3/2 x[2] x[3] Delta h3[q]
```

$$2\left|3/2\,\frac{V[c]}{V[r]} + 3/4\ \text{Delta}\ h3[d]\right| x[3]\ x[1]$$

$$+ 2\left|- 3/2\,\frac{\text{omega}\ L[3]\ I[max]}{V[r]} + 3/4\ \text{Delta}\ h3[q]\right| x[3]\ x[2]$$

$$+ 2\left|3/4\ I[max]\ \left|2\,\frac{V[c]}{V[r]} + \text{Delta}\ h3[d]\right| - 3\,\frac{V[c]\ I[max]}{V[r]}\right| x[3]$$

$$\text{Ans2} := 3\ x[1]\ \text{omega}\ L[1]\ x[2] - 3\,\frac{x[1]\ x[3]\ V[a]}{V[r]}$$

$$- 3/2\ x[1]\ x[3]\ \text{Delta}\ h1[d] - 3/2\ x[1]\ V[r]\ \text{Delta}\ h1[d]$$

$$+ 3\ x[1]\ \text{omega}\ L[2]\ x[2] - 3\,\frac{x[1]\ x[3]\ V[b]}{V[r]}$$

$$- 3/2\ x[1]\ x[3]\ \text{Delta}\ h2[d] - 3/2\ x[1]\ V[r]\ \text{Delta}\ h2[d]$$

$$+ 3\ x[1]\ \text{omega}\ L[3]\ x[2] - 3\,\frac{x[1]\ x[3]\ V[c]}{V[r]}$$

$$- 3/2\ x[1]\ x[3]\ \text{Delta}\ h3[d] - 3/2\ x[1]\ V[r]\ \text{Delta}\ h3[d]$$

$$\text{Ans3} := -3\ x[1]\ \text{omega}\ L[1]\ x[2] + 3\,\frac{x[2]\ x[3]\ \text{omega}\ L[1]\ I[max]}{V[r]}$$

$$- 3/2\ x[2]\ x[3]\ \text{Delta}\ h1[q] - 3/2\ x[2]\ V[r]\ \text{Delta}\ h1[q]$$

$$- 3\ x[1]\ \text{omega}\ L[2]\ x[2] + 3\,\frac{x[2]\ x[3]\ \text{omega}\ L[2]\ I[max]}{V[r]}$$

$$- 3/2\ x[2]\ x[3]\ \text{Delta}\ h2[q] - 3/2\ x[2]\ V[r]\ \text{Delta}\ h2[q]$$

$$- 3\, x[1]\, \omega\, L[3]\, x[2] + 3\, \frac{x[2]\, x[3]\, \omega\, L[3]\, I[max]}{V[r]}$$

$$- \frac{3}{2}\, x[2]\, x[3]\, \Delta h3[q] - \frac{3}{2}\, x[2]\, V[r]\, \Delta h3[q]$$

$$Ans4 := -3\, \frac{x[1]\, x[3]\, V[a]}{V[r]} - \frac{3}{2}\, x[1]\, x[3]\, \Delta h1[d]$$

$$- \frac{3}{2}\, x[1]\, V[r]\, \Delta h1[d] - 3\, \frac{x[1]\, x[3]\, V[b]}{V[r]}$$

$$- \frac{3}{2}\, x[1]\, x[3]\, \Delta h2[d] - \frac{3}{2}\, x[1]\, V[r]\, \Delta h2[d]$$

$$- 3\, \frac{x[1]\, x[3]\, V[c]}{V[r]} - \frac{3}{2}\, x[1]\, x[3]\, \Delta h3[d]$$

$$- \frac{3}{2}\, x[1]\, V[r]\, \Delta h3[d] + 3\, \frac{x[2]\, x[3]\, \omega\, L[1]\, I[max]}{V[r]}$$

$$- \frac{3}{2}\, x[2]\, x[3]\, \Delta h1[q] - \frac{3}{2}\, x[2]\, V[r]\, \Delta h1[q]$$

$$+ 3\, \frac{x[2]\, x[3]\, \omega\, L[2]\, I[max]}{V[r]} - \frac{3}{2}\, x[2]\, x[3]\, \Delta h2[q]$$

$$- \frac{3}{2}\, x[2]\, V[r]\, \Delta h2[q] + 3\, \frac{x[2]\, x[3]\, \omega\, L[3]\, I[max]}{V[r]}$$

$$- \frac{3}{2}\, x[2]\, x[3]\, \Delta h3[q] - \frac{3}{2}\, x[2]\, V[r]\, \Delta h3[q]$$

$$Ans5 := 3\, \frac{x[1]\, x[3]\, V[a]}{V[r]} + \frac{3}{2}\, x[1]\, x[3]\, \Delta h1[d]$$

$$- 3\, \frac{x[3]\, V[a]\, I[max]}{V[r]} + \frac{3}{2}\, x[3]\, I[max]\, \Delta h1[d]$$

$$- 3\,\frac{x[2]\,x[3]\,\omega\,L[1]\,I[max]}{V[r]} + 3/2\,x[2]\,x[3]\,\Delta\,h1[q]$$

$$+ 6\,\frac{x[1]\,x[3]\,V[b]}{V[r]} + 3\,x[1]\,x[3]\,\Delta\,h2[d]$$

$$+ 3\,x[3]\,I[max]\,\Delta\,h2[d] - 3\,\frac{x[2]\,x[3]\,\omega\,L[2]\,I[max]}{V[r]}$$

$$+ 3/2\,x[2]\,x[3]\,\Delta\,h2[q] + 3\,\frac{x[1]\,x[3]\,V[c]}{V[r]}$$

$$+ 3/2\,x[1]\,x[3]\,\Delta\,h3[d] - 3\,\frac{x[3]\,V[c]\,I[max]}{V[r]}$$

$$+ 3/2\,x[3]\,I[max]\,\Delta\,h3[d] - 3\,\frac{x[2]\,x[3]\,\omega\,L[3]\,I[max]}{V[r]}$$

$$+ 3/2\,x[2]\,x[3]\,\Delta\,h3[q]$$

$$Ans6 := - 3/2\,x[1]\,V[r]\,\Delta\,h1[d] - 3/2\,x[1]\,V[r]\,\Delta\,h2[d]$$

$$- 3/2\,x[1]\,V[r]\,\Delta\,h3[d] - 3/2\,x[2]\,V[r]\,\Delta\,h1[q]$$

$$- 3/2\,x[2]\,V[r]\,\Delta\,h2[q] - 3/2\,x[2]\,V[r]\,\Delta\,h3[q]$$

$$+ 3/2\,x[3]\,I[max]\,\Delta\,h1[d] + 3\,\frac{x[1]\,x[3]\,V[b]}{V[r]}$$

$$+ 3/2\,x[1]\,x[3]\,\Delta\,h2[d] - 3\,\frac{x[3]\,V[c]\,I[max]}{V[r]}$$

$$+ 3\,x[3]\,I[max]\,\Delta\,h2[d] + 3/2\,x[3]\,I[max]\,\Delta\,h3[d]$$

$$- 3\,\frac{x[3]\,V[a]\,I[max]}{V[r]}$$

```
//  V[b]              \
||3 ---- + 3/2 Delta h2[d]| x[3] - 3/2 V[r] Delta h1[d]
\\  V[r]              /

                                    \
   - 3/2 V[r] Delta h2[d] - 3/2 V[r] Delta h3[d]| x[1] + (
                                    /

   - 3/2 V[r] Delta h2[q] - 3/2 V[r] Delta h3[q]

                          /  V[a] I[max]    V[c] I[max]
   - 3/2 V[r] Delta h1[q]) x[2] + |-3 ---------- - 3 ----------
                          \     V[r]          V[r]

   + 3/2 I[max] Delta h1[d] + 3/2 I[max] Delta h3[d]

                 \
   + 3 I[max] Delta h2[d]| x[3]
                 /


- 3/2 (-2 x[1] x[3] V[b] - x[1] x[3] V[r] Delta h2[d]

          2                  2
   + x[1] V[r]  Delta h1[d] + x[1] V[r]  Delta h2[d]

          2             2
   + x[1] V[r]  Delta h3[d] + V[r]  Delta x[2] h2[q]

      2                  2
   + V[r]  Delta x[2] h3[q] + V[r]  Delta x[2] h1[q]

   + 2 I[max] x[3] V[a] + 2 I[max] x[3] V[c]

   - I[max] x[3] V[r] Delta h1[d] - I[max] x[3] V[r] Delta h3[d]

   - 2 I[max] x[3] V[r] Delta h2[d])/V[r]


/
|    (-V[r] Delta h2[d] - 2 V[b]) x[3]
|- 3/2 ---------------------------------
\              V[r]
```

$$- 3/2 \frac{\sqrt{V[r]^2\ \text{Delta h3[d]}^2 + V[r]^2\ \text{Delta h1[d]}^2 + V[r]^2\ \text{Delta h2[d]}^2}}{V[r]}$$

x[1] - 3/2

(V[r]^2 Delta h2[q]^2 + V[r]^2 2Delta h3[q]^2 + V[r]^2 Delta h1[q]^2) x[2]/

V[r] - 3/2 (2 V[a] I[max] + 2 V[c] I[max]

- I[max] Delta h1[d] V[r] - I[max] Delta h3[d] V[r]

- 2 I[max] Delta h2[d] V[r]) x[3]/V[r]

APPENDIX C:

ELEMENT FILE FOR UNBALANCED (MINIMUM CASE) INPUT VOLTAGE AND BALANCED INPUT LINE IMPEDANCE SIMULATION USING LYAPUNOV CONTROL

This Appendix shows the input file form PSIM used to simulate the Boost Type PWM Rectifier under unbalanced input voltage and balanced input line impedance.

```
.TIME 0.0002 0.5 0 3 0 0 0
SUM2P SUMP1 1 2 3 1 1
SUM2 SUM1 1 2 4 1 -1
P P1 5 6 0.67
P P2 3 7 0.33
P P3 4 8 0.58
SUM2 SUM2 6 7 9 1 -1
TG_1 TAN1 8 9 10
MULT MULT1 9 9 11
MULT MULT2 8 8 12
SUM2P SUMP2 11 12 13 1 1
SQROT SQ1 13 14
COMP COMP1 10 0 15
COMP COMP2 10 16 17
COMP COMP3 10 18 19
COMP COMP4 10 20 21
COMP COMP5 10 22 23
COMP COMP6 10 24 25
VDC VDC1 16 0 120
VDC VDC2 18 0 180
VDC VDC3 20 0 240
VDC VDC4 22 0 300
```

```
VDC VDC5 24 0 360
SUM3 SUM31 15 17 19 26 1 1 1
SUM3 SUM32 21 23 25 27 1 1 1
SUM2P SUMP3 26 27 28 1 1
SUM2 SUM3 28 29 30 1 -1
SUM2 SUM4 10 31 32 1 -1
P P4 30 31 60
VDC VDC6 29 0 1
SUM2 SUM5 33 32 34 1 -1
VDC VDC7 33 0 60
SIN SIN1 34 35
SIN SIN2 32 36
MULT MULT3 35 37 38
MULT MULT4 36 37 39
MULT MULT5 39 14 40
MULT MULT6 38 14 41
SUM2P SUMP4 41 40 42 1 1
SUM2 SUM6 37 42 43 1 -1
P P5 41 44 0.63
P P6 40 45 0.63
MONOC MONOC1 46 0 47 48 49
MONOC MONOC2 0 47 50 51 52
MONOC MONOC3 0 50 53 54 55
MONOC MONOC4 0 53 56 57 52
P P7 50 58 2
P P8 53 59 3
P P9 56 60 4
SUM3 SUM33 47 58 59 61 1 1 1
SUM3 SUM34 61 60 62 63 1 1 1
ANDGATE AND1 48 51 64
ANDGATE AND2 54 57 65
ANDGATE AND3 64 65 66
P P10 66 62 5
VDC VDC8 37 0 100u
LKUP2D LKUP2D7 68 67 69 Q1.tbl
LKUP2D LKUP2D8 68 67 70 Q2.tbl
LKUP2D LKUP2D9 68 67 71 Q3.tbl
LKUP2D LKUP2D10 68 67 72 Q4.tbl
LKUP2D LKUP2D11 68 67 73 Q5.tbl
LKUP2D LKUP2D12 68 67 74 Q6.tbl
ONCTRL B1 72 75
ONCTRL B2 69 76
ONCTRL B4 71 77
ONCTRL B5 70 78
ONCTRL B6 73 79
ONCTRL B3 74 80
```

LIM LIM1 63 67 1 5
UDELAY UDELAY1 44 49 10k
UDELAY UDELAY2 45 52 10k
UDELAY UDELAY3 43 55 10k
UDELAY UDELAY4 28 68 10k
VSQU VSQ1 46 0 2 10k 0.5 0 0 0
MOSFET S6 84 85 78 0 0 0 0
MOSFET S5 86 85 80 0 0 0 0
MOSFET S4 87 85 75 0 0 0 0
MOSFET S3 88 84 79 0 0 0 0
MOSFET S2 88 86 77 0 0 0 0
MOSFET S1 88 87 76 0 0 0 0
C C1 88 85 10000u 0 0
R R1 89 85 100 1
VP2 Vdc 90 85
L L1 91 87 3.8m 0 1
L L2 92 86 3.8m 0 1
L L3 93 84 3.8m 0 1
VCCVS VCCVS1 94 0 91 87 1.5
VCCVS VCCVS2 95 0 92 86 1.5
VCCVS VCCVS3 96 0 93 84 1.5
VDC Vref 97 0 270
MULT MULT15 97 98 99
DIVD DIVD2 99 100 101
SUM3 SUM310 102 103 104 100 3 3 3
MULT MULT16 101 105 106
SUM2 SUM18 109 106 110 1.5 -1.5
SUM2 SUM19 107 106 111 1.5 -1.5
SUM2 SUM20 108 106 112 1.5 -1.5
P P27 111 113 14
P P28 112 114 14
P P29 110 115 14
ABC2DQO ABC2 116 117 118 0 0 0 119
VGNL VGNL1 119 0 60 2 0 1 0 1
VSEN VSEN1 91 0 102 1
VSEN VSEN2 92 0 103 1
VSEN VSEN3 93 0 104 1
ISEN ISEN1 88 90 98 1
VSEN VSEN4 88 0 105 1
VDC Vref 120 0 270
MULT MULT24 121 0 122
MULT MULT25 122 123 124
SUM2 SUM26 120 105 121 -1.5 -1.5
MULT MULT26 125 0 126
MULT MULT27 126 127 128
SUM2 SUM27 120 105 125 -1.5 -1.5

```
MULT MULT28 129 0 130
MULT MULT29 130 131 132
SUM2 SUM28 120 105 129 -1.5 -1.5
VDC Vref 133 0 270
MULT MULT30 134 133 135
MULT MULT31 136 115 137
SUM2 SUM29 135 138 136 .667 -1
SUM2 SUM30 133 105 138 1 -1
SUM2 SUM35 0 98 134 1 -1
VDC Vref 139 0 270
MULT MULT32 140 139 141
MULT MULT33 142 114 143
SUM2 SUM36 141 144 142 0.667 -1
SUM2 SUM37 139 105 144 1 -1
SUM2 SUM38 0 98 140 1 -1
VDC Vref 145 0 270
MULT MULT34 146 145 147
MULT MULT35 148 113 149
SUM2 SUM39 147 150 148 0.667 -1
SUM2 SUM40 145 105 150 1 -1
SUM2 SUM41 0 98 146 1 -1
SUM2 SUM42 149 124 151 1 -1
SUM2 SUM43 137 128 152 1 -1
SUM2 SUM44 143 132 153 1 -1
P P40 0 127 0.0008
P P42 0 123 0.0008
MULT MULT39 0 97 109
MULT MULT37 0 97 107
MULT MULT40 0 97 108
P P43 0 131 0.0008
CTOP CTOP12 94 118
CTOP CTOP13 95 117
CTOP CTOP14 96 116
VP V31 1
VP V32 2
VSIN V1 91 0 165 60 0 0 0
VSIN V2 92 0 170 60 -120 0 0
VSIN V3 93 0 160 60 -240 0 0
COS COS1 154 5
COS COS2 155 1
COS COS3 156 2
L L6 90 89 10m 0 0
LIM LIM2 152 154 -1 1
LIM LIM3 151 155 -1 1
LIM LIM4 153 156 -1 1
VP V38 93
```

APPENDIX D:

ELEMENT FILE FOR UNBALANCED (SEVERE CASE) INPUT VOLTAGE AND BALANCED INPUT LINE IMPEDANCE SIMULATIONUSING LYAPUNOV CONTROL

This Appendix shows the input file form PSIM used to simulate the Boost Type PWM Rectifier under unbalanced input voltage and balanced input line impedance.

```
.TIME 0.0002 0.5 0 3 0 0 0
SUM2P SUMP1 1 2 3 1 1
SUM2 SUM1 1 2 4 1 -1
P P1 5 6 0.67
P P2 3 7 0.33
P P3 4 8 0.58
SUM2 SUM2 6 7 9 1 -1
TG_1 TAN1 8 9 10
MULT MULT1 9 9 11
MULT MULT2 8 8 12
SUM2P SUMP2 11 12 13 1 1
SQROT SQ1 13 14
COMP COMP1 10 0 15
COMP COMP2 10 16 17
COMP COMP3 10 18 19
COMP COMP4 10 20 21
COMP COMP5 10 22 23
COMP COMP6 10 24 25
VDC VDC1 16 0 120
VDC VDC2 18 0 180
VDC VDC3 20 0 240
VDC VDC4 22 0 300
```

```
VDC VDC4 22 0 300
VDC VDC5 24 0 360
SUM3 SUM31 15 17 19 26 1 1 1
SUM3 SUM32 21 23 25 27 1 1 1
SUM2P SUMP3 26 27 28 1 1
SUM2 SUM3 28 29 30 1 -1
SUM2 SUM4 10 31 32 1 -1
P P4 30 31 60
VDC VDC6 29 0 1
SUM2 SUM5 33 32 34 1 -1
VDC VDC7 33 0 60
SIN SIN1 34 35
SIN SIN2 32 36
MULT MULT3 35 37 38
MULT MULT4 36 37 39
MULT MULT5 39 14 40
MULT MULT6 38 14 41
SUM2P SUMP4 41 40 42 1 1
SUM2 SUM6 37 42 43 1 -1
P P5 41 44 0.63
P P6 40 45 0.63
MONOC MONOC1 46 0 47 48 49
MONOC MONOC2 0 47 50 51 52
MONOC MONOC3 0 50 53 54 55
MONOC MONOC4 0 53 56 57 52
P P7 50 58 2
P P8 53 59 3
P P9 56 60 4
SUM3 SUM33 47 58 59 61 1 1 1
SUM3 SUM34 61 60 62 63 1 1 1
ANDGATE AND1 48 51 64
ANDGATE AND2 54 57 65
ANDGATE AND3 64 65 66
P P10 66 62 5
VDC VDC8 37 0 100u
LKUP2D LKUP2D7 68 67 69 Q1.tbl
LKUP2D LKUP2D8 68 67 70 Q2.tbl
LKUP2D LKUP2D9 68 67 71 Q3.tbl
LKUP2D LKUP2D10 68 67 72 Q4.tbl
LKUP2D LKUP2D11 68 67 73 Q5.tbl
LKUP2D LKUP2D12 68 67 74 Q6.tbl
ONCTRL B1 72 75
ONCTRL B2 69 76
ONCTRL B4 71 77
ONCTRL B5 70 78
```

```
ONCTRL B6 73 79
ONCTRL B3 74 80
LIM LIM1 63 67 1 5
UDELAY UDELAY1 44 49 10k
UDELAY UDELAY2 45 52 10k
UDELAY UDELAY3 43 55 10k
UDELAY UDELAY4 28 68 10k
VSQU VSQ1 46 0 2 10k 0.5 0 0 0
MOSFET S6 84 85 78 0 0 0 0
MOSFET S5 86 85 80 0 0 0 0
MOSFET S4 87 85 75 0 0 0 0
MOSFET S3 88 84 79 0 0 0 0
MOSFET S2 88 86 77 0 0 0 0
MOSFET S1 88 87 76 0 0 0 0
C C1 88 85 10000u 0 0
R R1 89 85 100 1
VP2 Vdc 90 85
L L1 91 87 3.8m 0 1
L L2 92 86 3.8m 0 1
L L3 93 84 3.8m 0 1
VCCVS VCCVS1 94 0 91 87 1.5
VCCVS VCCVS2 95 0 92 86 1.5
VCCVS VCCVS3 96 0 93 84 1.5
VDC Vref 97 0 270
MULT MULT15 97 98 99
DIVD DIVD2 99 100 101
SUM3 SUM310 102 103 104 100 3 3 3
MULT MULT16 101 105 106
SUM2 SUM18 109 106 110 1.5 -1.5
SUM2 SUM19 107 106 111 1.5 -1.5
SUM2 SUM20 108 106 112 1.5 -1.5
P P27 111 113 14
P P28 112 114 14
P P29 110 115 14
ABC2DQO ABC2 116 117 118 0 0 0 119
VGNL VGNL1 119 0 60 2  0 1  0 1
VSEN VSEN1 91 0 102 1
VSEN VSEN2 92 0 103 1
VSEN VSEN3 93 0 104 1
ISEN ISEN1 88 90 98 1
VSEN VSEN4 88 0 105 1
VDC Vref 120 0 270
MULT MULT24 121 0 122
MULT MULT25 122 123 124
SUM2 SUM26 120 105 121 -1.5 -1.5
```

```
MULT MULT26 125 0 126
MULT MULT27 126 127 128
SUM2 SUM27 120 105 125 -1.5 -1.5
MULT MULT28 129 0 130
MULT MULT29 130 131 132
SUM2 SUM28 120 105 129 -1.5 -1.5
VDC Vref 133 0 270
MULT MULT30 134 133 135
MULT MULT31 136 115 137
SUM2 SUM29 135 138 136 .667 -1
SUM2 SUM30 133 105 138 1 -1
SUM2 SUM35 0 98 134 1 -1
VDC Vref 139 0 270
MULT MULT32 140 139 141
MULT MULT33 142 114 143
SUM2 SUM36 141 144 142 0.667 -1
SUM2 SUM37 139 105 144 1 -1
SUM2 SUM38 0 98 140 1 -1
VDC Vref 145 0 270
MULT MULT34 146 145 147
MULT MULT35 148 113 149
SUM2 SUM39 147 150 148 0.667 -1
SUM2 SUM40 145 105 150 1 -1
SUM2 SUM41 0 98 146 1 -1
SUM2 SUM42 149 124 151 1 -1
SUM2 SUM43 137 128 152 1 -1
SUM2 SUM44 143 132 153 1 -1
P P40 0 127 0.0008
P P42 0 123 0.0008
MULT MULT39 0 97 109
MULT MULT37 0 97 107
MULT MULT40 0 97 108
P P43 0 131 0.0008
CTOP CTOP12 94 118
CTOP CTOP13 95 117
CTOP CTOP14 96 116
VP V31 1
VP V32 2
VSIN V1 91 0 60 60 0 0 0
VSIN V2 92 0 170 60 -120 0 0
VSIN V3 93 0 60 60 -240 0 0
COS COS1 154 5
COS COS2 155 1
COS COS3 156 2
L L6 90 89 10m 0 0
```

```
LIM LIM2 152 154 -1 1
LIM LIM3 151 155 -1 1
LIM LIM4 153 156 -1 1
VP V38 93
```

APPENDIX E

ELEMENT FILE FOR BALANCED INPUT VOLTAGE AND UNBALANCED INPUT LINE IMPEDANCE (MINIMUM CASE) SIMULATION USING LYAPUNOV CONTROL

This Appendix shows the input file form PSIM used to simulate the Boost Type PWM Rectifier under balanced input voltage and unbalanced input line impedance.

```
.TIME 0.0002 0.5 0 3 0 0 0
SUM2P SUMP1 1 2 3 1 1
SUM2 SUM1 1 2 4 1 -1
P P1 5 6 0.67
P P2 3 7 0.33
P P3 4 8 0.58
SUM2 SUM2 6 7 9 1 -1
TG_1 TAN1 8 9 10
MULT MULT1 9 9 11
MULT MULT2 8 8 12
SUM2P SUMP2 11 12 13 1 1
SQROT SQ1 13 14
COMP COMP1 10 0 15
COMP COMP2 10 16 17
COMP COMP3 10 18 19
COMP COMP4 10 20 21
COMP COMP5 10 22 23
COMP COMP6 10 24 25
VDC VDC1 16 0 120
VDC VDC2 18 0 180
VDC VDC3 20 0 240
```

```
VDC VDC3 20 0 240
VDC VDC4 22 0 300
VDC VDC5 24 0 360
SUM3 SUM31 15 17 19 26 1 1 1
SUM3 SUM32 21 23 25 27 1 1 1
SUM2P SUMP3 26 27 28 1 1
SUM2 SUM3 28 29 30 1 -1
SUM2 SUM4 10 31 32 1 -1
P P4 30 31 60
VDC VDC6 29 0 1
SUM2 SUM5 33 32 34 1 -1
VDC VDC7 33 0 60
SIN SIN1 34 35
SIN SIN2 32 36
MULT MULT3 35 37 38
MULT MULT4 36 37 39
MULT MULT5 39 14 40
MULT MULT6 38 14 41
SUM2P SUMP4 41 40 42 1 1
SUM2 SUM6 37 42 43 1 -1
P P5 41 44 0.63
P P6 40 45 0.63
MONOC MONOC1 46 0 47 48 49
MONOC MONOC2 0 47 50 51 52
MONOC MONOC3 0 50 53 54 55
MONOC MONOC4 0 53 56 57 52
P P7 50 58 2
P P8 53 59 3
P P9 56 60 4
SUM3 SUM33 47 58 59 61 1 1 1
SUM3 SUM34 61 60 62 63 1 1 1
ANDGATE AND1 48 51 64
ANDGATE AND2 54 57 65
ANDGATE AND3 64 65 66
P P10 66 62 5
VDC VDC8 37 0 100u
LKUP2D LKUP2D7 68 67 69 Q1.tbl
LKUP2D LKUP2D8 68 67 70 Q2.tbl
LKUP2D LKUP2D9 68 67 71 Q3.tbl
LKUP2D LKUP2D10 68 67 72 Q4.tbl
LKUP2D LKUP2D11 68 67 73 Q5.tbl
LKUP2D LKUP2D12 68 67 74 Q6.tbl
ONCTRL B1 72 75
```

```
ONCTRL B2 69 76
ONCTRL B4 71 77
ONCTRL B5 70 78
ONCTRL B6 73 79
ONCTRL B3 74 80
LIM LIM1 63 67 1 5
UDELAY UDELAY1 44 49 10k
UDELAY UDELAY2 45 52 10k
UDELAY UDELAY3 43 55 10k
UDELAY UDELAY4 28 68 10k
VSQU VSQ1 46 0 2 10k 0.5 0 0 0
MOSFET S6 84 85 78 0 0 0 0
MOSFET S5 86 85 80 0 0 0 0
MOSFET S4 87 85 75 0 0 0 0
MOSFET S3 88 84 79 0 0 0 0
MOSFET S2 88 86 77 0 0 0 0
MOSFET S1 88 87 76 0 0 0 0
C C1 88 85 10000u 0 0
R R1 89 85 100 1
VP2 Vdc 90 85
L L1 91 87 1m 0 1
L L2 92 86 5m 0 1
L L3 93 84 10m 0 1
VCCVS VCCVS1 94 0 91 87 1.5
VCCVS VCCVS2 95 0 92 86 1.5
VCCVS VCCVS3 96 0 93 84 1.5
VDC Vref 97 0 270
MULT MULT15 97 98 99
DIVD DIVD2 99 100 101
SUM3 SUM310 102 103 104 100 3 3 3
MULT MULT16 101 105 106
SUM2 SUM18 109 106 110 1.5 -1.5
SUM2 SUM19 107 106 111 1.5 -1.5
SUM2 SUM20 108 106 112 1.5 -1.5
P P27 111 113 14
P P28 112 114 14
P P29 110 115 14
ABC2DQO ABC2 116 117 118 0 0 0 119
VGNL VGNL1 119 0 60 2  0 1  0 1
VSEN VSEN1 91 0 102 1
VSEN VSEN2 92 0 103 1
VSEN VSEN3 93 0 104 1
ISEN ISEN1 88 90 98 1
```

```
VSEN VSEN4 88 0 105 1
VDC Vref 120 0 270
MULT MULT24 121 0 122
MULT MULT25 122 123 124
SUM2 SUM26 120 105 121 -1.5 -1.5
MULT MULT26 125 0 126
MULT MULT27 126 127 128
SUM2 SUM27 120 105 125 -1.5 -1.5
MULT MULT28 129 0 130
MULT MULT29 130 131 132
SUM2 SUM28 120 105 129 -1.5 -1.5
VDC Vref 133 0 270
MULT MULT30 134 133 135
MULT MULT31 136 115 137
SUM2 SUM29 135 138 136 .667 -1
SUM2 SUM30 133 105 138 1 -1
SUM2 SUM35 0 98 134 1 -1
VDC Vref 139 0 270
MULT MULT32 140 139 141
MULT MULT33 142 114 143
SUM2 SUM36 141 144 142 0.667 -1
SUM2 SUM37 139 105 144 1 -1
SUM2 SUM38 0 98 140 1 -1
VDC Vref 145 0 270
MULT MULT34 146 145 147
MULT MULT35 148 113 149
SUM2 SUM39 147 150 148 0.667 -1
SUM2 SUM40 145 105 150 1 -1
SUM2 SUM41 0 98 146 1 -1
SUM2 SUM42 149 124 151 1 -1
SUM2 SUM43 137 128 152 1 -1
SUM2 SUM44 143 132 153 1 -1
P P40 0 127 0.0008
P P42 0 123 0.0008
MULT MULT39 0 97 109
MULT MULT37 0 97 107
MULT MULT40 0 97 108
P P43 0 131 0.0008
CTOP CTOP12 94 118
CTOP CTOP13 95 117
CTOP CTOP14 96 116
VP V31 1
```

```
VP V32 2
VSIN V1 91 0 170 60 0 0 0
VSIN V2 92 0 170 60 -120 0 0
VSIN V3 93 0 170 60 -240 0 0
COS COS1 154 5
COS COS2 155 1
COS COS3 156 2
L L6 90 89 10m 0 0
LIM LIM2 152 154 -1 1
LIM LIM3 151 155 -1 1
LIM LIM4 153 156 -1 1
VP V38 93
```

APPENDIX F

ELEMENT FILE FOR BALANCED INPUT VOLTAGE AND UNBALANCED INPUT LINE IMPEDANCE (SEVERE CASE) SIMULATION USING LYAPUNOV CONTROL

This Appendix shows the input file form PSIM used to simulate the Boost Type PWM Rectifier under balanced input voltage and unbalanced input line impedance.

```
.TIME 0.0002 0.5 0 3 0 0 0
SUM2P SUMP1 1 2 3 1 1
SUM2 SUM1 1 2 4 1 -1
P P1 5 6 0.67
P P2 3 7 0.33
P P3 4 8 0.58
SUM2 SUM2 6 7 9 1 -1
TG_1 TAN1 8 9 10
MULT MULT1 9 9 11
MULT MULT2 8 8 12
SUM2P SUMP2 11 12 13 1 1
SQROT SQ1 13 14
COMP COMP1 10 0 15
COMP COMP2 10 16 17
COMP COMP3 10 18 19
COMP COMP4 10 20 21
COMP COMP5 10 22 23
COMP COMP6 10 24 25
VDC VDC1 16 0 120
VDC VDC2 18 0 180
VDC VDC3 20 0 240
```

```
VDC VDC3 20 0 240
VDC VDC4 22 0 300
VDC VDC5 24 0 360
SUM3 SUM31 15 17 19 26 1 1 1
SUM3 SUM32 21 23 25 27 1 1 1
SUM2P SUMP3 26 27 28 1 1
SUM2 SUM3 28 29 30 1 -1
SUM2 SUM4 10 31 32 1 -1
P P4 30 31 60
VDC VDC6 29 0 1
SUM2 SUM5 33 32 34 1 -1
VDC VDC7 33 0 60
SIN SIN1 34 35
SIN SIN2 32 36
MULT MULT3 35 37 38
MULT MULT4 36 37 39
MULT MULT5 39 14 40
MULT MULT6 38 14 41
SUM2P SUMP4 41 40 42 1 1
SUM2 SUM6 37 42 43 1 -1
P P5 41 44 0.63
P P6 40 45 0.63
MONOC MONOC1 46 0 47 48 49
MONOC MONOC2 0 47 50 51 52
MONOC MONOC3 0 50 53 54 55
MONOC MONOC4 0 53 56 57 52
P P7 50 58 2
P P8 53 59 3
P P9 56 60 4
SUM3 SUM33 47 58 59 61 1 1 1
SUM3 SUM34 61 60 62 63 1 1 1
ANDGATE AND1 48 51 64
ANDGATE AND2 54 57 65
ANDGATE AND3 64 65 66
P P10 66 62 5
VDC VDC8 37 0 100u
LKUP2D LKUP2D7 68 67 69 Q1.tbl
LKUP2D LKUP2D8 68 67 70 Q2.tbl
LKUP2D LKUP2D9 68 67 71 Q3.tbl
LKUP2D LKUP2D10 68 67 72 Q4.tbl
LKUP2D LKUP2D11 68 67 73 Q5.tbl
LKUP2D LKUP2D12 68 67 74 Q6.tbl
ONCTRL B1 72 75
```

```
ONCTRL B2 69 76
ONCTRL B4 71 77
ONCTRL B5 70 78
ONCTRL B6 73 79
ONCTRL B3 74 80
LIM LIM1 63 67 1 5
UDELAY UDELAY1 44 49 10k
UDELAY UDELAY2 45 52 10k
UDELAY UDELAY3 43 55 10k
UDELAY UDELAY4 28 68 10k
VSQU VSQ1 46 0 2 10k 0.5 0 0 0
MOSFET S6 84 85 78 0 0 0 0
MOSFET S5 86 85 80 0 0 0 0
MOSFET S4 87 85 75 0 0 0 0
MOSFET S3 88 84 79 0 0 0 0
MOSFET S2 88 86 77 0 0 0 0
MOSFET S1 88 87 76 0 0 0 0
C C1 88 85 10000u 0 0
R R1 89 85 100 1
VP2 Vdc 90 85
L L1 91 87 1m 0 1
L L2 92 86 5m 0 1
L L3 93 84 8m 0 1
VCCVS VCCVS1 94 0 91 87 1.5
VCCVS VCCVS2 95 0 92 86 1.5
VCCVS VCCVS3 96 0 93 84 1.5
VDC Vref 97 0 270
MULT MULT15 97 98 99
DIVD DIVD2 99 100 101
SUM3 SUM310 102 103 104 100 3 3 3
MULT MULT16 101 105 106
SUM2 SUM18 109 106 110 1.5 -1.5
SUM2 SUM19 107 106 111 1.5 -1.5
SUM2 SUM20 108 106 112 1.5 -1.5
P P27 111 113 14
P P28 112 114 14
P P29 110 115 14
ABC2DQO ABC2 116 117 118 0 0 0 119
VGNL VGNL1 119 0 60 2  0 1  0 1
VSEN VSEN1 91 0 102 1
VSEN VSEN2 92 0 103 1
VSEN VSEN3 93 0 104 1
ISEN ISEN1 88 90 98 1
```

```
VSEN VSEN4 88 0 105 1
VDC Vref 120 0 270
MULT MULT24 121 0 122
MULT MULT25 122 123 124
SUM2 SUM26 120 105 121 -1.5 -1.5
MULT MULT26 125 0 126
MULT MULT27 126 127 128
SUM2 SUM27 120 105 125 -1.5 -1.5
MULT MULT28 129 0 130
MULT MULT29 130 131 132
SUM2 SUM28 120 105 129 -1.5 -1.5
VDC Vref 133 0 270
MULT MULT30 134 133 135
MULT MULT31 136 115 137
SUM2 SUM29 135 138 136 .667 -1
SUM2 SUM30 133 105 138 1 -1
SUM2 SUM35 0 98 134 1 -1
VDC Vref 139 0 270
MULT MULT32 140 139 141
MULT MULT33 142 114 143
SUM2 SUM36 141 144 142 0.667 -1
SUM2 SUM37 139 105 144 1 -1
SUM2 SUM38 0 98 140 1 -1
VDC Vref 145 0 270
MULT MULT34 146 145 147
MULT MULT35 148 113 149
SUM2 SUM39 147 150 148 0.667 -1
SUM2 SUM40 145 105 150 1 -1
SUM2 SUM41 0 98 146 1 -1
SUM2 SUM42 149 124 151 1 -1
SUM2 SUM43 137 128 152 1 -1
SUM2 SUM44 143 132 153 1 -1
P P40 0 127 0.0008
P P42 0 123 0.0008
MULT MULT39 0 97 109
MULT MULT37 0 97 107
MULT MULT40 0 97 108
P P43 0 131 0.0008
CTOP CTOP12 94 118
CTOP CTOP13 95 117
CTOP CTOP14 96 116
VP V31 1
```

```
VP V32 2
VSIN V1 91 0 170 60 0 0 0
VSIN V2 92 0 170 60 -120 0 0
VSIN V3 93 0 170 60 -240 0 0
COS COS1 154 5
COS COS2 155 1
COS COS3 156 2
L L6 90 89 10m 0 0
LIM LIM2 152 154 -1 1
LIM LIM3 151 155 -1 1
LIM LIM4 153 156 -1 1
VP V38 93
```

APPENDIX G

PSIM PROGRAM

The PSIM is simulation package designed specifically for power electronics circuit modeling and motor control. Created by Powersim Inc., PSIM is a user friendly simulation package that provides a unique simulation environment for power electronics converters, motor, and control loop design. With its many built-in element, it is an ideal simulator for both circuit-oriented and equation solving simulation. In PSIM a circuit is basically represented in four part, power circuit, control circuit, sensors, and switch controllers. Power circuits are made up of components such as resistors, capacitors, inductors, transformers, and coupled inductors. Control circuits are presented in block diagrams in forms such as s-domain, z-domain, logic components such as logic gates and flip-flops, nonlinear components such multipliers and divider. Sensors are used to measure signals such as current and voltage that the values are then passed to control circuits. Gating signals are then generated from the control circuit and sent back to the power circuit through the switch controllers that in turn control the switch [26].

Some of the nontraditional elements from PSIM used in the simulation are:

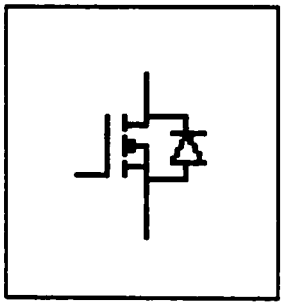

Figure F.1. N-channel MOSFET Switch

Parameters:

On Resistance - Resistance of the MOSFET transistor during the on state, in Ohm

Diode Voltage Drop- Conduction voltage drop of the anti-parallel diode, in V

Initial Position- Flag for initial transistor position (0: open; 1: closed)

Current Flag- Flag for current output of the whole switch module (0: no output; 1: with output)

An n-channel MOSFET Figure F.1 consists of a transistor in anti-parallel with a diode. This device is turned on when the gating signal is high and the drain-to-source is positively biased. It is turned off when the gating is low or the current drops to zero.

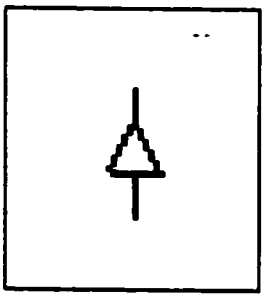

Figure F.2. (ONCTRL) On-Off Switch Controller

The on-off switch controller Figure F.2 interfaces between the control circuit and the power circuit. The input is a logic signal (0 or 1) from the control circuit. The output is connected to the gate (base) node of a switch (or multiple switches) to control the conduction of the switch. The signal level of 1 is for switch on and 0 for switch off.

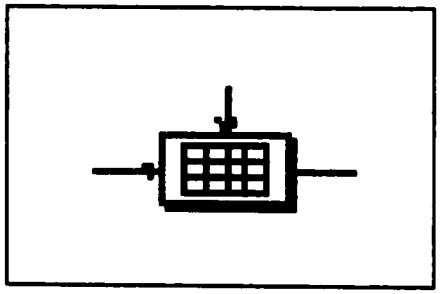

Figure F.3. (LKUP2D) 2-Dimensional Lookup Table

A file name of the file storing the lookup table Figure F.3 is specified using a block diagram. The 2-dimensional lookup table has two inputs and one output. The output data is stored in a 2-dimensional matrix. The two input correspond to the row and column indices of the matrix. For example, if the row index is 3 and the column index is 4, the output will be A(3,4) where A is the data matrix.

The data for the lookup table are stored in a file and have the following format:

m, n

A(1,1), A(1,2), ..., A(1,n)

A(2,1), A(2,2), ..., A(2,n)

... ...

A(m,1), A(m,2), ..., A(m,n)

where m and n are the number of rows and columns, respectively. Since the row and the column index must be an integer, the input value is automatically converted to an integer. If either the row or the column index is out of the range (for example, if the row index is less than 1 or greater than m), the output will be zero.

Example:

The following shows a 2-dimensional lookup table:

3, 4

1., -2., 4., 1.

2., 3., 5., 8.

3., 8., -2., 9.

If the row index is 2 and the column index is 4, the output will be 8. If the row index is 5, regardless of the column index, the output will be 0.

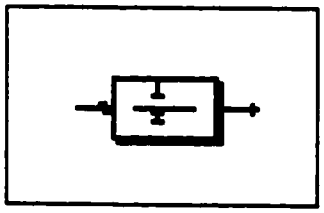

Figure F.4. (UDELAY) Unit Delay Block

A unit delay block Figure F.4 is used to delays the input by one sampling period.

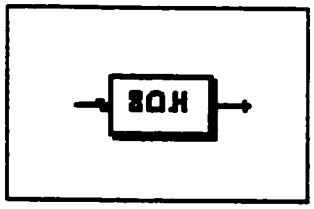

Figure F.5. (ZOH) Zero-Order Hold

Figure F.5 is a zero-order sampling/hold block (ZOH). The ZOH samples the input at the beginning of a clock cycle, and holds the sampled value until the next clock cycle. The difference between the element ZOH and the sampling/hold element SAMP is that, while the clock is provided externally in SAMP, the clock is free-running for ZOH.

For example, if the sampling frequency of ZOH is 1000, the sampling will occur at 0., 0.001 sec., 0.002 sec., etc.

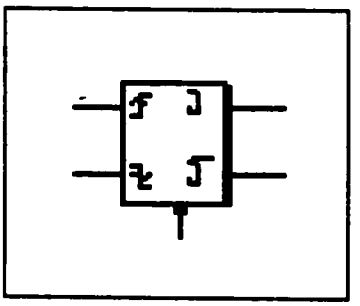

Figure F.6. (MONOC) Controlled Monostable Multivibrator

The controlled monostable multivibrator Figure F.6 allows the pulse width to be specified externally. The node at the bottom of block is for the input that defines the pulse width.

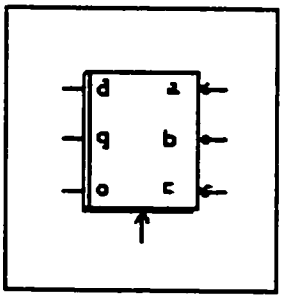

Figure F.7. (ABC2DQO) abc to dqo Transformation Block

This block Figure F.7 transforms 3-phase abc quantities to dqo quantities. This block can be used in both the power circuit and the control circuit. Note that only the voltage quantities can be transformed used this block. To transform current quantities, they must first be converted to voltage quantities using current-controlled voltage sources.

The transformation equations from abc to dqo are:

$$V_d = \frac{2}{3}\left[V_a \cos\alpha + V_b \cos(\alpha - \frac{2\pi}{3}) + V_c \cos(\alpha + \frac{2\pi}{3})\right]$$

$$V_q = \frac{2}{3}\left[V_a \sin\alpha + V_b \sin(\alpha - \frac{2\pi}{3}) + V_c \sin(\alpha + \frac{2\pi}{3})\right]$$

$$V_0 = \frac{1}{3}\left[V_a + V_b + V_c\right]$$

Examples:

Let phases a, b, and c to be symmetrical, and X = wt.

If V_a = 10sin(wt), then Vd = 0, Vq = 10.

If V_a = 10sin(wt + pi / 6), then Vd = 5, Vq = 8.66.

If V_a = 10sin(wt - pi / 6), then Vd = -5, Vq = 8.66.

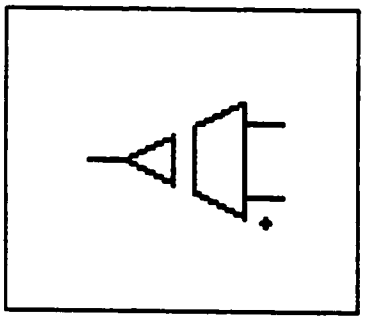

Figure F.8. (VSEN) Voltage Sensor

The voltage sensor Figure F.8 measures the voltage of the power circuit and passes the value to the control circuit.

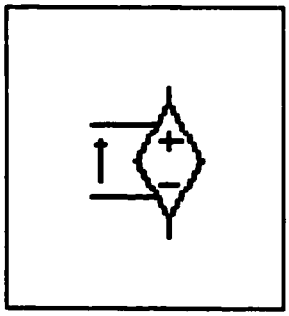

Figure F.9. (VCCVS) Current-Controlled Voltage Source

Figure F.9 is Current-controlled voltage sourceblock. The voltage source value is equal to the gain multiplied by the controlling current. The control nodes, on the left, should be connected across a resistor/inductor/capacitor branch, and the arrow indicates the direction of the controlling current.

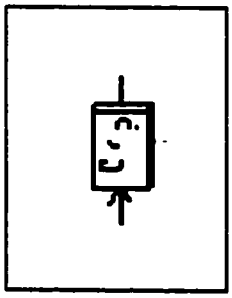

Figure F.10. (CTOP) Control-power Interface Block

In PSIM, power circuits and control circuits are separated and are solved sequentially. The control-power interface block Figure F.10allows a control circuit quantity to be

passed unchanged to the power circuit. The output of the interface block is treated as a constant voltage source in the power circuit. By using this block, some of the functions that can only be generated in the control circuit can be passed to the power circuit.